School of Electrical Engineering and Computing
Department of Electrical and Computer Engineering

Robust Transceiver Designs for MIMO Relay Communication Systems

Lenin Gopal

This thesis is presented for the degree of
Doctor of Philosophy
of
Curtin University

July 2015

Declaration

To the best of my knowledge and belief this thesis contains no material previously published by any other person except where due acknowledgment has been made.

This thesis contains no material which has been accepted for the award of any other degree or diploma in any university.

Signature: .....

Date: .....

To

my parents, my wife Gowsalya Devi, my daughter Aboorva and my son Avannish

Acknowledgements

First and foremost, I would like to express my sincere gratitude to my thesis supervisors Associate Prof. Zhuquan Zang and Associate Prof. Yue Rong for their inspiration, motivation, immense knowledge, constant support and encouragement during the entire period of my PhD study. Their invaluable guidance and timely correspondence directed me to reach the goal. They were constantly patient and caring in their instructive and research support, which guided me to pursue the right path.

Besides my supervisors, I would like to extend my gratitude to Associate Prof. Chua Han Bing, Chairperson of my thesis committee, for his necessary administrative guidance and help at all levels of this research work.

My earnest thanks also go to Associate Prof. Ravindra Nath Mukerjee, Associate Prof. C. Palanichamy, Dr. M. V. Prasanna and Mr. Mohd Amaluddin Yusoff for their continuous encouragement, insightful comments, proof reading and motivation to complete the thesis on schedule.

I am grateful to the Faculty of Engineering and Science, Curtin University, Sarawak, Malaysia for the financial and administrative support they have provided me during the course of my doctoral study.

I would like to acknowledge my wife, Gowsalya Devi, who deserves a doctorate herself for the patience, sacrifice, and care she has shown during the entire period of my PhD study. My sincere thanks also go to all my friends and colleagues, especially Dr. G. Rajamohan, Dr. Moola Mohan Reddy and Mr. S. Veeramani for their continuous support in thesis preparation.

Most of all, I am indebted to my unconditionally loving parents and kids Aboorva and Avannish, whose moral support in my research endeavours has made this dissertation possible. I would like to finish off by thanking my Creator for making my life beautiful.

Abstract

Recently cooperative wireless communications have attracted considerable attention, due to their potential to provide reliable, cost effective and wide-area coverage of wireless networks. In cooperative wireless communication systems, relay node can be deployed in between the source and the destination nodes to reduce the transmission power from the source to neighbouring nodes and mitigate the channel fading and shadowing effects. In this scenario, the source signals travel through two hops before they are received by the destination node. Such system is called as multiple-input multiple-output (MIMO) relay system. In this dissertation, practical aspects of wireless channels such as channel uncertainty and channel estimation errors are considered for transceiver design problems in a non-regenerative MIMO relay system.

An optimal structure of the relay precoding matrix is derived to minimize the mean-squared error (MSE) in the signal waveform estimation with the assumption that the relay knows the channel covariance information (CCI) of the relay-destination link and also the full channel state information (CSI) of the source-relay link. The proposed scheme outperforms the conventional relay algorithms in terms of both MSE and bit-error-rate (BER).

Next, an iterative covariance algorithm is proposed for non-regenerative MIMO relay system with direct link. It is assumed that the full CSI of the source-relay link and CCI of the relay-destination link as well as the source-destination link are available at the relay node. In order to reduce computational complexity of the proposed iterative covariance algorithm, a suboptimal covariance algorithm is proposed. The developed iterative covariance algorithm outperforms the conventional CCI based MSE algorithms.

Next, an iterative joint source and relay precoder design is proposed for a non-regenerative MIMO relay system with the assumption that the relay

knows the mean and CCI of the relay-destination link and the full CSI of the source-relay link. In order to reduce computational complexity of the proposed iterative design algorithm, a suboptimal relay-only precoder design algorithm is proposed. The performance of the proposed iterative joint source and relay precoder design algorithm is very close to that of the algorithm using the full CSI.

Next, Tomlinson-Harashima (TH) precoder based non-linear transceiver design is proposed for a non-regenerative MIMO relay system, it is assumed that the CCI of the relay-destination link is available at the relay node. First, the structure of the optimal TH precoding matrix and the source precoding matrix is derived. Then an iterative algorithm is developed to optimize the relay precoding matrix. To reduce the computational complexity of the iterative algorithm, a simplified precoding matrices design algorithm is proposed. The proposed precoding matrices design algorithms outperform the existing algorithms.

Finally, the transceiver design is investigated for a non-regenerative multicasting MIMO relay system, where one transmitter broadcasts common message to multiple receivers with the aid of a relay node. The transmitter, relay, and receivers are equipped with multiple antennas. It is assumed that the true (unknown) channel matrices have Gaussian distribution, the estimated channels are the mean value of this distribution. The channel estimation errors follow the well-known Kronecker model. Two robust transceiver design algorithms are proposed to jointly design the transmitter, relay, and receiver matrices to minimize the maximal MSE of the signal waveform estimation among all receivers. In particular, it is proved that the MSE at each receiver can be decomposed into the sum of the MSEs of the first-hop and second-hop channels. Based on this MSE decomposition, transceiver design algorithms are developed with low computational complexity. Numerical simulations demonstrate the improved robustness of the proposed transceiver design algorithm against the mismatch between the true and estimated channels.

Author's Note

Parts of this thesis and concepts from it have been previously published in the following journal and/or conference papers.

Journal Papers

[1] L. Gopal, Y. Rong, and Z. Zang, "Robust MMSE transceiver design for nonregenerative multicasting MIMO relay systems", *IEEE Trans. Signal Process.*, revised and resubmitted, May. 2015.

[2] L. Gopal, Y. Rong, and Z. Zang, "Tomlinson-Harashima precoding based transceiver design for MIMO relay systems with channel covariance information", *IEEE Trans. Wireless Commun.*, to appear, 2015.

Conference Papers

[1] L. Gopal, Y. Rong, and Z. Zang, "Simplified robust design for nonrenerative multicasting MIMO relay systems", in *Proc. 22nd Int. Conf. Telecommun.*, Sydney, Australia, Apr. 27-29, 2015.

[2] L. Gopal, Y. Rong, and Z. Zang, "MMSE based transceiver design for MIMO relay systems with mean and covariance feedback", in *Proc. 77th IEEE Veh. Tech. Conf.*, Dresden, Germany, Jun. 2-5, 2013.

[3] L. Gopal, Y. Rong, and Z. Zang, "Channel covariance information based transceiver design for AF MIMO relay systems with direct Link", in *Proc. 18th Asia-Pacific Conf. Commun.*, Jeju Iceland, South Korea, Oct. 15-17, 2012.

[4] L. Gopal, Y. Rong, and Z. Zang, "Joint MMSE transceiver design in non-regenerative MIMO relay systems with covariance feedback", in *Proc. 17th Asia-Pacific Conf. Commun.*, Sabah, Malaysia, Oct. 2-5, 2011.

Contents

List of Figures

List of Tables

List of symbols

AF	amplify-and-forward
AGI	arithmetic-geometric inequality
BER	bit-error-rate
CCI	channel covariance information
CSI	channel state information
DF	decode-and-forward
DFE	decision-feedback equalizer
EVD	eigenvalue decomposition
GMD	geometric mean decomposition
i.i.d.	independent and identically distributed
JMMSE	joint MMSE
KKT	Karush-Kuhn-Tucker
LTE	long-term evolution
MI	mutual information
MIMO	multiple-input multiple-output
MMSE	minimum MSE
MSE	mean-squared error
NAF	naive amplify-and-forward

NMSE	normalized MSE
PSD	positive semidefinite
QAM	quadrature amplitude modulation
QPSK	quadrature phase-shift keying
SISO	single-input single-output
SNR	signal-to-noise ratio
SVD	singular value decomposition
TH	Tomlinson-Harashima

Chapter 1

Introduction

In the next generation wireless communication systems, relaying is essential to provide reliable and cost effective, wide-area coverage for wireless networks in a variety of applications. If the link-quality between the source and destination nodes degrades in a cellular environment, relay nodes can be deployed in between the source-destination link to mitigate the strong shadowing, multipath fading, path losses and high interferences. The main aim of this thesis is to develop advanced robust signal processing algorithms for multiple-input multiple-output (MIMO) relay communication systems. In this introductory chapter, necessary background of the MIMO relay systems is presented briefly using partial channel state information (CSI) and an overview of the thesis contributions is described in the following section.

1.1 MIMO Wireless Communication Systems

Due to high demand in multimedia applications, next-generation wireless communication systems are expected to support higher data rate compared to the current systems. However, wireless communication channel is strongly impaired by multi-path fading. The multi-path fading effects can severely degrade the performance of wireless communication systems in terms of quality and reliability of the received signal at the receiver. Designing the high data rate, high reliability wireless communication systems is extremely challenging task.

MIMO technology provides a number of benefits that it effectively mitigates the multi-path fading as well as resource constraints [1]. Wireless system's spectral efficiency can be improved by deploying multiple antennas at the transmitter and receiver ends.

By deploying multiple antennas at the transmitter and receiver ends, higher data rate can be achieved without increasing the additional power or bandwidth expenditure as compared to the single-input single-output (SISO) systems. By spatially multiplexing several data streams onto the MIMO channel, the system can provide an additional *degree-of-freedom* which leads to increase in the channel capacity [2–8]. The advantage of a MIMO system is that it has the ability to convert multipath fading into a benefit for the user [2, 9–11]. The performance improvements resulting from the use of MIMO systems are due to the following unique features of MIMO configuration [5, 7].

- Array gain: Due to a coherent combining effect of the received signals at the receiver, increases the receive signal-to-noise ratio (SNR). Achieving array gain requires CSI between the transmitter and receiver and depends on the number of transmit and receive antennas.

- Spatial diversity gain: In wireless communication systems, the received signal level undergoes multi-path fading. The spatial diversity gain mitigates the fading effects of wireless channels. Spatial diversity gain depends on signal being transmitted over multiple copies of the transmitted signals in time, frequency, or space. Spatial diversity is preferred over time/frequency diversity as it does not incur any cost in transmission time or bandwidth. A MIMO channel with M_{T} transmit and M_{R} receive antennas can achieve $M_{\mathrm{T}}M_{\mathrm{R}}$th-order spatial diversity.

- MIMO systems provide higher data rate through spatial multiplexing gain which is achieved by transmitting independent data streams from different antennas. By exploiting the spatial information of the signal, the receiver can separate the different streams, and the capacity scales linearly, with minimum number of transmit antennas and receiver antennas, i.e., $\min\{M_{\mathrm{T}}, M_{\mathrm{R}}\}$ [7, 9].

- Interference occurs due to multiple users operating in the same time and frequency band. When multiple antennas are used, spatial filters preserve the signals coming from a certain spatial location, while suppressing signals from other spatial locations. Therefore, MIMO systems can separate signals which differ in spatial dimensions, just as a conventional filter which can separate signals of different frequency band. Interference mitigation can also be implemented at the transmitter, where the aim is to minimize the interference power sent towards the co-channel users while delivering the signal to the intended user.

However, it can be noticed that in general, it may not be possible to exploit all the benefits of MIMO technology simultaneously due to conflicting demands on the spatial degrees of freedom between spatial diversity gain and spatial multiplexing gain. The level of these conflicts are resolved based on the type of signaling scheme and transceiver design [5].

MIMO technologies have become the core of many components in the next-generation wireless standards viz. the mobile communication systems, long-term evolution (LTE) systems, and the IEEE 802.xx family of standards viz. IEEE 802.16e, IEEE 802.16j, IEEE 802.16m, and IEEE 802.11n [12]. MIMO technology is compatible with any modulation scheme, hence future wireless standards will use MIMO techniques to achieve higher data rate.

1.2 MIMO Relay Communication Systems

Wireless relaying is essential to provide reliable and cost effective, wide-area coverage for wireless networks in a variety of applications. In a cellular environment, a relay can be deployed in areas where there are strong shadowing effects, such as inside buildings and tunnels. For mobile ad-hoc networks, relaying is essential not only to overcome shadowing due to obstacles but also to reduce transmission power from source to neighbouring nodes [13–16]. For tactical applications, dynamic deployment of relays is useful to enhance the networks reliability, throughput, and minimize interception by unwanted users.

There are two types of relay strategies: regenerative scheme and non-regenerative scheme [17–19]. In regenerative strategy, the relay decodes the information received from source and forwards the re-encoded signal to the destination. Whereas in non-regenerative strategy, the relay amplifies the received signal from source and retransmits the signal to the destination. Compared with the regenerative scheme, the non-regenerative strategy has a lower computational complexity and is easy to implement in a cooperative environment.

On the other hand, MIMO system can provide spatial diversity and multiplexing gains to wireless communication systems [20]. When nodes in a relay network have multiple transmit/receive antennas, such system is termed a MIMO relay system. Transceiver designs for a two-hop non-regenerative MIMO relay system have been proposed to maximize the mutual information (MI) between the source-destination link

[21, 22]. Relay precoding algorithms have been investigated to minimize the mean-squared error (MSE) of the signal waveform estimation at the destination node [23–28]. The proposed precoder designs in [21–28] have been developed with the assumption that the full CSI of the source-relay and relay-destination links is available at the relay node.

However, in practice, the environment is mostly surrounded by scatters and shadowing effects. Due to the scattered and shadowing environments, the received signal is uncorrelated at the destination. Hence, the full CSI of the wireless channel is too difficult to estimate at the relay node. Hence, a more practical assumption is that only partial information of the wireless channel is available at the relay node. Relay precoder design schemes have been proposed in [29–31] for maximizing the ergodic capacity of a non-regenerative MIMO relay system with the assumption that the channel covariance information (CCI) of the relay-destination link is available at the relay node. Minimum MSE (MMSE) based transceiver designs have been investigated in [32–35] with the assumption that CCI of the relay-destination link and the full CSI of the source-relay link is known at the relay node.

Linear transceiver designs have been considered for non-regenerative MIMO relay systems in the work of [29, 30, 32–35]. Compared with linear transceivers, non-linear transceivers have a better MSE and bit-error-rate (BER) performances. Recently, non-linear transceiver based non-regenerative MIMO relay system designs have been proposed in [36, 37]. Non-linear transceiver can be incorporated at the receiver as a decision-feedback equalizer (DFE) and/or at the transmitter in the form of a Tomlinson-Harashima (TH) precoder. In general, the TH precoding based non-linear transceiver design provides better MSE and BER performances than the DFE-based transceiver design, as the latter suffers from error propagation.

The performance of the TH precoding scheme has been well studied for single-hop MIMO systems [38], [39]. Recently, the TH precoding scheme has also been developed for dual-hop non-regenerative MIMO relay systems [40] with the assumption that the full CSI of the wireless channel is available at the relay node. In [40–43], channel uncertainty has been considered for designing the TH precoding based non-regenerative MIMO relay systems. Due to the non-linear nature of the precoding scheme, the TH precoding is highly sensitive to the time-varying nature of the wireless channel [44].

The foregoing algorithms are developed by assuming that the exact CSI of the channels is available at the relay node. However, in practical communication systems,

the exact CSI is not available, and therefore, has to be estimated. There is always a mismatch between the true and estimated CSI. Hence, the performance of the earlier proposed algorithms will degrade due to such CSI mismatch. Furthermore, the proposed algorithms are not tested under multiple receivers.

Recently, a two-hop non-regenerative multicasting MIMO relay system has been investigated in [45, 46] where one transmitter multicasts common message to multiple receivers with the aid of a relay node. The transmitter, relay, and receivers are all equipped with multiple antennas. The multicasting transceiver design in [45, 46] is proposed with the assumption that the full CSI of all channels is available at the relay node. As described earlier, in the practical communication systems, the exact CSI is not available, and therefore, has to be estimated. There is always a mismatch between the true and estimated CSI. Hence, the performance of the algorithm in [45, 46] will also degrade due to such CSI mismatch.

1.3 Thesis Objectives

The objective of this research is to develop new and innovative robust transceiver design schemes for a non-regenerative MIMO relay system to minimize the MSE of the estimated signal at the destination node. Distinctively, the objectives of this research are to:

- develop new and innovative MMSE based robust transceiver design schemes for MIMO relay systems with theoretical justifications using computationally efficient convex optimization algorithms.
- investigate the currently popular transceiver design approaches to minimize the MSE of the MIMO relay systems for further improvement.
- evaluate and validate the effectiveness of the proposed transceiver design schemes using numerical analysis and computer simulation.

1.4 Thesis Overview and Contributions

In next generation wireless communication systems, multiple users equipped with multiple antennas will transmit simultaneously to the base station with multiple receive antennas and vice versa [47, 48]. However, in the case of long source-destination link

distance, relay node is necessary to efficiently mitigate the pathloss of wireless channel. Non-regenerative MIMO relays are very useful in extending the network coverage and improving the link quality of the network.

Recently, relay precoding schemes have been proposed [23–28] to minimize the MSE of the signal waveform estimation at the destination node. The precoder designs in [21–28] assume that the full CSI of the source-relay and relay-destination links is available at the relay node. However, the exact CSI is not available at the relay node. Hence, a more practical assumption is that only partial CSI of the wireless channel is available at the relay node. MMSE based linear transceiver designs [32–35] and non-linear transceiver design [49] have been proposed with the assumption that the CCI of the relay-destination link and the full CSI of the source-relay link are known at the relay node.

However, in practical communication systems, the CSI is unknown at the relay node, and therefore, has to be estimated. There is always mismatch between the true and the estimated CSI due to channel noise, quantization errors and outdated channel estimates. Hence, the performance of the earlier proposed algorithms will be degraded due to such CSI mismatch. Therefore, in this thesis, it is assumed that the true channel matrices have Gaussian distribution, with the estimated channels as the mean value, and the channel estimation errors follow the well-known Kronecker model. Based on this assumption, robust advanced signal processing algorithms are proposed to jointly design the transmitter, relay, and receiver matrices to minimize the maximal mean MSE of the non-regenerative multicasting MIMO relay systems. The proposed joint source and relay optimization problems for non-regenerative MIMO relay systems are highly nonconvex, in nature, hence, main contribution of this thesis is that the nonconvex optimization problems are transformed into suitable forms which can be efficiently solved by using standard convex optimization tools.

In Chapter 2, the problem of transceiver design is addressed for a non-regenerative MIMO relay system with the assumption that CCI of the relay-destination link and the full CSI of the source-relay link are known at the relay node. Chapter 3, a design scheme is proposed for a non-regenerative MIMO relay system with covariance feedback and direct link. In the proposed design scheme, it is assumed that the full CSI of the source-relay link and partial channel state information such as CCI of the relay-destination link are available at the relay node. The problem of transceiver design in a non-regenerative MIMO relay system is investigated in Chapter 4 with the assumption that the mean and CCI of the relay-destination link and the full CSI of the source-relay

link are known at the relay node. In Chapter 5, the performance of the TH precoder based non-linear transceiver design is investigated for a non-regenerative MIMO relay system with the assumption that the full CSI of the source-relay link is known, while only the CCI of the relay-destination link is available at the relay node. Chapter 6 proposes a robust transceiver design for a non-regenerative multicasting MIMO relay system with the assumption that the actual CSI is assumed as a Gaussian random matrix with the estimated CSI as the mean value, and estimated errors of the channels are derived from the well-known Kronecker model. Chapter 7 summarizes the thesis and highlights some interesting future works.

Chapter 2: MIMO Relay Design with Covariance Feedback

In this chapter, the optimal structure of the non-regenerative MIMO relay matrix is derived which minimizes the MSE of the symbol estimation at the destination node. It is assumed that the covariance feedback of the relay-destination link is available at the relay node. It is further assumed that the full CSI of the source-relay link is known at the relay node. Simulation results demonstrate that the proposed scheme has better performance in terms of MSE and BER as compared to the conventional MSE schemes proposed in the literature for non-regenerative MIMO relay schemes.

Chapter 2 is based on the following conference publication:

- L. Gopal, Y. Rong, and Z. Zang, "Joint MMSE transceiver design in non-regenerative MIMO relay systems with covariance feedback", in *Proc. 17th Asia-Pacific Conf. Commun.*, Sabah, Malaysia, Oct. 2-5, 2011.

Chapter 3: MIMO Relay Design with CCI Feedback and Direct Link

In this chapter, a design scheme for non-regenerative MIMO relay system is developed to minimize the MSE of the signal estimation at the destination node. In the proposed design scheme, an optimal precoding matrix is derived with the assumption that the full CSI of the source-relay link and partial CSI such as CCI of the relay-destination link are available at the relay node. In practical cases, if the destination is closer to the source, the source-destination link cannot be ignored. Hence, in this chapter, it is assumed that the partial CSI of the source-destination link is known at the relay node. Based on this assumption, an iterative optimal covariance algorithm is developed to achieve the minimum MSE of the estimated signal at the destination node. Numerical examples show that the developed optimal covariance algorithm outperforms the conventional CCI based MSE algorithms.

The material in Chapter 3 is based on the following conference publication:

- L. Gopal, Y. Rong, and Z. Zang, "Channel covariance information based transceiver design for AF MIMO relay systems with direct Link", in *Proc. 18th Asia-Pacific Conf. Commun.*, Jeju Iceland, South Korea, Oct. 15-17, 2012.

Chapter 4: MIMO Relay Design with Mean and Covariance Feedback

In this chapter, the problem of transceiver design in a non-regenerative MIMO relay system is addressed, where linear signal processing is applied at the source, relay and destination nodes to minimize the MSE of the signal waveform estimation at the destination node. In the proposed design scheme, optimal structure of the source and relay precoding matrices are obtained with the assumption that the mean and CCI of the relay-destination link and the full CSI of the source-relay link are known at the relay node. Based on this assumption, an iterative joint source and relay precoder design is proposed to achieve the minimum MSE of the estimated signal at the destination node. In order to reduce computational complexity of the proposed iterative design, a suboptimal relay-only precoder design is proposed. Numerical examples show that the performance of the proposed iterative joint source and relay precoder design is very close to that of the algorithm using full CSI.

Chapter 4 is based on the following conference publication:

- L. Gopal, Y. Rong, and Z. Zang, "MMSE based transceiver design for MIMO relay systems with mean and covariance feedback", in *Proc. 77th IEEE Veh. Tech. Conf.*, Dresden, Germany, Jun. 2-5, 2013.

Chapter 5: Non-linear MIMO Relay Design with Covariance Feedback

In this chapter, the performance of the TH precoder based non-linear transceiver design is investigated for a non-regenerative MIMO relay system with the assumption that the full CSI of the source-relay link is known, while only the CCI of the relay-destination link is available at the relay node. First, the optimal structure of the TH precoding matrix and the source precoding matrix are derived to minimize the MSE of the signal waveform estimation at the destination. Then, an iterative algorithm to optimize the relay precoding matrix is developed. To reduce the computational complexity of the iterative algorithm, a simplified precoding matrices design scheme is proposed. Numerical results show that the proposed precoding matrices design schemes outperform existing algorithms.

The material in Chapter 5 is based on the following journal submission:

- L. Gopal, Y. Rong, and Z. Zang, "Tomlinson-Harashima precoding based transceiver design for MIMO relay systems with channel covariance information", *IEEE Trans. Wireless Commun.*, to appear, 2015.

Chapter 6: Robust Design for Multicasting MIMO Relay Systems

The increasing demand for mobile applications such as streaming media, software updates, and location-based services involving group communications has triggered the need for wireless multicasting technology. The broadcasting nature of the wireless channel makes it naturally suitable for multicasting applications, since a single transmission may be simultaneously received by a number of users. However, wireless channel is subject to signal fading. By exploiting the spatial diversity, multi-antenna techniques can be applied to combat channel fading [7]. Hence, in this chapter, the transceiver design is investigated for non-regenerative multicasting MIMO relay systems, where one transmitter broadcasts common message to multiple receivers with the aid of a relay node and it is assumed that the transmitter, relay, and receivers are all equipped with multiple antennas. In the proposed design, it is assumed that the true channel matrices have Gaussian distribution, with the estimated channels as the mean value, and the channel estimation errors follow the well-known Kronecker model. In this chapter, two robust algorithms are proposed, namely suboptimal robust and optimal robust algorithms, to jointly design the transmitter, relay, and receiver matrices to minimize the maximal MSE of the signal waveform estimation among all receivers. In particular, it is proved that the MSE at each receiver can be decomposed into the sum of the MSEs of the first-hop and second-hop channels. Based on this MSE decomposition, transceiver design algorithms are developed with low computational complexity. Numerical simulations demonstrate the improved robustness of the proposed transceiver design algorithms against the mismatch between the true and estimated channels.

Chapter 6 is based on the following journal submission:

- L. Gopal, Y. Rong, and Z. Zang, "Robust MMSE transceiver design for nonregenerative multicasting MIMO relay systems", *IEEE Trans. Signal Process.*, revised and resubmitted, May. 2015.

and conference submission:

- L. Gopal, Y. Rong, and Z. Zang, "Simplified robust design for nonrenerative multicasting MIMO relay systems", in *Proc. 22nd Int. Conf. Telecommun.*, Sydney, Australia, Apr. 27-29, 2015.

1.5 Notations

The notations used in this thesis are as follows: Lower case letters are used to denote scalars, e.g. s, n. Bold face lower case letters denote vectors, e.g. $\mathbf{s}$, $\mathbf{n}$. Bold face upper case letters are reserved for matrices, e.g. $\mathbf{S}$, $\mathbf{N}$. For matrices, $(\cdot)^T, (\cdot)^*, (\cdot)^H, (\cdot)^{-1}$, and $(\cdot)^\dagger$ denote transpose, conjugate, Hermitian transpose, inverse, and pseudo-inverse operations, respectively. $\text{rank}(\cdot)$ and $\text{tr}(\cdot)$ denote the rank and trace of matrices, respectively. $\otimes$ denotes the matrix kronecker product. $\text{E}[\cdot]$ represents the statistical expectation. An N dimensional identity matrix is denoted as either $\mathbf{I}_N$ or $\mathbf{I}$. Note that the scope of any variable in each chapter is limited to that particular chapter.

Chapter 2

MIMO Relay Design with Covariance Feedback

In this chapter, the transceiver design in a non-regenerative MIMO relay system is addressed by deriving the optimal structure of the relay precoding matrix. Linear signal processing is applied at the relay and destination nodes to minimize the MSE of the estimated signal waveform. The optimal structure of the relay precoding matrix is derived with the assumption that the CCI of the relay-destination link and the full CSI of the source-relay link are known at the relay node. Following, a review of previous contribution available in the literature is presented in Section 2.1, system model of a two-hop non-regenerative MIMO relay system is introduced in Section 2.2. The MIMO relay precoder design algorithm is proposed in Section 2.3. Simulation results are presented in Section 2.4 to justify the significance of the proposed algorithms before summarizing the chapter in Section 2.5.

2.1 Overview of Existing Techniques

Wireless relaying is essential to provide reliable, cost effective and wide-area coverage for wireless networks in a variety of applications. In a cellular environment, a relay can be deployed in areas where there are strong shadowing effects, such as inside the buildings and tunnels. For mobile ad-hoc networks, relaying is essential not only to overcome shadowing due to obstacles but also to reduce transmission power from source to neighbouring nodes. For tactical applications, dynamic deployment of relays is useful

to enhance the network reliability, throughput, and minimize interception by unwanted users.

There are two types of relay strategies: non-regenerative scheme and regenerative scheme [17–19, 50]. Compared with the regenerative scheme, the non-regenerative scheme is easy to implement, and thus is embraced by industry.

A relay precoding scheme in non-regenerative MIMO relaying has been proposed to increase the capacity between the source and destination with further signal processing [21, 22, 51–54]. In this scheme, the relay multiplies the received signal by a linear precoding matrix and retransmits the precoded signal to the destination. The precoding matrix is designed by minimizing the MSE of the estimated signal waveform at the destination node [23–25, 55–57]. An optimal precoding matrix based on the maximum SNR criterion is developed in [24, 55]. A unified framework is developed to jointly optimize the source precoding matrix and the relay amplifying matrix for a broad class of objective functions [25]. The full CSI for entire link is assumed to be available at the relay node [23–25, 55–57].

In a practical system with a limited feedback rate, the assumption that the full CSI for the relay-destination link is known at the relay node is not feasible, especially in the situation when the mobile node is moving rapidly. The covariance matrix is more stable than the instantaneous channel matrix because the scattering environment changes more slowly compared to the mobile location. The precoding matrix is derived for maximizing the ergodic capacity when only the partial CSI for the relay-destination link is available at the relay node in [29–31, 58]. A covariance feedback based MMSE estimator is proposed in [33] and the estimator is only suitable for a MIMO relay system, where the number of antennas at the destination is greater than the relay antennas.

In this chapter, optimal precoder design is proposed to minimize the MSE of the estimated signal in a non-regenerative MIMO relay system, when the covariance information for the relay-destination link is available at the relay. It is assumed that the full CSI of the source-relay link and CCI of the relay destination link are known at the relay node. By restraining power consumption at the relay node, the optimal precoding matrix is derived to minimize the MSE of the estimated signal at the destination node. The proposed algorithm is not constrained by the number of antennas at the destination as in [33]. Simulation results presented in Section 2.4 show the effectiveness of the proposed MSE scheme.

2.2 MIMO Relay System Model without Direct Link

In this section, the non-regenerative MIMO relay system is considered as shown in Fig. 2.1, where the source, relay and destination nodes have N_S, N_R and N_D antennas, respectively. In this system model, it is assumed that there is no direct link exist between the source and destination nodes due to long distance between these two nodes. The

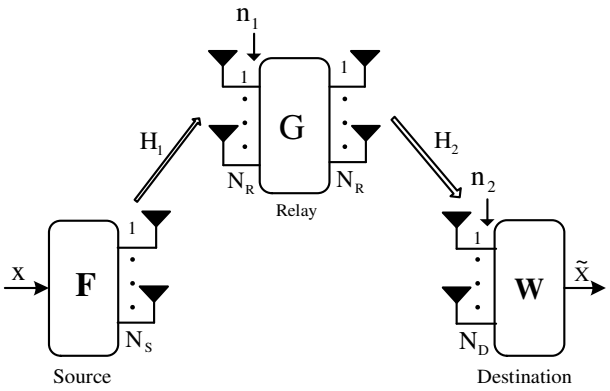

Figure 2.1: Block diagram of linear non-regenerative MIMO relay communication system without direct link.

data transmission takes place over two time slots. The received signal at the relay node during the first time slot is given by

$$\mathbf{y}_1 = \mathbf{H}_1\mathbf{F}\mathbf{x} + \mathbf{n}_1 \tag{2.1}$$

where $\mathbf{F} \in \mathbb{C}^{N_S \times N_S}$ is a precoding matrix of the source node, $\mathbf{H}_1 \in \mathbb{C}^{N_R \times N_S}$ is the channel matrix of the source-relay link, $\mathbf{x} \in \mathbb{C}^{N_S \times 1}$ is the transmitted vector with covariance matrix $E\{\mathbf{x}\mathbf{x}^H\} = \sigma_x^2\mathbf{I}_{N_S}$, $\mathbf{n}_1 \in \mathbb{C}^{N_R \times 1}$ is the circularly symmetric complex Gaussian noise vector with zero mean and covariance matrix $E\{\mathbf{n}_1\mathbf{n}_1^H\} = \sigma_1^2\mathbf{I}_{N_R}$. The received signal at the destination node during the second time slot is given by

$$\mathbf{y}_2 = \mathbf{H}_2\mathbf{G}\mathbf{H}_1\mathbf{F}\mathbf{x} + \mathbf{H}_2\mathbf{G}\mathbf{n}_1 + \mathbf{n}_2 \tag{2.2}$$

where $\mathbf{H}_2 \in \mathbb{C}^{N_D \times N_R}$ is the channel matrix of the relay-destination link, $\mathbf{G} \in \mathbb{C}^{N_R \times N_R}$ is a precoding matrix of the relay, $\mathbf{n}_2 \in \mathbb{C}^{N_D \times 1}$ is the circularly symmetric complex Gaussian noise vector with zero mean and covariance matrix $E\{\mathbf{n}_2\mathbf{n}_2^H\} = \sigma_2^2\mathbf{I}_{N_D}$. The combined channel and noise matrices can be introduced

$$\mathbf{H} = \sigma_x\mathbf{H}_2\mathbf{G}\mathbf{H}_1 \tag{2.3}$$

and

$$\mathbf{n} = \mathbf{H}_2\mathbf{G}\mathbf{n}_1 + \mathbf{n}_2 \tag{2.4}$$

where $\mathbf{H} \in \mathbb{C}^{N_D \times N_S}$ is the equivalent MIMO channel matrix, and $\mathbf{n} \in \mathbb{C}^{N_D \times 1}$ represents the equivalent noise vector and for simplicity, the source precoding matrix $\mathbf{F}$ is assumed as $\mathbf{F} = \mathbf{I}_{N_S}$. Now (2.2) can be written as

$$\mathbf{y}_2 = \mathbf{H}\mathbf{x} + \mathbf{n}. \tag{2.5}$$

Similar to [30, 31], it is assumed that the channel of the relay-destination link is correlated at the transmit antennas and is uncorrelated at the receive antennas. The model is suitable for an environment where the relay is not influenced by local scatters and the destination is fully surrounded by local scatters [11]. It is assumed that $\mathbf{H}_2$ can be expressed as

$$\mathbf{H}_2 = \mathbf{H}_\omega \mathbf{\Sigma}^{1/2} \tag{2.6}$$

where $\mathbf{H}_\omega$ is an $N_D \times N_R$ Gaussian matrix having independent and identically distributed (i.i.d.) circularly symmetric complex entries with zero mean and unit variance, and $\mathbf{\Sigma}$ is an $N_R \times N_R$ covariance matrix of $\mathbf{H}_2$ at the relay end. To reduce implementation complexity, linear receiver precoder matrix $\mathbf{W}$ is applied at the destination, the estimated signal is given by

$$\tilde{\mathbf{x}} = \mathbf{W}\mathbf{H}\mathbf{x} + \mathbf{W}\mathbf{n}. \tag{2.7}$$

It is assumed that the average power used by the source is upper bounded by P_s, and the average power used by the relay is upper bounded by P_r. Since the transmitted signal from the relay is $\mathbf{G}\mathbf{y}_1 = \mathbf{G}\mathbf{H}_1\mathbf{x} + \mathbf{G}\mathbf{n}_1$, the power constraint on the relay can be expressed as

$$p(\mathbf{G}) = tr\Big\{\mathbf{G}(\sigma_x^2\mathbf{H}_1\mathbf{H}_1^H + \sigma_1^2\mathbf{I}_{N_R})\mathbf{G}^H\Big\} \leq P_r. \tag{2.8}$$

Our goal is to design $\mathbf{G}$ and $\mathbf{W}$ so as to obtain the estimated signal which minimizes the following MSE function subject to the power constraint (2.8).

$$J(\mathbf{G}, \mathbf{W}) = tr\Big\{E\Big[(\tilde{\mathbf{x}} - \mathbf{x})(\tilde{\mathbf{x}} - \mathbf{x})^H\Big]\Big\} \tag{2.9}$$

Mathematically, this problem can be formulated as

$$\begin{aligned} (\mathbf{G}, \mathbf{W}) &= \arg\min_{(\mathbf{G},\mathbf{W})} J(\mathbf{G}, \mathbf{W}), \\ s.t.\ p(\mathbf{G}) &\leq P_r. \end{aligned} \tag{2.10}$$

After substituting (2.7) into (2.9), the MSE function (2.9) is simplified to

$$J(\mathbf{G},\mathbf{W})=tr\Big\{\sigma_x^2\Big(\mathbf{WH}-\mathbf{I}_{N_S}\Big)\Big(\mathbf{WH}-\mathbf{I}_{N_S}\Big)^H+\mathbf{WR}_n\mathbf{W}^H\Big\} \tag{2.11}$$

where $\mathbf{R}_n$ is the equivalent noise covariance matrix, given by

$$\begin{aligned}\mathbf{R}_n&=E\Big[\mathbf{n}\mathbf{n}^H\Big]\\&=E\Big[\big(\mathbf{H}_2\mathbf{G}\mathbf{n}_1+\mathbf{n}_2\big)\big(\mathbf{H}_2\mathbf{G}\mathbf{n}_1+\mathbf{n}_2\big)^H\Big]\\&=\sigma_1^2\mathbf{H}_2\mathbf{G}\mathbf{G}^H\mathbf{H}_2^H+\sigma_2^2\mathbf{I}_{N_D}.\end{aligned} \tag{2.12}$$

Note that directly solving the constrained optimization problem (2.10) is difficult due to the fact that both the cost function $J(\mathbf{G},\mathbf{W})$ and the power constraint are non-linear function of $\mathbf{G}$ and $\mathbf{W}$. In the following section a suboptimal approach will be used to tackle the constrained non-linear optimization problem. First, the problem will be solved for the optimal linear receiver $\mathbf{W}$ for any given precoding matrix $\mathbf{G}$ which satisfies the power constraint (2.8). Then, the optimal precoding matrix $\mathbf{G}$ will be derived by solving a closely related constrained optimization problem.

2.3 Proposed MIMO Relay Precoder Design

For any given precoding matrix $\mathbf{G}$ which satisfies the power constraint (2.8), the optimal linear receiver $\mathbf{W}$ that minimizes the MSE function $J(\mathbf{G},\mathbf{W})$ is the same as the MMSE (Wiener filter) receiver [59], which is given by

$$\mathbf{W}=\sigma_x^2\mathbf{H}^H(\sigma_x^2\mathbf{H}\mathbf{H}^H+\mathbf{R}_n)^{-1}. \tag{2.13}$$

After substituting (2.13) into (2.11), the MSE function is obtained as

$$J(\mathbf{G})=\sigma_x^2 tr\Big\{\mathbf{I}_{N_S}-\sigma_x^2\mathbf{H}^H(\sigma_x^2\mathbf{H}\mathbf{H}^H+\mathbf{R}_n)^{-1}\mathbf{H}\Big\}. \tag{2.14}$$

Using the following matrix inversion lemma [60]

$$(\mathbf{A}+\mathbf{BCD})^{-1}=\mathbf{A}^{-1}-\mathbf{A}^{-1}\mathbf{B}(\mathbf{D}\mathbf{A}^{-1}\mathbf{B}+\mathbf{C}^{-1})^{-1}\mathbf{D}\mathbf{A}^{-1}, \tag{2.15}$$

the MSE function (2.14) can be written as

$$J(\mathbf{G})=\sigma_x^2 tr\Big\{\Big[\mathbf{I}_{N_S}+\sigma_x^2\mathbf{H}^H\mathbf{R}_n^{-1}\mathbf{H}\Big]^{-1}\Big\}. \tag{2.16}$$

Substituting (2.3) and (2.12) into (2.16), the MSE function can be expressed as

$$J(\mathbf{G})=\sigma_x^2 tr\Big\{\Big[\mathbf{I}_{N_S}+\sigma_x^2\mathbf{H}_1^H\mathbf{G}^H\mathbf{H}_2^H \times\Big(\sigma_1^2\mathbf{H}_2\mathbf{G}\mathbf{G}^H\mathbf{H}_2^H+\sigma_2^2\mathbf{I}_{N_D}\Big)^{-1}\mathbf{H}_2\mathbf{G}\mathbf{H}_1\Big]^{-1}\Big\}. \tag{2.17}$$

Now the problem is reduced to find the optimal $\mathbf{G}$ that minimize $J(\mathbf{G})$ subject to the power constraint (2.8). The singular value decomposition (SVD) of $\mathbf{H}_1$ can be introduced as

$$\mathbf{H}_1=\mathbf{U}_1\mathbf{\Lambda}_1^{1/2}\mathbf{V}_1^H \tag{2.18}$$

where $\mathbf{\Lambda}_1=\text{diag}\{\Lambda_{1,1}\cdots\Lambda_{1,N_R}\}$ is a diagonal matrix with $\Lambda_{1,1}\geq\cdots\geq\Lambda_{1,N_R}$. The eigenvalue decomposition of $\mathbf{\Sigma}$ can be introduced as $\mathbf{\Sigma}=\mathbf{V}_\Sigma\mathbf{\Lambda}_\Sigma\mathbf{V}_\Sigma^H$ where $\mathbf{\Lambda}_\Sigma=\text{diag}\{\Lambda_{\Sigma,1}\cdots\Lambda_{\Sigma,N_R}\}$ with $\Lambda_{\Sigma,1}\geq\cdots\geq\Lambda_{\Sigma,N_R}$. The columns of $\mathbf{V}_\Sigma$ are the right eigenvectors of $\mathbf{\Sigma}$ for the corresponding eigenvalues. Then $\mathbf{H}_2$ can be rewritten as

$$\mathbf{H}_2=\mathbf{Z}\mathbf{\Lambda}_\Sigma^{1/2}\mathbf{V}_\Sigma^H \tag{2.19}$$

where $\mathbf{Z}\triangleq\mathbf{H}_2\mathbf{V}_\Sigma\mathbf{\Lambda}_\Sigma^{-1/2}$. Then $\mathbf{Z}$ has the same distribution as $\mathbf{H}_w$ because $\mathbf{H}_2\mathbf{V}_\Sigma\mathbf{\Lambda}_\Sigma^{-1/2}=\mathbf{H}_\omega\mathbf{V}_\Sigma$. The optimal precoding matrix $\mathbf{G}$ which minimizes (2.17) can be expressed as

$$\mathbf{G}=\mathbf{V}_\Sigma\mathbf{\Lambda}_G^{1/2}\mathbf{U}_1^H \tag{2.20}$$

where $\mathbf{\Lambda}_G=\text{diag}\{\Lambda_{G,1}\cdots\Lambda_{G,N_R}\}$. Using the matrix inversion lemma (2.15), the MSE function (2.17) can be written as

$$J(\mathbf{G})=\sigma_x^2 tr\Big\{\Big[\mathbf{I}_{N_S}+\frac{\sigma_x^2}{\sigma_1^2}\mathbf{H}_1^H\Big[\mathbf{I}_{N_R} -\Big(\mathbf{I}_{N_R}+\frac{\sigma_1^2}{\sigma_2^2}\mathbf{G}^H\mathbf{H}_2^H\mathbf{H}_2\mathbf{G}\Big)^{-1}\Big]\mathbf{H}_1\Big]^{-1}\Big\}. \tag{2.21}$$

Substituting (2.18)-(2.20) in (2.21), now the MSE function is given by

$$J(\mathbf{\Lambda_G})=\sigma_x^2 tr\Big\{\Big[\mathbf{I}_{N_S}+\frac{\sigma_x^2}{\sigma_1^2}\mathbf{V}_1\mathbf{\Lambda}_1^{1/2}\mathbf{U}_1^H \times\Big[\mathbf{I}_{N_R}-\mathbf{D}_1\Big]\mathbf{U}_1\mathbf{\Lambda}_1^{1/2}\mathbf{V}_1^H\Big]^{-1}\Big\} \tag{2.22}$$

where

$$\mathbf{D}_1=\Big(\mathbf{I}_{N_R}+\frac{\sigma_1^2}{\sigma_2^2}\mathbf{U}_1\mathbf{\Lambda}_G^{1/2}\mathbf{\Lambda}_\Sigma^{1/2}\mathbf{Z}^H\mathbf{Z}\mathbf{\Lambda}_\Sigma^{1/2}\mathbf{\Lambda}_G^{1/2}\mathbf{U}_1^H\Big)^{-1}.$$

Using the SVD and trace properties, the MSE function (2.22) can be simplified to

$$J(\mathbf{\Lambda_G})=\sigma_x^2 tr\Big\{\Big[\mathbf{I}_{N_S}+\frac{\sigma_x^2}{\sigma_1^2}\Big(\mathbf{\Lambda}_1-\mathbf{\Lambda}_1^{1/2}\mathbf{D}_2\mathbf{\Lambda}_1^{1/2}\Big)\Big]^{-1}\Big\}$$
$$=\sigma_x^2\sigma_1^2 tr\Big\{\Big[\sigma_1^2\mathbf{I}_{N_S}+\sigma_x^2\Big(\mathbf{\Lambda}_1-\mathbf{\Lambda}_1^{1/2}\mathbf{D}_2\mathbf{\Lambda}_1^{1/2}\Big)\Big]^{-1}\Big\} \tag{2.23}$$

where

$$\mathbf{D}_2=\Big(\mathbf{I}_{N_R}+\frac{\sigma_1^2}{\sigma_2^2}\mathbf{\Lambda}_G^{1/2}\mathbf{\Lambda}_\Sigma^{1/2}\mathbf{Z}^H\mathbf{Z}\mathbf{\Lambda}_\Sigma^{1/2}\mathbf{\Lambda}_G^{1/2}\Big)^{-1}.$$

It can be seen from (2.23) that $J(\mathbf{\Lambda_G})$ depends on $\mathbf{Z}$, which is random and unknown. In the following, $E_{\mathbf{Z}}[J(\mathbf{\Lambda_G})]$ is optimized, where $E_{\mathbf{Z}}[.]$ indicates that the expectation is taken with respect to the random matrix $\mathbf{Z}$. Now $E_{\mathbf{Z}}[J(\mathbf{\Lambda_G})]$ can be expressed as

$$E_{\mathbf{Z}}[J(\mathbf{\Lambda_G})]=\sigma_x^2\sigma_1^2 E_{\mathbf{Z}}\Big[tr\Big\{\Big[\sigma_1^2\mathbf{I}_{N_S}+\sigma_x^2$$
$$\times\Big(\mathbf{\Lambda}_1-\mathbf{\Lambda}_1^{1/2}\mathbf{D}_2\mathbf{\Lambda}_1^{1/2}\Big)\Big]^{-1}\Big\}\Big] \tag{2.24}$$

where

$$\mathbf{D}_2=\Big(\mathbf{I}_{N_R}+\frac{\sigma_1^2}{\sigma_2^2}\mathbf{\Lambda}_G^{1/2}\mathbf{\Lambda}_\Sigma^{1/2}\mathbf{Z}^H\mathbf{Z}\mathbf{\Lambda}_\Sigma^{1/2}\mathbf{\Lambda}_G^{1/2}\Big)^{-1}.$$

Now the work is left to determine the diagonal elements $\mathbf{\Lambda}_G$ of precoder matrix $\mathbf{G}$. The optimal precoder allocates power according to the eigenmodes of $\mathbf{H}_1\mathbf{H}_1^H$ and $\mathbf{\Sigma}$.

Direct minimization of (2.24) for the optimal power allocation is difficult. In the following, the lower bound of the MSE is used together with the power constraint (2.8) to derive the suboptimal power allocation for the precoder matrix $\mathbf{G}$. Assume that the MSE function is convex in $\mathbf{Z}^H\mathbf{Z}$ and has the following lower bound using Jensen's inequality

$$J_L(\mathbf{\Lambda_G})=\sigma_x^2\sigma_1^2 tr\Big\{\Big[\sigma_1^2\mathbf{I}_{N_S}+\sigma_x^2\mathbf{\Lambda}_1-\sigma_x^2\mathbf{\Lambda}_1^{1/2}\mathbf{D}_3\mathbf{\Lambda}_1^{1/2}\Big]^{-1}\Big\} \tag{2.25}$$

where

$$\mathbf{D}_3=\Big(\mathbf{I}_{N_R}+\frac{\sigma_1^2}{\sigma_2^2}\mathbf{\Lambda}_G^{1/2}\mathbf{\Lambda}_\Sigma^{1/2}E_{\mathbf{Z}}[\mathbf{Z}^H\mathbf{Z}]\mathbf{\Lambda}_\Sigma^{1/2}\mathbf{\Lambda}_G^{1/2}\Big)^{-1}.$$

Now the MSE function 2.25 is simplified to

$$J_L(\mathbf{\Lambda_G})=\sigma_x^2\sigma_1^2 tr\Big\{\Big[\sigma_1^2\mathbf{I}_{N_S}+\sigma_x^2\mathbf{\Lambda}_1$$
$$-\sigma_x^2\mathbf{\Lambda}_1\Big(\mathbf{I}_{N_R}+\frac{\sigma_1^2}{\sigma_2^2}\mathbf{\Lambda}_G\mathbf{\Lambda}_\Sigma N_D\Big)^{-1}\Big]^{-1}\Big\} \tag{2.26}$$

where $E_{\mathbf{Z}}(\mathbf{Z}^H\mathbf{Z})=N_D\mathbf{I}_{N_R}$. Inserting (2.18) and (2.20) into (2.8), the power constraint for the relay node can be expressed as

$$p(\mathbf{\Lambda_G})=tr\Big\{\mathbf{V}_\Sigma\mathbf{\Lambda}_G^{1/2}\mathbf{U}_1^H\Big(\sigma_x^2\mathbf{U}_1\mathbf{\Lambda}_1\mathbf{U}_1^H+\sigma_1^2\mathbf{I}_{N_R}\Big)$$
$$\times\mathbf{U}_1\mathbf{\Lambda}_G^{1/2}\mathbf{V}_\Sigma^H\Big\}\leq P_r. \tag{2.27}$$

Using the SVD and trace properties, the power constraint (2.27) can be simplified to

$$p(\mathbf{\Lambda_G}) = tr\Big\{\big(\sigma_x^2\mathbf{\Lambda}_1 + \sigma_1^2\mathbf{I}_{N_R}\big)\mathbf{\Lambda}_G\Big\} \leq P_r. \tag{2.28}$$

From (2.26) and (2.28), the constrained optimization problem can be expressed as

$$\min_{\{\Lambda_{G,i}\}} \ \sigma_x^2 \sum_{i=1}^{N_S} \frac{\sigma_1^2 N_D \Lambda_{\Sigma,i}\Lambda_{G,i} + \sigma_2^2}{(\sigma_x^2\Lambda_{1,i} + \sigma_1^2)N_D\Lambda_{\Sigma,i}\Lambda_{G,i} + \sigma_2^2} \tag{2.29}$$

$$s.t. \sum_{i=1}^{N_S}(\sigma_x^2\Lambda_{1,i} + \sigma_1^2)\Lambda_{G,i} \leq P_r. \tag{2.30}$$

Using the Karush-Kuhn-Tucker(KKT) conditions [61], the optimal diagonal elements of $\Lambda_{G,i}$ are obtained as

$$\Lambda_{G,i} = \frac{1}{(\sigma_x^2\Lambda_{1,i} + \sigma_1^2)N_D\Lambda_{\Sigma,i}}\left(\sqrt{\frac{\sigma_x^2\sigma_2^2 N_D\Lambda_{1,i}\Lambda_{\Sigma,i}}{\mu(\sigma_x^2\Lambda_{1,i} + \sigma_1^2)}} - \sigma_2^2\right)^+ \tag{2.31}$$

where $(x)^+ = \max(x, 0)$, and μ should be chosen to meet the power constraint (2.30). Inserting (2.31) and (2.18)-(2.20) into (2.13) leads to obtain the optimal receiver matrix $\mathbf{W}$.

2.4 Numerical Examples

In this section, the performance of the proposed algorithm is presented by numerical examples. The channel matrices $\mathbf{H}_1$ and $\mathbf{H}_\omega$ are generated as complex Gaussian variables with zero mean and unit variance. The symbols are generated from QPSK constellation.

The elements of covariance matrix $\mathbf{\Sigma}$ of $\mathbf{H}_2$ are generated by $\Sigma_{i,j} = J_0(\triangle\pi|i-j|)$ [11], where $J_0(.)$ is the zeroth order Bessel function of the first kind, $\triangle$ the angle of fading spread. The SNRs for the source-relay and relay-destination links are defined as $\text{SNR}_1 = \frac{\sigma_x^2}{\sigma_1^2}$, $\text{SNR}_2 = \frac{P_r}{N_R\sigma_2^2}$.

The performance of the proposed joint MMSE covariance (JMMSE-COV) algorithm is compared with that of the full CSI algorithm [23], the MMSE-COV algorithm [33], pseudo match-and-forward (PMF) algorithm [22] and the traditional amplify-and-forward (AF) algorithm. The full CSI algorithm, also known as JMMSE [23] provides the lower-bound of the proposed algorithm. In the conventional AF algorithm, the relay precoder is obtained by $\mathbf{G} = \alpha\mathbf{I}_{N_R}$, where α is determined to meet the power constraint (2.30).

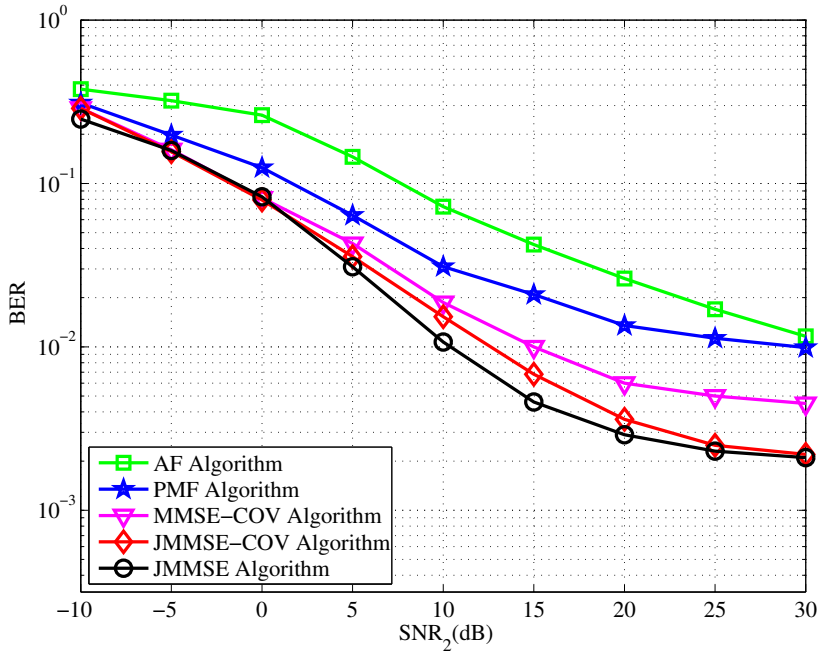

Figure 2.2: BER versus SNR_2 while fixing $\mathrm{SNR}_1 = 20\mathrm{dB}$, $\triangle = 5^o$, $N_S = N_R = N_D$=4.

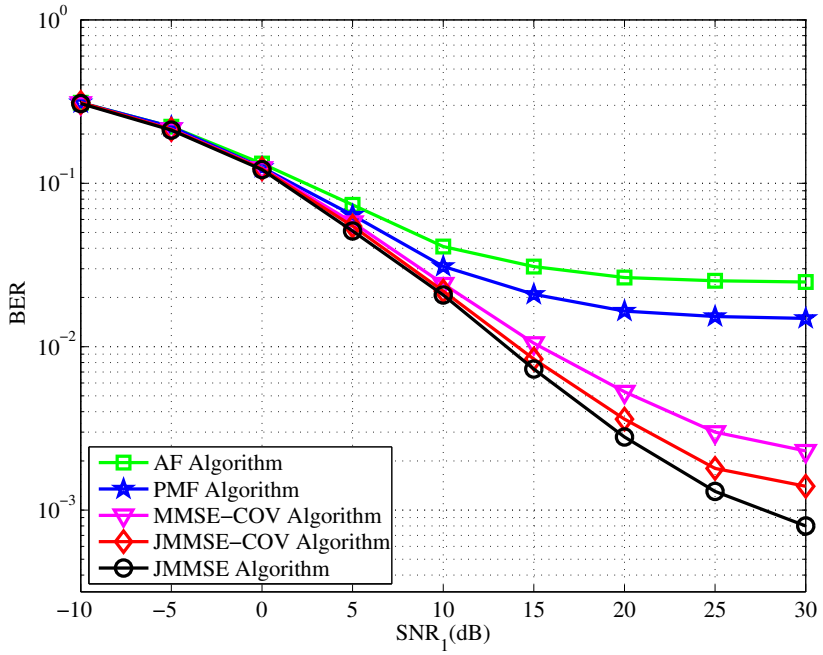

Figure 2.3: BER versus SNR_1 while fixing $\mathrm{SNR}_2 = 20\mathrm{dB}$, $\triangle = 5^o$, $N_S = N_R = N_D$=4.

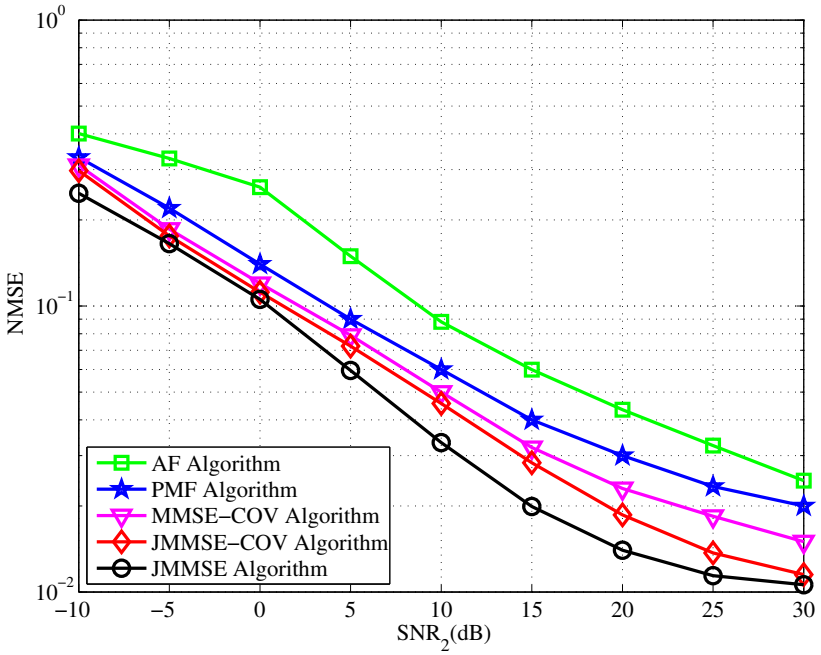

Figure 2.4: NMSE versus SNR_2 while fixing $\mathrm{SNR}_1 = 20\mathrm{dB}$, $\triangle = 5^o$, $N_S = N_R = N_D$=4.

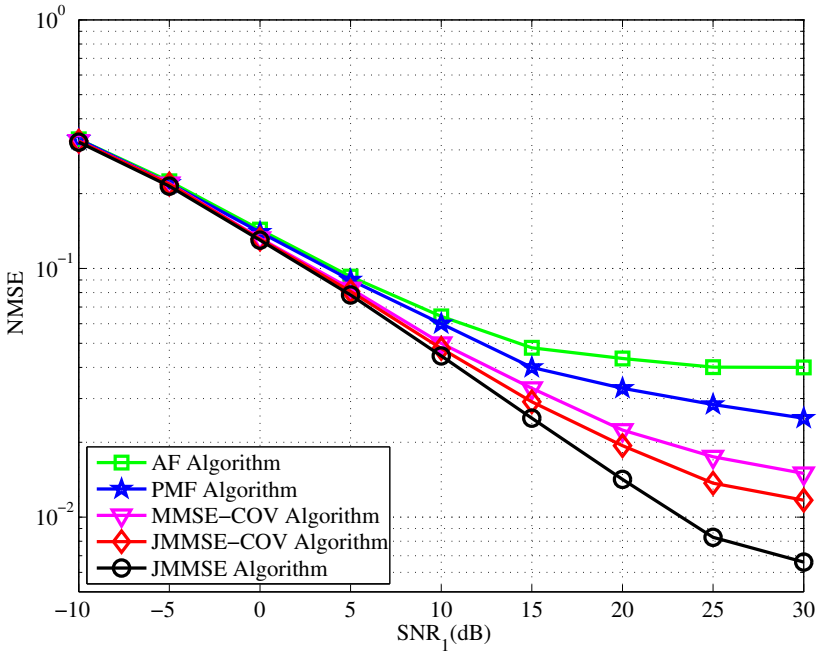

Figure 2.5: NMSE versus SNR_1 while fixing $\mathrm{SNR}_2 = 20\mathrm{dB}$, $\triangle = 5^o$, $N_S = N_R = N_D$=4.

In the first example, the performance of the MSE algorithms is studied in terms of BER versus SNR_2 while fixing SNR_1 = 20dB and the number of antennas at the source, relay and destination nodes are fixed as $N_S = N_R = N_D$=4. The angle spread is considered as $\triangle = 5^o$. The simulation result is averaged over 1000 independent channel realization. It can be seen in Fig. 2.2 that the proposed JMMSE-COV algorithm shows better BER performance over all range of SNR_2 than the MMSE-COV, PMF and AF algorithms. For high SNR_2, the BER performance of the proposed MSE algorithm is closer to the JMMSE algorithm.

In the second example, the BER performance is compared for various SNR_1 while fixing SNR_2= 20dB and similar to [33], the MIMO relay system is simulated with $N_S = N_R = N_D$ =4. In this example, the angle spread is fixed as $\triangle = 5^o$. Randomly generated 1000 QPSK constellations are transmitted from the source node for each channel realization. It can be noticed from the Fig. 2.3 that the proposed JMSE-COV algorithm performance is similar to the MMSE-COV, PMF and AF algorithms in low SNR_1 (e.g. $\text{SNR}_1 < 5$dB) because the received signal at the relay is impaired by the noise. For high SNR_1, the proposed algorithm shows better BER performance than the MMSE-COV algorithm, PMF algorithm and the conventional AF algorithm. In other words, the proposed algorithm outperforms the MMSE-COV, PMF and AF algorithms.

In the third example, the normalized MSE (NMSE) performance of the proposed algorithm is compared for various SNR_2 while fixing SNR_1 = 20dB. In the example, the angle spread is set as $\triangle = 5^o$ and $N_S = N_R = N_D$ =4. In this example, 1000 QPSK samples are randomly generated at source node for each channel realization. From Fig. 2.4, it can be concluded that AF and PMF algorithms produce much higher MSE as compared to the proposed JMMSE-COV algorithm even at high SNR_2. It is clearly shown in Fig. 2.4 that the proposed JMMSE-COV algorithm offers improved performance in terms of NMSE compared to the MMSE-COV algorithm.

In the final example, the NMSE performance of the proposed algorithm is compared for varying SNR_1 while fixing SNR_2 = 20dB. In the example as shown in Fig. 2.5, the angle of delay spread is set as $\triangle = 5^o$ and source, relay and destination nodes antennas are fixed as $N_S = N_R = N_D$ =4. In this example, 1000 QPSK samples are randomly generated at source node for each channel realization. From Fig. 2.5, it can be seen that AF and PMF algorithms have much higher NMSE as compared to the proposed JMMSE-COV algorithm at high SNR_1. It can be noticed from the Fig. 2.5 that the

proposed JMMSE-COV algorithm outperforms the MMSE-COV algorithm in terms of NMSE.

2.5 Chapter Summary

In this chapter, the optimal structure of the non-regenerative MIMO relay matrix is derived to minimize the MSE of the symbol estimation at the destination node with the assumption that the covariance feedback of the relay-destination link is available at the relay node. It is assumed that the relay knows the full CSI of the source-relay link. Simulation results show that the derived optimal solution which minimize the upper-bound of the MSE is achieved and the simulation results demonstrate that the proposed scheme has better performance in terms of NMSE and BER as compared to the conventional MSE schemes.

Chapter 3

MIMO Relay Design with Covariance Feedback and Direct Link

In this chapter, transceiver design schemes are proposed for non-regenerative MIMO relay system with direct link which minimizes the MSE of the signal waveform estimation at the destination node. In the proposed design schemes, an optimal precoding matrix is derived with the assumption that the full CSI of the source-relay link and partial CSI such as CCI of the relay-destination link are available at the relay node. In practical cases, if the destination node is closer to the source node, the source-destination link cannot be ignored. Hence, in the proposed design, it is assumed that the relay knows the partial CSI of the source-destination link. An overview of the existing techniques is provided in Section 3.1. In Section 3.2, the system model of the proposed precoding matrix design is introduced for a non-regenerative MIMO relay system with direct link. In Section 3.3, two non-regenerative MIMO relay precoder design schemes, such as iterative optimal covariance algorithm and suboptimal covariance algorithm are developed to achieve the minimum MSE of the signal estimation at the destination node. The performance of the proposed MIMO relay design schemes is demonstrated through numerical simulations in Section 3.4. Finally, the chapter is summarized in Section 3.5.

3.1 Overview of Existing Techniques

Recently, cooperative wireless communications attract much research interest. By deploying a wireless relay in cooperative wireless communications, wireless networks coverage area can be extended and reliable and cost effective wireless network applications can be provided. In cooperative wireless communications, a relay can be deployed inside a building or tunnel to mitigate the effects of shadowing [50].

Two types of relaying schemes, regenerative and non-regenerative , have been proposed in [17, 19, 50]. In regenerative strategy, the relay decodes the information received from source and forwards the re-encoded signal to the destination. Whereas in non-regenerative strategy, the relay amplifies the received signal from source and retransmits the signal to the destination. When compared with the regenerative strategy, the non-regenerative strategy has a lower computational complexity and is easy to implement in the cooperative environment.

Relay precoding algorithms [21, 22, 51–54] for non-regenerative MIMO relay systems have been developed to maximize the capacity of the source-destination link. In these algorithms, a precoding matrix is multiplied with the received signal at the relay node for further signal processing. A precoding matrix is proposed to minimize the receiver estimation error which is known as MSE of the signal at the destination node [23–26, 55–57, 62]. The optimal precoding matrix design is investigated well in [26–28, 62–64] for non-regenerative MIMO relay system with the assumption that the relay knows the full CSI of the source-relay, source-destination and relay-destination links.

In practice, the environment is mostly surrounded by scatters and shadowing effects. Due to the scattered and shadowing environments, the received signal is uncorrelated at the destination. Hence, the full CSI of the relay-destination link and the source-destination link is difficult to obtain at the relay node. For this model, the channel covariance matrix is more suitable than the instantaneous channel matrix.

Optimal precoder is designed for maximizing the ergodic capacity of the non-regenerative MIMO relay system with the assumption that the CCI of the relay-destination link is available at the relay node [29–31, 58]. MMSE based estimators are investigated in [32, 33] with the assumption that the CCI of the relay-destination link is known at the relay node. However, the optimal precoding matrix with the direct link is not investigated in [32, 33]. In practice, the source-destination link provides valuable spatial diversity to the non-regenerative MIMO relay system and can be advantageously exploited.

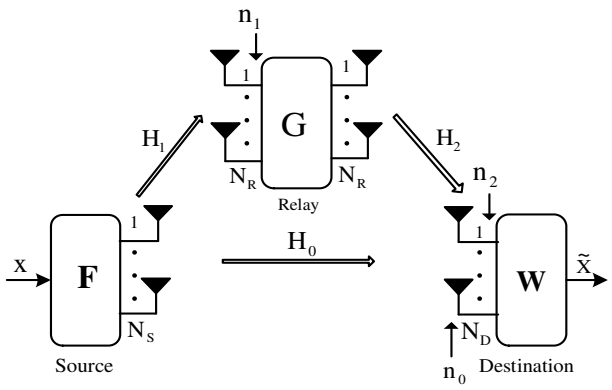

Figure 3.1: Block diagram of non-regenerative MIMO relay communication system with direct link.

In this chapter, an iterative optimal covariance algorithm is proposed to minimize the MSE of the signal estimation at the destination in a non-regenerative MIMO relay system with direct link. Considering that the computational complexity of the developed optimal covariance algorithm may be high for practical implementation of the relay system, a suboptimal covariance algorithm is proposed. In the proposed two algorithms, it is assumed that the relay knows the full CSI of the source-relay link, the CCI of the relay-destination link and the direct source-destination link. Simulation results verify the performance of the proposed optimal and suboptimal covariance based MSE algorithms.

3.2 MIMO Relay System Model with Direct Link

A typical three node non-regenerative MIMO relay system is considered as shown in Fig. 3.1. It is assumed that the source and destination nodes have N_S and N_D antennas, respectively, and relay node has N_R antennas. In the considered MIMO relay system model, it is assumed that there is a direct link between the source and destination nodes. The signal transmission between the source and destination node is completed in two time slots. During the first time slot, the source transmits $\mathbf{x}$. The received signal at the destination and the relay during the first time slot is given by

$$\begin{aligned} \mathbf{y}_0 &= \mathbf{H}_0\mathbf{F}\mathbf{x} + \mathbf{n}_0 \\ \mathbf{y}_1 &= \mathbf{H}_1\mathbf{F}\mathbf{x} + \mathbf{n}_1 \end{aligned} \tag{3.1}$$

where $\mathbf{F} \in \mathbb{C}^{N_S \times N_S}$ is a precoding matrix of the source node, $\mathbf{H}_0 \in \mathbb{C}^{N_D \times N_S}$ is the channel matrix of the direct source-destination link, $\mathbf{x} \in \mathbb{C}^{N_S \times 1}$ is the transmitted vector with covariance matrix $E\{\mathbf{x}\mathbf{x}^H\} = \sigma_x^2 \mathbf{I}_{N_S}$, $\mathbf{n}_0 \in \mathbb{C}^{N_D \times 1}$ is the circularly symmetric complex Gaussian noise vector with zero mean and unit variance matrix, $\mathbf{H}_1 \in \mathbb{C}^{N_R \times N_S}$ is the channel matrix of the source-relay link, $\mathbf{n}_1 \in \mathbb{C}^{N_R \times 1}$ is the circularly symmetric complex Gaussian noise vector with zero mean and covariance matrix $E\{\mathbf{n}_1 \mathbf{n}_1^H\} = \sigma_1^2 \mathbf{I}_{N_R}$. The received signal at the destination in the second time slot is given by

$$\mathbf{y}_2 = \mathbf{H}_2 \mathbf{G} \mathbf{H}_1 \mathbf{F} \mathbf{x} + \mathbf{H}_2 \mathbf{G} \mathbf{n}_1 + \mathbf{n}_2 \tag{3.2}$$

where $\mathbf{H}_2 \in \mathbb{C}^{N_D \times N_R}$ is the channel matrix of the relay-destination link, $\mathbf{G} \in \mathbb{C}^{N_R \times N_R}$ is a precoding matrix of the relay node, $\mathbf{n}_2 \in \mathbb{C}^{N_D \times 1}$ is the circularly symmetric complex Gaussian noise vector with zero mean and covariance matrix $E\{\mathbf{n}_2 \mathbf{n}_2^H\} = \sigma_2^2 \mathbf{I}_{N_D}$. In a more compact way, the signal models (3.1) and (3.2) for the non-regenerative MIMO relay system can be written as

$$\begin{aligned} \mathbf{y} &\triangleq \begin{bmatrix} \mathbf{y}_2 \\ \mathbf{y}_0 \end{bmatrix} \\ &= \begin{bmatrix} \mathbf{H}_2 \mathbf{G} \mathbf{H}_1 \\ \mathbf{H}_0 \end{bmatrix} \mathbf{F} \mathbf{x} + \begin{bmatrix} \mathbf{H}_2 \mathbf{G} \mathbf{n}_1 + \mathbf{n}_2 \\ \mathbf{n}_0 \end{bmatrix}. \end{aligned} \tag{3.3}$$

It is assumed that the relay knows the full CSI of the source-relay link and CCI of the relay-destination link and the direct source-destination link. However, the channel information is unavailable at the source node. The combined channel and noise matrices can be introduced as

$$\mathbf{H} \triangleq \begin{bmatrix} \mathbf{H}_2 \mathbf{G} \mathbf{H}_1 \\ \mathbf{H}_0 \end{bmatrix} \tag{3.4}$$

and

$$\mathbf{n} = \begin{bmatrix} \mathbf{H}_2 \mathbf{G} \mathbf{n}_1 + \mathbf{n}_2 \\ \mathbf{n}_0 \end{bmatrix} \tag{3.5}$$

where $\mathbf{H} \in \mathbb{C}^{2N_D \times N_S}$ is the equivalent MIMO channel matrix, $\mathbf{n} \in \mathbb{C}^{2N_D \times 1}$ represents the equivalent noise vector and for simplicity, the source precoding matrix $\mathbf{F}$ is defined as $\mathbf{F} = \mathbf{I}_{N_S}$. Inserting (3.4) and (3.5) into (3.3), the signal model for the non-regenerative MIMO relay system can be written as

$$\mathbf{y} = \mathbf{H}\mathbf{x} + \mathbf{n}. \tag{3.6}$$

Consider a scenario that the destination node is moving rapidly [30, 31], so the channel is correlated at the transmitter and is uncorrelated at the receiver for the relay-destination link and the direct source-destination link. This model is appropriate for

an environment where the destinations is fully surrounded by local scatters [11]. With this assumption, the channel matrices $\mathbf{H}_0$ and $\mathbf{H}_2$ can be modeled as [30–32]

$$\begin{aligned}\mathbf{H}_0 &= \mathbf{H}_{\omega_0}\boldsymbol{\Sigma}_0^{1/2} \\ \mathbf{H}_2 &= \mathbf{H}_{\omega_2}\boldsymbol{\Sigma}_2^{1/2}\end{aligned} \tag{3.7}$$

where $\mathbf{H}_{\omega_0} \in \mathbb{C}^{N_D \times N_S}$ and $\mathbf{H}_{\omega_2} \in \mathbb{C}^{N_D \times N_R}$ are Gaussian matrices having i.i.d. circularly symmetric complex entries, $\boldsymbol{\Sigma}_0$ an $N_S \times N_S$ covariance matrix of $\mathbf{H}_0$ and $\boldsymbol{\Sigma}_2$ an $N_R \times N_R$ covariance matrix of $\mathbf{H}_2$ at the relay side. Here, it is assumed that the destination node feedbacks the two covariances matrices, $\boldsymbol{\Sigma}_0$ and $\boldsymbol{\Sigma}_2$, to the relay node.

A linear receiver precoder matrix $\mathbf{W}$ is applied at the destination to reduce implementation complexity. The estimated signal at the destination node can be written as

$$\tilde{\mathbf{x}} = \mathbf{W}\mathbf{y} = \mathbf{W}\mathbf{H}\mathbf{x} + \mathbf{W}\mathbf{n}. \tag{3.8}$$

Since the transmitted signal from the relay is $\mathbf{G}\mathbf{y}_1 = \mathbf{G}\mathbf{H}_1\mathbf{x} + \mathbf{G}\mathbf{n}_1$, the power constraint on the relay can be expressed as [21]

$$p(\mathbf{G}) = tr\Big\{\mathbf{G}(\sigma_x^2\mathbf{H}_1\mathbf{H}_1^H + \sigma_1^2\mathbf{I}_{N_R})\mathbf{G}^H\Big\} \leq P_r \tag{3.9}$$

where P_r is the upper bounded average power used by the relay. Now, our goal is to obtain $\mathbf{G}$ and $\mathbf{W}$ to minimize the MSE of the estimated signal at the destination node. Using the precoder matrix G and the linear receiver $\mathbf{W}$, the MSE function of the estimated signal can be written as [59]

$$J(\mathbf{G}, \mathbf{W}) = tr\Big\{E\Big[(\tilde{\mathbf{x}} - \mathbf{x})(\tilde{\mathbf{x}} - \mathbf{x})^H\Big]\Big\}. \tag{3.10}$$

Mathematically, the design problem can be formulated as

$$(\mathbf{G}, \mathbf{W}) = \underset{(\mathbf{G},\mathbf{W})}{\arg\min}\, J(\mathbf{G}, \mathbf{W}), \quad \text{s.t. } p(\mathbf{G}) \leq P_r. \tag{3.11}$$

After substituting (3.8) into (3.10), the MSE function (3.10) is simplified to

$$J(\mathbf{G}, \mathbf{W}) = tr\Big\{\sigma_x^2\Big(\mathbf{W}\mathbf{H} - \mathbf{I}_{N_S}\Big)\Big(\mathbf{W}\mathbf{H} - \mathbf{I}_{N_S}\Big)^H + \mathbf{W}\mathbf{R}_n\mathbf{W}^H\Big\} \tag{3.12}$$

where $\mathbf{R}_n$ is the equivalent noise covariance matrix, given by

$$\mathbf{R}_n = E\Big[\mathbf{n}\mathbf{n}^H\Big]. \tag{3.13}$$

Substituting (3.5) into (3.13), the noise covariance matrix $\mathbf{R}_n$ is given by

$$\begin{aligned}\mathbf{R}_n &= E\left[\begin{bmatrix}\mathbf{H}_2\mathbf{G}\mathbf{n}_1+\mathbf{n}_2\\ \mathbf{n}_0\end{bmatrix}\begin{bmatrix}\mathbf{H}_2\mathbf{G}\mathbf{n}_1+\mathbf{n}_2\\ \mathbf{n}_0\end{bmatrix}^H\right]\\ &= \begin{bmatrix}\sigma_1^2\mathbf{H}_2\mathbf{G}\mathbf{G}^H\mathbf{H}_2^H+\sigma_2^2\mathbf{I}_{N_D} & \mathbf{0}_{N_D\times N_D}\\ \mathbf{0}_{N_D\times N_D} & \mathbf{I}_{N_D}\end{bmatrix}.\end{aligned} \tag{3.14}$$

Note that the constrained optimization problem (3.11) is not easy to solve directly due to the fact that the optimization function $J(\mathbf{G},\mathbf{W})$ is a non-linear and non-convex function of $\mathbf{G}$ and $\mathbf{W}$ and the power constraint is non-linear function of $\mathbf{G}$. In the following sections an iterative based optimal covariance algorithm and suboptimal covariance algorithm are proposed to solve the constrained non-linear optimization problem.

3.3 Proposed MIMO Relay Precoder Design

For any given precoding matrix $\mathbf{G}$ which satisfies the power constraint (3.9), the optimal linear receiver $\mathbf{W}$ that minimizes the MSE function $J(\mathbf{G},\mathbf{W})$ is the MMSE (Wiener filter) receiver [59], which is given by

$$\mathbf{W} = \sigma_x^2\mathbf{H}^H(\sigma_x^2\mathbf{H}\mathbf{H}^H+\mathbf{R}_n)^{-1}. \tag{3.15}$$

After substituting (3.15) into (3.12), the MSE function is obtained as

$$J(\mathbf{G}) = \sigma_x^2 tr\Big\{\mathbf{I}_{N_S}-\sigma_x^2\mathbf{H}^H(\sigma_x^2\mathbf{H}\mathbf{H}^H+\mathbf{R}_n)^{-1}\mathbf{H}\Big\}. \tag{3.16}$$

Using the matrix inversion lemma (2.15), the MSE function (3.16) can be written as

$$J(\mathbf{G}) = \sigma_x^2 tr\Big\{\Big[\mathbf{I}_{N_S}+\sigma_x^2\mathbf{H}^H\mathbf{R}_n^{-1}\mathbf{H}\Big]^{-1}\Big\}. \tag{3.17}$$

Substituting (3.4) and (3.14) into (3.17), the MSE function can be expressed as

$$\begin{aligned}J(\mathbf{G}) = \sigma_x^2 tr\Big\{&\big[\mathbf{I}_{N_S}+\sigma_x^2\mathbf{H}_0^H\mathbf{H}_0+\sigma_x^2\mathbf{H}_1^H\mathbf{G}^H\mathbf{H}_2^H\\ &\times\big(\sigma_1^2\mathbf{H}_2\mathbf{G}\mathbf{G}^H\mathbf{H}_2^H+\sigma_2^2\mathbf{I}_{N_D}\big)^{-1}\mathbf{H}_2\mathbf{G}\mathbf{H}_1\big]^{-1}\Big\}.\end{aligned} \tag{3.18}$$

Using the matrix inversion lemma (2.15), the MSE function (3.18) can be written as

$$\begin{aligned}J(\mathbf{G}) = \sigma_x^2 tr\Big\{&\Big[\mathbf{I}_{N_S}+\sigma_x^2\mathbf{H}_0^H\mathbf{H}_0+\frac{\sigma_x^2}{\sigma_1^2}\mathbf{H}_1^H\Big[\mathbf{I}_{N_R}\\ &-\Big(\mathbf{I}_{N_R}+\frac{\sigma_1^2}{\sigma_2^2}\mathbf{G}^H\mathbf{H}_2^H\mathbf{H}_2\mathbf{G}\Big)^{-1}\Big]\mathbf{H}_1\Big]^{-1}\Big\}.\end{aligned} \tag{3.19}$$

Now the problem is reduced to find the optimal $\mathbf{G}$ that minimize $J(\mathbf{G})$ subject to the power constraint (3.9). The eigenvalue decomposition (EVD) of $\mathbf{\Sigma}_0$ can be introduced as

$$\mathbf{\Sigma}_0 = \mathbf{V}_{\Sigma_0}\mathbf{\Lambda}_{\Sigma_0}\mathbf{V}_{\Sigma_0}^H \tag{3.20}$$

where $\mathbf{\Lambda}_{\Sigma_0} = \text{diag}\{\Lambda_{\Sigma_0,1}\cdots\Lambda_{\Sigma_0,N_S}\}$ with $\Lambda_{\Sigma_0,1} \geq \cdots \geq \Lambda_{\Sigma_0,N_S}$. The columns of $\mathbf{V}_{\Sigma_0}$ are the eigenvectors of $\mathbf{\Sigma}_0$ for the corresponding eigenvalues. Substituting (3.20) into (3.7), the channel matrix $\mathbf{H}_0$ can be written as

$$\mathbf{H}_0 \triangleq \widetilde{\mathbf{H}}_{\omega_0}\mathbf{\Lambda}_{\Sigma_0}^{1/2}\mathbf{V}_{\Sigma_0}^H \tag{3.21}$$

where $\widetilde{\mathbf{H}}_{\omega_0} \triangleq \mathbf{H}_{\omega_0}\mathbf{V}_{\Sigma_0}$ has the same distribution as $\mathbf{H}_{\omega_0}$, because the unitary matrix $\mathbf{V}_{\Sigma_0}$ does not change the statistical distribution of $\mathbf{H}_{\omega_0}$. The SVD of $\mathbf{H}_1$ can be expressed as

$$\mathbf{H}_1 = \mathbf{U}_1\mathbf{\Lambda}_1^{1/2}\mathbf{V}_1^H \tag{3.22}$$

where $\mathbf{\Lambda}_1 = \text{diag}\{\Lambda_{1,1}\cdots\Lambda_{1,R_1}\}$ is a diagonal matrix with $\Lambda_{1,1} \geq \cdots \geq \Lambda_{1,R_1}$, $R_1 = \min(N_S, N_R)$, and the dimensions of $\mathbf{U}_1$ and $\mathbf{V}_1$ are $N_R \times R_1$, $N_S \times R_1$, respectively. Now, the EVD of $\mathbf{\Sigma}_2$ is introduced as

$$\mathbf{\Sigma}_2 = \mathbf{V}_{\Sigma_2}\mathbf{\Lambda}_{\Sigma_2}\mathbf{V}_{\Sigma_2}^H \tag{3.23}$$

where $\mathbf{\Lambda}_{\Sigma_2} = \text{diag}\{\Lambda_{\Sigma_2,1}\cdots\Lambda_{\Sigma_2,N_R}\}$ with $\Lambda_{\Sigma_2,1} \geq \cdots \geq \Lambda_{\Sigma_2,N_R}$. The columns of $\mathbf{V}_{\Sigma_2}$ are the eigenvectors of $\mathbf{\Sigma}_2$ for the corresponding eigenvalues. Substituting (3.23) into (3.7), the channel matrix $\mathbf{H}_2$ can be rewritten as

$$\mathbf{H}_2 \triangleq \widetilde{\mathbf{H}}_{\omega_2}\mathbf{\Lambda}_{\Sigma_2}^{1/2}\mathbf{V}_{\Sigma_2}^H \tag{3.24}$$

where $\widetilde{\mathbf{H}}_{\omega_2} \triangleq \mathbf{H}_{\omega_2}\mathbf{V}_{\Sigma_2}$ has the same distribution as $\mathbf{H}_{\omega_2}$. The optimal precoding matrix $\mathbf{G}$ which minimizes (3.19) can be expressed as

$$\mathbf{G} = \mathbf{V}_{\Sigma_2}\widetilde{\mathbf{G}}\mathbf{U}_1^H. \tag{3.25}$$

Substituting (3.21)-(3.25) into (3.19), now the MSE function is given by

$$\begin{aligned} J(\widetilde{\mathbf{G}}) = \sigma_x^2 tr\Big\{\Big[\mathbf{I}_{N_S} + \sigma_x^2\mathbf{V}_{\Sigma_0}\mathbf{\Lambda}_{\Sigma_0}^{1/2}\widetilde{\mathbf{H}}_{\omega_0}^H\widetilde{\mathbf{H}}_{\omega_0}\mathbf{\Lambda}_{\Sigma_0}^{1/2}\mathbf{V}_{\Sigma_0}^H \\ + \frac{\sigma_x^2}{\sigma_1^2}\mathbf{V}_1\mathbf{\Lambda}_1^{1/2}\mathbf{U}_1^H\Big[\mathbf{I}_{N_R} - \mathbf{D}_1\Big]\mathbf{U}_1\mathbf{\Lambda}_1^{1/2}\mathbf{V}_1^H\Big]^{-1}\Big\} \end{aligned} \tag{3.26}$$

where

$$\mathbf{D}_1 = \Big(\mathbf{I}_{N_R} + \frac{\sigma_1^2}{\sigma_2^2}\mathbf{U}_1\widetilde{\mathbf{G}}^H\mathbf{\Lambda}_{\Sigma_2}^{1/2}\widetilde{\mathbf{H}}_{\omega_2}^H\widetilde{\mathbf{H}}_{\omega_2}\mathbf{\Lambda}_{\Sigma_2}^{1/2}\widetilde{\mathbf{G}}\mathbf{U}_1^H\Big)^{-1}.$$

Since $\mathbf{U}_1^H\mathbf{U}_1 = \mathbf{I}_{R_1}$, the MSE function (3.26) can be simplified to

$$J(\widetilde{\mathbf{G}}) = \sigma_x^2 tr\Big\{\Big[\mathbf{I}_{N_S} + \sigma_x^2\mathbf{V}_{\Sigma_0}\mathbf{\Lambda}_{\Sigma_0}^{1/2}\widetilde{\mathbf{H}}_{\omega_0}^H\widetilde{\mathbf{H}}_{\omega_0}\mathbf{\Lambda}_{\Sigma_0}^{1/2}\mathbf{V}_{\Sigma_0}^H + \frac{\sigma_x^2}{\sigma_1^2}\Big(\mathbf{V}_1\mathbf{\Lambda}_1\mathbf{V}_1^H - \mathbf{V}_1\mathbf{\Lambda}_1^{1/2}\mathbf{D}_2\mathbf{\Lambda}_1^{1/2}\mathbf{V}_1^H\Big)\Big]^{-1}\Big\} \tag{3.27}$$

where

$$\mathbf{D}_2 = \Big(\mathbf{I}_{R_1} + \frac{\sigma_1^2}{\sigma_2^2}\widetilde{\mathbf{G}}^H\mathbf{\Lambda}_{\Sigma_2}^{1/2}\widetilde{\mathbf{H}}_{\omega_2}^H\widetilde{\mathbf{H}}_{\omega_2}\mathbf{\Lambda}_{\Sigma_2}^{1/2}\widetilde{\mathbf{G}}\Big)^{-1}.$$

It can be seen from (3.27) that $J(\widetilde{\mathbf{G}})$ depends on $\widetilde{\mathbf{H}}_{\omega_0}$ and $\widetilde{\mathbf{H}}_{\omega_2}$, which are random and unknown. In the following, $E_{\mathbf{H}_{\omega_{0,2}}}[J(\widetilde{\mathbf{G}})]$ is optimized, where $E_{\mathbf{H}_{\omega_{0,2}}}[.]$ indicates that the expectation is taken with respect to the random matrices $\widetilde{\mathbf{H}}_{\omega_0}$ and $\widetilde{\mathbf{H}}_{\omega_2}$. Now $E_{\mathbf{H}_{\omega_{0,2}}}[J(\widetilde{\mathbf{G}})]$ can be expressed as

$$E_{\mathbf{H}_{\omega_{0,2}}}[J(\widetilde{\mathbf{G}})] = \sigma_x^2\sigma_1^2 E_{\mathbf{H}_{\omega_{0,2}}}\Big[tr\Big\{\Big[\sigma_1^2\mathbf{I}_{N_S} + \sigma_x^2\sigma_1^2\mathbf{V}_{\Sigma_0}\mathbf{\Lambda}_{\Sigma_0}^{1/2}\widetilde{\mathbf{H}}_{\omega_0}^H\widetilde{\mathbf{H}}_{\omega_0}\mathbf{\Lambda}_{\Sigma_0}^{1/2}\mathbf{V}_{\Sigma_0}^H + \sigma_x^2\mathbf{V}_1\mathbf{\Lambda}_1\mathbf{V}_1^H - \sigma_x^2\mathbf{V}_1\mathbf{\Lambda}_1^{1/2}\mathbf{D}_2\mathbf{\Lambda}_1^{1/2}\mathbf{V}_1^H\Big]^{-1}\Big\}\Big]. \tag{3.28}$$

Now the work is left to determine $\widetilde{\mathbf{G}}$ of precoder matrix $\mathbf{G}$. The optimal precoder allocates power according to the eigenmodes of $\mathbf{H}_1\mathbf{H}_1^H$, $\mathbf{\Sigma}_0$ and $\mathbf{\Sigma}_2$.

Direct minimization of (3.28) for the optimal power allocation is difficult. In the following, the lower bound of the MSE is used together with the power constraint (3.9) to derive the optimal power allocation for the precoder matrix $\mathbf{G}$. Since $J(\widetilde{\mathbf{G}})$ is convex in $\widetilde{\mathbf{H}}_{\omega_0}^H\widetilde{\mathbf{H}}_{\omega_0}$ and $\widetilde{\mathbf{H}}_{\omega_2}^H\widetilde{\mathbf{H}}_{\omega_2}$, which is proved in Appendix 3.A, Jensen's inequality [65] is used to derive the following lower bound

$$J_L(\widetilde{\mathbf{G}}) = \sigma_x^2\sigma_1^2 tr\Big\{\Big[\sigma_1^2\mathbf{I}_{N_S} + \sigma_x^2\sigma_1^2\mathbf{V}_{\Sigma_0}\mathbf{\Lambda}_{\Sigma_0}^{1/2}E_{\mathbf{H}_{\omega_0}}[\widetilde{\mathbf{H}}_{\omega_0}^H\widetilde{\mathbf{H}}_{\omega_0}] \times\mathbf{\Lambda}_{\Sigma_0}^{1/2}\mathbf{V}_{\Sigma_0}^H + \sigma_x^2\mathbf{V}_1\mathbf{\Lambda}_1\mathbf{V}_1^H - \sigma_x^2\mathbf{V}_1\mathbf{\Lambda}_1^{1/2}\mathbf{D}_3\mathbf{\Lambda}_1^{1/2}\mathbf{V}_1^H\Big]^{-1}\Big\}$$

where

$$\mathbf{D}_3 = \Big(\mathbf{I}_{R_1} + \frac{\sigma_1^2}{\sigma_2^2}\widetilde{\mathbf{G}}^H\mathbf{\Lambda}_{\Sigma_2}^{1/2}E_{\mathbf{H}_{\omega_2}}[\widetilde{\mathbf{H}}_{\omega_2}^H\widetilde{\mathbf{H}}_{\omega_2}]\mathbf{\Lambda}_{\Sigma_2}^{1/2}\widetilde{\mathbf{G}}\Big)^{-1}.$$

Now the MSE function is simplified to

$$J_L(\widetilde{\mathbf{G}}) = \sigma_x^2\sigma_1^2 tr\Big\{\Big[\sigma_1^2\mathbf{I}_{N_S} + \sigma_x^2\sigma_1^2 N_D\mathbf{V}_{\Sigma_0}\mathbf{\Lambda}_{\Sigma_0}\mathbf{V}_{\Sigma_0}^H + \sigma_x^2\mathbf{V}_1\mathbf{\Lambda}_1\mathbf{V}_1^H - \sigma_x^2\mathbf{V}_1\mathbf{\Lambda}_1^{1/2}\mathbf{D}_4\mathbf{\Lambda}_1^{1/2}\mathbf{V}_1^H\Big]^{-1}\Big\} \tag{3.29}$$

where

$$\mathbf{D}_4 = \Big(\mathbf{I}_{R_1} + \frac{\sigma_1^2 N_D}{\sigma_2^2}\widetilde{\mathbf{G}}^H\mathbf{\Lambda}_{\Sigma_2}\widetilde{\mathbf{G}}\Big)^{-1}.$$

Here, it is assumed that $E_{\mathbf{H}_{\omega_0}}\left[\widetilde{\mathbf{H}}_{\omega_0}^H\widetilde{\mathbf{H}}_{\omega_0}\right] = E_{\mathbf{H}_{\omega_2}}\left[\widetilde{\mathbf{H}}_{\omega_2}^H\widetilde{\mathbf{H}}_{\omega_2}\right] = N_D\mathbf{I}_{N_R}$. Substituting (3.22) and (3.25) into (3.9), the power constraint for the relay node can be expressed as

$$p(\widetilde{\mathbf{G}}) = tr\Big\{\mathbf{V}_{\Sigma_2}\widetilde{\mathbf{G}}\mathbf{U}_1^H\Big(\sigma_x^2\mathbf{U}_1\mathbf{\Lambda}_1\mathbf{U}_1^H + \sigma_1^2\mathbf{I}_{N_R}\Big)\mathbf{U}_1\widetilde{\mathbf{G}}^H\mathbf{V}_{\Sigma_2}^H\Big\} \leq P_r. \tag{3.30}$$

Using the SVD and trace properties, the power constraint (3.30) can be simplified to

$$p(\widetilde{\mathbf{G}}) = tr\Big\{\widetilde{\mathbf{G}}\big(\sigma_x^2\mathbf{\Lambda}_1 + \sigma_1^2\mathbf{I}_{R_1}\big)\widetilde{\mathbf{G}}^H\Big\} \leq P_r. \tag{3.31}$$

The remaining task is to optimize $\widetilde{\mathbf{G}}$. From (3.29) and (3.31), the constrained optimization problem can be written as

$$\begin{aligned}\min\ \ J_L(\widetilde{\mathbf{G}}) = \sigma_x^2\sigma_1^2 tr\Big\{\Big[&\sigma_1^2\mathbf{I}_{N_S} + \sigma_x^2\sigma_1^2 N_D\mathbf{V}_{\Sigma_0}\mathbf{\Lambda}_{\Sigma_0}\mathbf{V}_{\Sigma_0}^H \\ &+\sigma_x^2\mathbf{V}_1\mathbf{\Lambda}_1\mathbf{V}_1^H - \sigma_x^2\mathbf{V}_1\mathbf{\Lambda}_1^{1/2}\mathbf{D}_4\mathbf{\Lambda}_1^{1/2}\mathbf{V}_1^H\Big]^{-1}\Big\} \qquad (3.32)\\ \text{s.t.}\ \ p(\widetilde{\mathbf{G}}) = tr\Big\{\widetilde{\mathbf{G}}\big(\sigma_x^2\mathbf{\Lambda}_1 + \sigma_1^2\mathbf{I}_{R_1}\big)\widetilde{\mathbf{G}}^H\Big\} &\leq P_r. \qquad (3.33)\end{aligned}$$

3.3.1 Optimal Covariance Algorithm

The constrained optimization problem (3.32)-(3.33) does not have a closed-form solution due to the presence of the direct link channel $\mathbf{H}_0$. The problem (3.32)-(3.33) can be solved by resorting to numerical methods, such as the projected gradient algorithm [61]. The relay precoding matrix $\widetilde{\mathbf{G}}$ is optimized by solving the following constrained optimization problem

$$\min\ J_L(\tilde{\mathbf{G}}) = \sigma_x^2\sigma_1^2 tr\Big\{\Big[\mathbf{B} - \mathbf{C}\mathbf{D}_4\mathbf{C}^H\Big]^{-1}\Big\} \tag{3.34}$$

$$\text{s.t.}\ p(\tilde{\mathbf{G}}) = tr\Big\{\widetilde{\mathbf{G}}\mathbf{M}\widetilde{\mathbf{G}}^H\Big\} \leq P_r \tag{3.35}$$

where

$$\begin{aligned}\mathbf{B} &= \sigma_1^2\mathbf{I}_{N_S} + \sigma_x^2\sigma_1^2 N_D\mathbf{V}_{\Sigma_0}\mathbf{\Lambda}_{\Sigma_0}\mathbf{V}_{\Sigma_0}^H + \sigma_x^2\mathbf{V}_1\mathbf{\Lambda}_1\mathbf{V}_1^H\\ \mathbf{C} &= \sigma_x\mathbf{V}_1\mathbf{\Lambda}_1^{1/2}\\ \mathbf{M} &= \sigma_x^2\mathbf{\Lambda}_1 + \sigma_1^2\mathbf{I}_{R_1}\end{aligned}$$

The gradient of (3.34) is given by

$$\nabla J_L(\tilde{\mathbf{G}}) = \frac{-2\sigma_1^2 N_D}{\sigma_2^2}\Big[\mathbf{D}_4\mathbf{C}^H\big(\mathbf{B} - \mathbf{C}\mathbf{D}_4\mathbf{C}^H\big)^{-2}\mathbf{C}\mathbf{D}_4\widetilde{\mathbf{G}}^H\mathbf{\Lambda}_{\Sigma_2}\Big]^H \tag{3.36}$$

where the derivatives $\partial tr(\mathbf{\Theta}\mathbf{X}^{-1})/\partial\mathbf{X} = -(\mathbf{X}^{-1}\mathbf{\Theta}\mathbf{X}^{-1})^T$ and $\partial tr(\mathbf{\Theta}\mathbf{X})/\partial\mathbf{X} = \mathbf{\Theta}^T$ are used to obtain (3.36). The problem (3.34)-(3.35) can be solved by the projected gradient algorithm to optimize the matrix elements of $\widetilde{\mathbf{G}}$.

3.3.2 Suboptimal Covariance Algorithm

Now a relay matrix design algorithm is proposed which is suboptimal, but has a significant computational complexity reduction compared with the gradient projection-based optimal design. Similar to [23–33], it can be assumed that the matrix $\widetilde{\mathbf{G}} = [\mathbf{\Lambda}_G^{1/2}, \mathbf{0}_{R_1\times(N_R-R_1)}]^T$, where $\mathbf{\Lambda}_G = \text{diag}\{\Lambda_{G,1}\cdots\Lambda_{G,R_1}\}$. Hence, the equation (3.25) can be rewritten as

$$\mathbf{G} = \bar{\mathbf{V}}_{\Sigma_2}\mathbf{\Lambda}_G^{1/2}\mathbf{U}_1^H \tag{3.37}$$

where $\bar{\mathbf{V}}_{\Sigma_2}$ is a matrix taking the first R_1 columns of $\mathbf{V}_{\Sigma_2}$. Then, the constrained optimization problem is reduced to

$$\begin{aligned}\min\ J_L(\mathbf{\Lambda}_G) = \sigma_x^2\sigma_1^2 tr\Big\{\Big[\sigma_1^2\mathbf{I}_{N_S} + \sigma_x^2\sigma_1^2 N_D\mathbf{V}_{\Sigma_0}\mathbf{\Lambda}_{\Sigma_0}\mathbf{V}_{\Sigma_0}^H \\ +\sigma_x^2\mathbf{V}_1\mathbf{\Lambda}_1\Big[\mathbf{I}_{R_1}-\Big(\mathbf{I}_{R_1}+\frac{\sigma_1^2N_D}{\sigma_2^2}\mathbf{\Lambda}_G\bar{\mathbf{\Lambda}}_{\Sigma_2}\Big)^{-1}\Big]\mathbf{V}_1^H\Big]^{-1}\Big\}\end{aligned} \tag{3.38}$$

$$\text{s.t. } p(\mathbf{\Lambda}_G) = tr\Big\{\big(\sigma_x^2\mathbf{\Lambda}_1 + \sigma_1^2\mathbf{I}_{R_1}\big)\mathbf{\Lambda}_G\Big\} \le P_r \tag{3.39}$$

where $\bar{\mathbf{\Lambda}}_{\Sigma_2} = \text{diag}\{\Lambda_{\Sigma_2,1}\cdots\Lambda_{\Sigma_2,R_1}\}$. To proceed further, the matrix inversion lemma (2.15) is used to rewrite the MSE function (3.38) as

$$\begin{aligned}J_L(\mathbf{\Lambda}_G) = \sigma_x^2 tr\Big\{\Big[\mathbf{I}_{N_S} + \sigma_x^2 N_D\mathbf{V}_{\Sigma_0}\mathbf{\Lambda}_{\Sigma_0}\mathbf{V}_{\Sigma_0}^H + \frac{\sigma_x^2N_D}{\sigma_2^2}\mathbf{V}_1\mathbf{\Lambda}_1 \\ \times\mathbf{\Lambda}_G\bar{\mathbf{\Lambda}}_{\Sigma_2}\Big(\mathbf{I}_{R_1} + \frac{\sigma_1^2N_D}{\sigma_2^2}\bar{\mathbf{\Lambda}}_{\Sigma_2}\mathbf{\Lambda}_G\Big)^{-1}\mathbf{V}_1^H\Big]^{-1}\Big\}.\end{aligned} \tag{3.40}$$

An upper-bound of (3.40) is considered as follows. By introducing $\mathbf{E}_1 = \frac{\sigma_x^2N_D}{\sigma_2^2}\mathbf{\Lambda}_1\mathbf{\Lambda}_G\bar{\mathbf{\Lambda}}_{\Sigma_2}\Big(\mathbf{I}_{R_1} + \frac{\sigma_1^2N_D}{\sigma_2^2}\bar{\mathbf{\Lambda}}_{\Sigma_2}\mathbf{\Lambda}_G\Big)^{-1}$, the MSE function (3.40) can be written as

$$J_L(\mathbf{\Lambda}_G) = \sigma_x^2 tr\Big\{\Big[\mathbf{I}_{N_S} + \mathbf{V}_1\mathbf{E}_1\mathbf{V}_1^H + \sigma_x^2N_D\mathbf{V}_{\Sigma_0}\mathbf{\Lambda}_{\Sigma_0}\mathbf{V}_{\Sigma_0}^H\Big]^{-1}\Big\}. \tag{3.41}$$

Here $\bar{\mathbf{V}}_1 = [\mathbf{V}_1, \mathbf{V}_1^{\perp}]$ is introduced such that $\bar{\mathbf{V}}_1$ is an $N_s\times N_s$ unitary matrix. Obviously, if $R_1 = N_s$, $\bar{\mathbf{V}}_1 = \mathbf{V}_1$. Then (3.41) can be equivalently rewritten as

$$J_L(\mathbf{\Lambda}_G) = \sigma_x^2 tr\Big\{\Big[\mathbf{A} + \sigma_x^2N_D\bar{\mathbf{V}}_1^H\mathbf{V}_{\Sigma_0}\mathbf{\Lambda}_{\Sigma_0}\mathbf{V}_{\Sigma_0}^H\bar{\mathbf{V}}_1\Big]^{-1}\Big\} \tag{3.42}$$

where

$$\mathbf{A} = \mathbf{I}_{N_S} + \big[\mathbf{I}_{R_1}, \mathbf{0}_{R_1\times(N_s-R_1)}\big]^T\mathbf{E}_1\big[\mathbf{I}_{R_1}, \mathbf{0}_{R_1\times(N_s-R_1)}\big].$$

Applying the matrix inversion lemma (2.15), the MSE function (3.42) can be rewritten as

$$J_L(\mathbf{\Lambda}_G) = \sigma_x^2\Big[tr(\mathbf{A}^{-1}) - tr\big(\mathbf{A}^{-1}\big(\mathbf{C}+\mathbf{A}^{-1}\big)^{-1}\mathbf{A}^{-1}\big)\Big] \tag{3.43}$$

where $\mathbf{C} = \sigma_x^2 N_D(\bar{\mathbf{V}}_1^H \mathbf{V}_{\Sigma_0} \mathbf{\Lambda}_{\Sigma_0} \mathbf{V}_{\Sigma_0}^H \bar{\mathbf{V}}_1)^{-1}$. By using the following inequality from [28]

$$\begin{aligned} & tr\big(\mathbf{A}^{-1}\big(\mathbf{C}+\mathbf{A}^{-1}\big)^{-1}\mathbf{A}^{-1}\big) \\ & \geq tr\big(\mathbf{A}^{-1}\big(\mathrm{diag}\big(\mathbf{C}\big)+\mathbf{A}^{-1}\big)^{-1}\mathbf{A}^{-1}\big), \end{aligned} \tag{3.44}$$

an upper-bound of $J_L(\mathbf{\Lambda}_G)$ is given by

$$J_U(\mathbf{\Lambda}_G) = \sigma_x^2\Big[tr(\mathbf{A}^{-1}) - tr\big(\mathbf{A}^{-1}\big(\mathrm{diag}(\mathbf{C})+\mathbf{A}^{-1}\big)^{-1}\mathbf{A}^{-1}\big)\Big]. \tag{3.45}$$

From (3.45), the diagonal elements of $\mathbf{\Lambda_G}$ can be obtained by solving the following optimization problem with scalar variables

$$\min_{\{\Lambda_{G,i}\}} \sum_{i=1}^{R_1} \frac{\big(\sigma_1^2 N_D \Lambda_{\Sigma_2,i}\Lambda_{G,i} + \sigma_2^2\big)\sigma_x^2\lambda_{c,i}}{D_5\Lambda_{G,i} + \sigma_2^2\lambda_{c,i} + \sigma_2^2} \tag{3.46}$$

$$\text{s.t.} \sum_{i=1}^{R_1} (\sigma_x^2\Lambda_{1,i} + \sigma_1^2)\Lambda_{G,i} \leq P_r \tag{3.47}$$

where

$$D_5 = (\sigma_1^2\lambda_{c,i} + \sigma_x^2\Lambda_{1,i}\lambda_{c,i} + \sigma_1^2)N_D\Lambda_{\Sigma_2,i},$$

$$\lambda_{c,i} = \sigma_x^2 N_D \mathrm{diag}\Big((\bar{\mathbf{V}}_1^H \mathbf{V}_{\Sigma_0} \mathbf{\Lambda}_{\Sigma_0} \mathbf{V}_{\Sigma_0}^H \bar{\mathbf{V}}_1)^{-1}\Big).$$

Using the KKT conditions [61], the optimal diagonal elements of $\Lambda_{G,i}$ are obtained as

$$\Lambda_{G,i} = \frac{1}{D_5}\left(\sqrt{\frac{\sigma_x^4\sigma_2^2 N_D \Lambda_{1,i}\Lambda_{\Sigma_2,i}\lambda_{c,i}^2}{\mu(\sigma_x^2\Lambda_{1,i}+\sigma_1^2)}} - \sigma_2^2\lambda_{c,i} - \sigma_2^2\right)^+ \tag{3.48}$$

where $(x)^+ = \max(x, 0)$ and μ should be chosen to meet the power constraint (3.47).

3.4 Numerical Examples

In this section, the performance of the proposed schemes is illustrated by numerical examples. The entries of channel matrices $\mathbf{H}_{\omega_0}$, $\mathbf{H}_1$ and $\mathbf{H}_{\omega_2}$ are generated as complex Gaussian variables with zero mean and unit variances. The symbols are generated from QPSK constellation.

The elements of covariance matrices $\mathbf{\Sigma}_0$ of $\mathbf{H}_0$ and $\mathbf{\Sigma}_2$ of $\mathbf{H}_2$ are generated by $\Sigma_{i,j}$ $= J_0(\triangle\pi|i-j|)$ [11], where $J_0(.)$ is the zeroth order Bessel function of the first kind, $\triangle$ the angle of fading spread. The SNRs for the direct source-destination, the source-relay and relay-destination links are defined as $\mathrm{SNR}_0 = \frac{\sigma_x^2}{\sigma_0^2}$, $\mathrm{SNR}_1 = \frac{\sigma_x^2}{\sigma_1^2}$ and $\mathrm{SNR}_2 = \frac{P_r}{N_R\sigma_2^2}$.

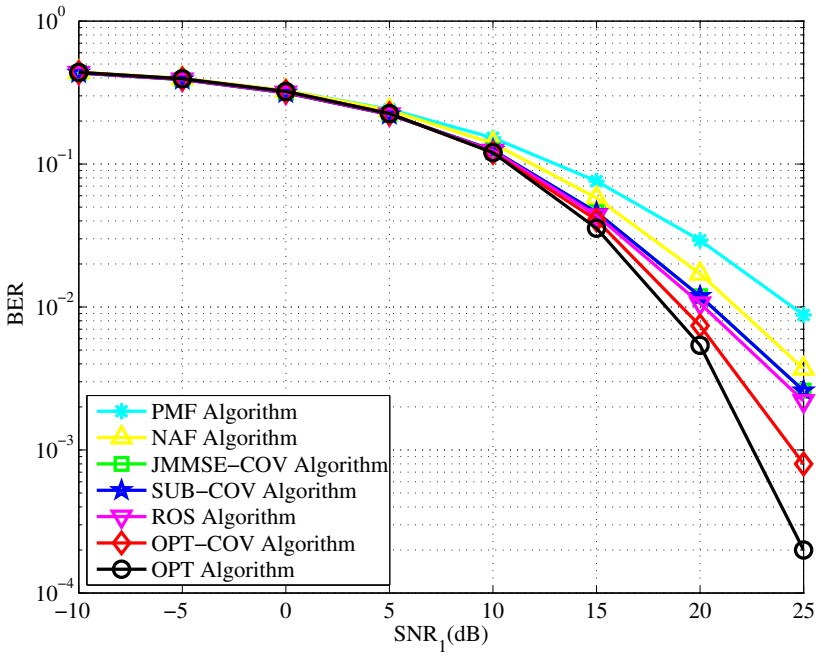

Figure 3.2: BER versus SNR_1 while fixing $N_S = N_R = N_D = 4$, $\triangle_0 = 1^o$, $\triangle_2 = 30^o$, $\mathrm{SNR}_2 = 20dB$, $\mathrm{SNR}_0 = \mathrm{SNR}_1 - 10dB$.

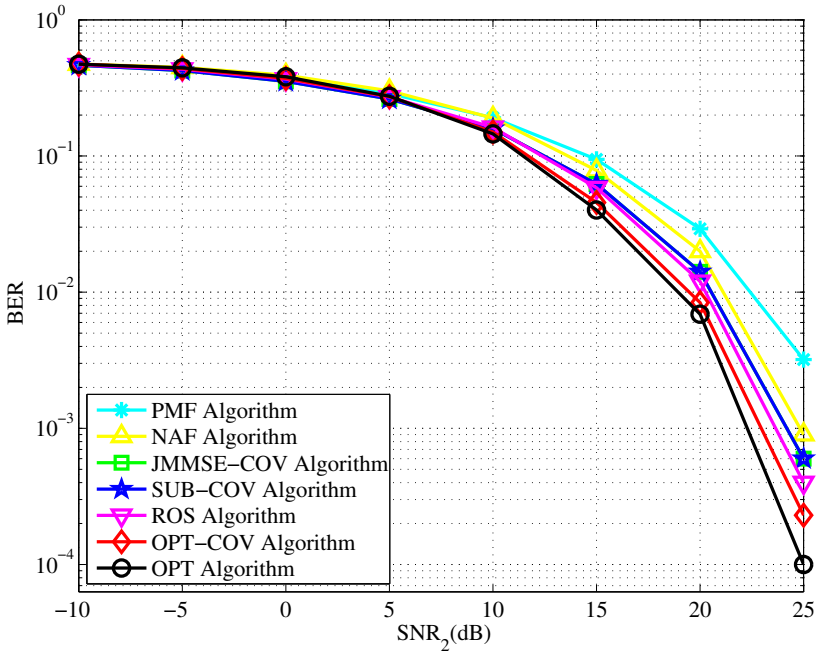

Figure 3.3: BER versus SNR_2 while fixing $N_S = N_R = N_D = 4$, $\triangle_0 = 1^o$, $\triangle_2 = 30^o$, $\mathrm{SNR}_1 = 20dB$, $\mathrm{SNR}_0 = \mathrm{SNR}_1 - 10dB$.

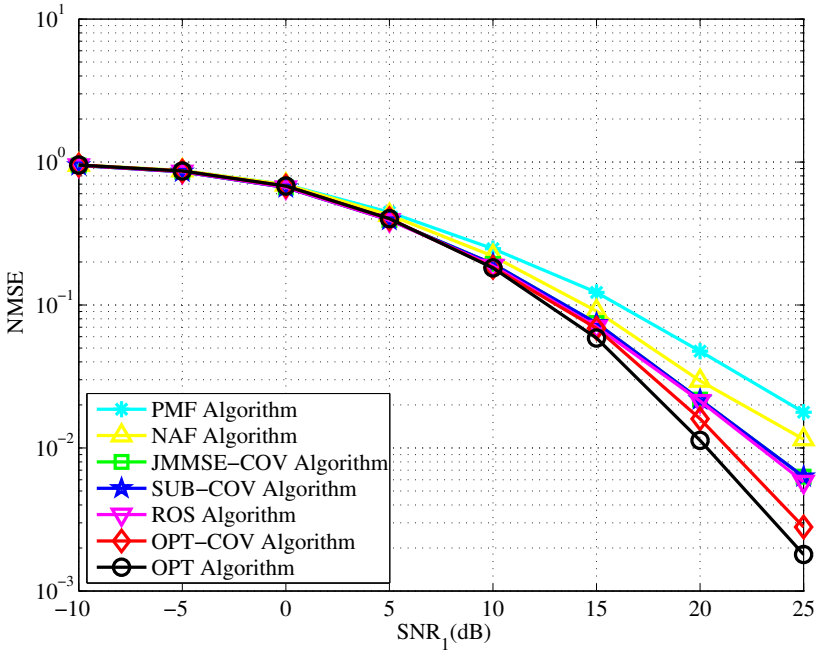

Figure 3.4: NMSE versus SNR_1 while fixing $N_S = N_R = N_D = 4$, $\triangle_0 = 1^o$, $\triangle_2 = 30^o$, $\mathrm{SNR}_2 = 20dB$, $\mathrm{SNR}_0 = \mathrm{SNR}_1 - 10dB$.

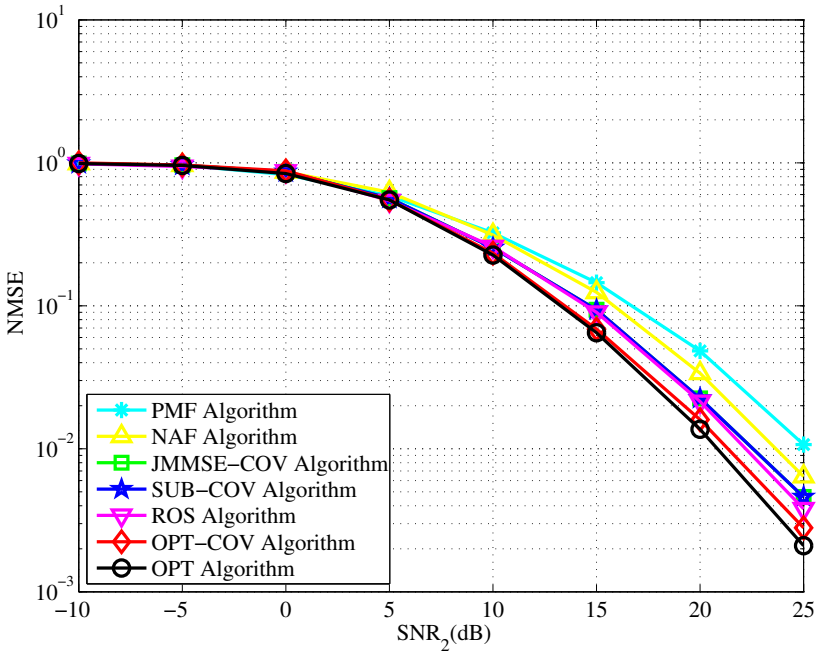

Figure 3.5: NMSE versus SNR_2 while fixing $N_S = N_R = N_D = 4$, $\triangle_0 = 1^o$, $\triangle_2 = 30^o$, $\mathrm{SNR}_1 = 20dB$, $\mathrm{SNR}_0 = \mathrm{SNR}_1 - 10dB$.

The performance of the proposed optimal covariance (OPT-COV) algorithm and the suboptimal covariance (SUB-COV) algorithm is compared with the naive amplify-and-forward (NAF) algorithm [22], the PMF algorithm [22], ROS algorithm [26], the JMMSE-COV algorithm [32], OPT algorithm [26]. The full CSI scheme, also known as OPT algorithm [26] provides the lower-bound of the proposed schemes. For the proposed OPT-COV algorithm, the projected gradient method is applied to optimize $\widetilde{\mathbf{G}}$ in (3.34)-(3.35).

In the first example, the BER performance of the proposed algorithms is compared with the existing MSE algorithms. The Fig. 3.2 shows the performance of the MSE algorithms in terms of BER versus SNR_1. The non-regenerative MIMO relay system is simulated with $N_S = N_R = N_D = 4$. A scenario is considered as assumed in section 3.2 that the source node is moving rapidly. Hence, to implement the assumption in simulation, the distance between the relay to destination link is fixed, where the source to relay and source to destination distances are varied. For establishing the scenario, the SNR of the relay-destination link is set as $\text{SNR}_2 = 20dB$ and the SNR of the source-destination link is fixed as $\text{SNR}_0 = \text{SNR}_1 - 10dB$. The angle spread is set as $\triangle_0 = 1^o$ for the direct source-destination link and $\triangle_2 = 30^o$ for the relay-destination link. In this example, 1000 samples are randomly generated at source node for each channel realization. It can be seen from the Fig. 3.2 that the PMF algorithm has worst performance than all other MSE algorithms. The proposed SUB-COV algorithm performance is similar to the JMMSE-COV and ROS algorithms. At high SNR_1, the proposed OPT-COV algorithm shows better BER performance than the NAF, PMF, ROS, JMMSE-COV and SUB-COV algorithms.

In the second example, the BER performance of the proposed algorithms is compared with the existing MSE algorithms. The Fig. 3.3 shows the performance of MSE algorithms in terms of BER versus SNR_2. In the example, the source, relay and destination nodes antennas of the non-regenerative MIMO relay system are set as $N_S = N_R = N_D = 4$. A scenario is considered as assumed in section 3.2 that the destination node is moving rapidly. Hence, to implement the assumption in simulation, it is set that the distance between the source to relay link is fixed, where the relay to destination and source to destination distances are varied. For establishing the scenario, the SNR values are set as $\text{SNR}_1 = 20dB$, $\text{SNR}_0 = \text{SNR}_1 - 10dB$. The angle spread is fixed as $\triangle_0 = 1^o$ for the direct source-destination link and $\triangle_2 = 30^o$ for the relay-destination link. In this example, 1000 samples are randomly generated at source node for each

channel realization. It can be noticed from the Fig. 3.3 that the proposed SUB-COV algorithm outperforms the NAF and PMF algorithms and it performance is similar to the JMMSE-COV algorithm. The performance of the SUB-COV algorithm is closer to the ROS algorithm. At high SNR_2 (SNR_2 >10dB), the proposed OPT-COV algorithm shows better BER performance than the NAF, PMF, ROS, JMMSE-COV and SUB-COV algorithms.

In the third example, the NMSE performance of the proposed algorithm is studied for various SNR_1 while fixing $\text{SNR}_2 = 20\text{dB}$, $\text{SNR}_1 = 20dB$, and $\text{SNR}_0 = \text{SNR}_1 - 10dB$ for satisfying the assumption in the section 3.2. In the example, the angle spreads and number of antennas are set as $\triangle_0 = 1^o$, $\triangle_2 = 30^o$, $N_S = N_R = N_D$=4. In this example, 1000 samples are randomly generated at source node for each channel realization. It can be noticed from the Fig. 3.4 that NAF and PMF algorithms produce much higher NMSE as compared to the proposed SUB-COV algorithm at high SNR_1. It can be depicted from the Fig. 3.4 that the performance of the proposed SUB-COV algorithm is similar to the ROS and JMMSE-COV algorithms. It is clearly shown in Fig. 3.4 that the proposed OPT-COV algorithm outperforms in terms of NMSE as compared to the NAF, PMF, JMMSE-COV, SUB-COV and ROS algorithms.

In the final example, a non-regenerative MIMO relay system is simulated with $N_S = N_R = N_D$ =4. The QPSK constellations are used to modulate the symbols at the source node. Fig. 2.5 shows the NMSE performance of the proposed algorithms for varying SNR_2 while fixing SNR_1 =20dB and $\text{SNR}_0 = \text{SNR}_1 - 10dB$. Angle of the delay spread for the source-destination link is set as $\triangle_0 = 1^o$ and the relay-destination link is set as $\triangle_2 = 30^o$. The simulation result is averaged over 1000 QPSK samples which are randomly generated at source node for each channel realization. From the Fig. 3.5, it can be noticed that the proposed SUB-COV algorithm excels the NAF and PMF algorithms in terms of NMSE at high SNR_2 ($\text{SNR}_2 > 5dB$). The proposed OPT-COV algorithm has a better NMSE performance as compared to the NAF, PMF, JMMSE-COV, SUB-COV and ROS algorithms.

3.5 Chapter Summary

In this chapter, the general structure of the optimal relay precoding matrix for linear non-regenerative MIMO relay communication systems is derived. The proposed relay matrix minimizes the MSE of the signal waveform estimation at the destination node in

the presence of the direct source-destination link. It is assumed that the relay knows the full CSI of the source-relay link and the partial CSI (covariance feedback) of the direct source-destination link and the relay-destination link. Simulation results demonstrate that the proposed iterative based optimal covariance algorithm has improved NMSE and BER performances compared with the conventional covariance feedback based MSE algorithms.

3.A Appendix

Regarding the convexity of (3.28) for $\widetilde{\mathbf{H}}_{\omega_0}^H\widetilde{\mathbf{H}}_{\omega_0}$ and $\widetilde{\mathbf{H}}_{\omega_2}^H\widetilde{\mathbf{H}}_{\omega_2}$, it can be noted that by using the matrix inversion lemma (2.15), the MSE function (3.28) can be rewritten as

$$\begin{aligned}E_{\mathbf{H}_{\omega_{0,2}}}[J(\widetilde{\mathbf{G}})]=&\sigma_x^2\sigma_1^2E_{\mathbf{H}_{\omega_{0,2}}}\Big[tr\Big\{\Big[\sigma_1^2\mathbf{I}_{N_S}+\sigma_x^2\sigma_1^2\mathbf{V}_{\Sigma_0}\mathbf{\Lambda}_{\Sigma_0}^{1/2}\big[\widetilde{\mathbf{H}}_{\omega_0}^H\widetilde{\mathbf{H}}_{\omega_0}\big]\mathbf{\Lambda}_{\Sigma_0}^{1/2}\mathbf{V}_{\Sigma_0}^H\\&+\sigma_x^2\mathbf{V}_1\mathbf{\Lambda}_1^{1/2}\widetilde{\mathbf{G}}^H\mathbf{\Lambda}_{\Sigma_2}^{1/2}\Big(\mathbf{\Lambda}_{\Sigma_2}^{1/2}\widetilde{\mathbf{G}}\widetilde{\mathbf{G}}^H\mathbf{\Lambda}_{\Sigma_2}^{1/2}+\frac{\sigma_2^2}{\sigma_1^2}\big[\widetilde{\mathbf{H}}_{\omega_2}^H\widetilde{\mathbf{H}}_{\omega_2}\big]^{-1}\Big)^{-1}\\&\times\mathbf{\Lambda}_{\Sigma_2}^{1/2}\widetilde{\mathbf{G}}\mathbf{\Lambda}_1^{1/2}\mathbf{V}_1^H\Big]^{-1}\Big\}\Big].\end{aligned}$$

From [66], $f(\mathbf{X})=\mathbf{X}^{-1}$ is a matrix-convex function of $\mathbf{X}$. Hence, the MSE function (3.28) is a convex function for $\widetilde{\mathbf{H}}_{\omega_0}^H\widetilde{\mathbf{H}}_{\omega_0}$ and $\widetilde{\mathbf{H}}_{\omega_2}^H\widetilde{\mathbf{H}}_{\omega_2}$.

Chapter 4

MIMO Relay Design with Mean and Covariance Feedback

In this chapter, the problem of transceiver design in a non-regenerative MIMO relay system is addressed, where linear signal processing is applied at the source, relay and destination nodes to minimize the MSE of the signal waveform estimation at the destination node. In the proposed design scheme, optimal structures of the source and relay precoding matrices are derived with the assumption that the mean and CCI of the relay-destination link and the full CSI of the source-relay link are known at the relay node. Overview of the existing work is described in Section 4.1. In Section 4.2, a system model of the proposed precoding matrix design is introduced for a non-regenerative MIMO relay system with mean and covariance feedback. In Section 4.3, two non-regenerative MIMO relay precoder design schemes, such as an iterative joint source and relay precoder design scheme and suboptimal relay only precoder design scheme are proposed to achieve the minimum MSE of the signal estimation at the destination node. The performance of the proposed MIMO relay design schemes is verified through numerical simulations which is presented in Section 4.4. Finally, the chapter is summarized in Section 4.5.

4.1 Overview of Existing Techniques

Recently cooperative communication has attracted considerable attention, due to its potential to provide reliable, cost effective and wide-area coverage of wireless networks.

In cooperative communication systems, relay node can be deployed in between the source and destination to reduce the transmission power from the source to neighbouring nodes and mitigate the shadowing effects.

In general there are two kinds of relay strategies, including regenerative scheme and non-regenerative scheme [17, 19, 50]. In terms of implementation complexity, the non-regenerative scheme has a lower computational complexity, since for this scheme, the relay node amplifies the received signal from the source node and retransmits the signal to the destination node.

On the other hand, multiple antennas can provide spacial diversity and multiplexing gains to wireless communication systems. This benefits can be incorporated in the cooperative communication systems by deploying multiple antennas at the transceiver. Due to this fact, non-regenerative MIMO relay systems have received much research interest [21–25, 28–34, 37, 51–55, 67].

Recently, relay precoding scheme [21, 22, 51–54] for non-regenerative MIMO relaying has been investigated to maximize the capacity between the source and destination with further signal processing. In this scheme, the relay multiplies the received signal by a precoding matrix and retransmits the precoded signal to the destination node. The precoding matrix is designed to minimize the MSE of the signal waveform estimation at the destination node [23, 25, 56, 57]. The optimal precoding matrix design is investigated well in [23, 25, 56, 57, 67] for non-regenerative MIMO relay system with the assumption that the relay knows the full CSI of the source-relay and relay-destination links.

In a practical system with a limited feedback rate, the assumption that the relay knows the full CSI for the relay-destination link is not feasible, especially in the situation when the destination node is moving rapidly. The channel mean and covariance matrices are more stable than the instantaneous channel matrix because the scattering environment changes more slowly compared to the destination node location.

Optimal precoder is designed for maximizing the ergodic capacity of the non-regenerative MIMO relay systems with the assumption that the CCI of the relay-destination link is available at the relay node [29–31, 58]. Recently, MMSE based estimators are investigated in [32–34] with the assumption that the covariance channel information of the relay-destination link is known at the relay node. An optimal transmit strategy is proposed for maximizing the cut-set bound on the ergodic capacity of the two-hop decode-and-forward (DF) MIMO relay systems with the mean and covariance feedback [68]. However, the optimal precoding matrix design with the mean feedback of the

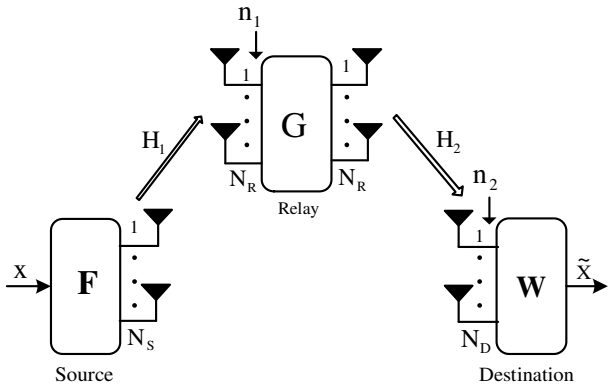

Figure 4.1: Non-regenerative MIMO relay system

relay-destination link is not investigated for non-regenerative MIMO relay systems in [32–34, 68].

In this chapter, an iterative joint source and relay precoder design is proposed to minimize the MSE of the symbol estimation in a non-regenerative MIMO relay system, when the mean and covariance information for the relay-destination link are available at the relay node. It is considered that the computational complexity of the developed iterative scheme may be high for practical implementation of the relay system. Hence, a suboptimal relay-only precoder design scheme is proposed. In the proposed two algorithms, it is assumed that the relay knows the full CSI of the source-relay link and mean and CCI of the relay-destination link. Simulation results verify the performance of the proposed optimal and suboptimal mean and covariance based algorithms.

4.2 System Model and Problem Formulation

Consider a non-regenerative MIMO relay system as shown in Fig. 4.1, where the source, relay and destination nodes have N_S, N_R and N_D antennas, respectively. It is assumed that there is no direct link between the source and destination nodes due to long distance between these two points. The data transmission takes place over two hops. The received signal at the relay during the first hop is given by

$$\mathbf{y}_1 = \mathbf{H}_1\mathbf{F}\mathbf{x} + \mathbf{n}_1 \tag{4.1}$$

where $\mathbf{H}_1 \in \mathbb{C}^{N_R \times N_S}$ is the channel matrix of the source-relay link, $\mathbf{F} \in \mathbb{C}^{N_S \times N_S}$ is the source precoding matrix, $\mathbf{x} \in \mathbb{C}^{N_S \times 1}$ is the transmitted signal vector with covariance matrix $E\{\mathbf{x}\mathbf{x}^H\} = \sigma_x^2\mathbf{I}_{N_S}$, $\mathbf{n}_1 \in \mathbb{C}^{N_R \times 1}$ is the circularly symmetric complex Gaussian

noise vector with zero mean and covariance matrix $E\{\mathbf{n}_1\mathbf{n}_1^H\} = \sigma_1^2\mathbf{I}_{N_R}$. The received signal at the destination in the second hop is given by

$$\mathbf{y}_2 = \mathbf{H}_2\mathbf{G}\mathbf{H}_1\mathbf{F}\mathbf{x} + \mathbf{H}_2\mathbf{G}\mathbf{n}_1 + \mathbf{n}_2 \tag{4.2}$$

where $\mathbf{H}_2 \in \mathbb{C}^{N_D \times N_R}$ is the channel matrix of the relay-destination link, $\mathbf{G} \in \mathbb{C}^{N_R \times N_R}$ is the relay precoding matrix, $\mathbf{n}_2 \in \mathbb{C}^{N_D \times 1}$ is the circularly symmetric complex Gaussian noise vector with zero mean and covariance matrix $E\{\mathbf{n}_2\mathbf{n}_2^H\} = \sigma_2^2\mathbf{I}_{N_D}$. The combined channel and noise matrices can be written

$$\mathbf{H} = \mathbf{H}_2\mathbf{G}\mathbf{H}_1\mathbf{F} \tag{4.3}$$

and

$$\mathbf{n} = \mathbf{H}_2\mathbf{G}\mathbf{n}_1 + \mathbf{n}_2 \tag{4.4}$$

where $\mathbf{H} \in \mathbb{C}^{N_D \times N_S}$ is the equivalent MIMO channel matrix, and $\mathbf{n} \in \mathbb{C}^{N_D \times 1}$ represents the equivalent noise vector. Now (4.2) can be written as

$$\mathbf{y}_2 = \mathbf{H}\mathbf{x} + \mathbf{n}. \tag{4.5}$$

Consider a scenario that the channel of the relay-destination link is correlated at the transmit antennas and is uncorrelated at the receive antennas. This model is suitable for an environment where the relay is not surrounded by local scatterers [11] and the destination node is hindered by local scatterers [30, 31]. With this assumption, the channel matrix $\mathbf{H}_2$ can be modeled as

$$\mathbf{H}_2 = \bar{\mathbf{H}}_\mu + \mathbf{H}_\omega\mathbf{\Sigma}^{1/2} \tag{4.6}$$

where $\bar{\mathbf{H}}_\mu \in \mathbb{C}^{N_D \times N_R}$ is the mean of $\mathbf{H}_2$, $\mathbf{H}_\omega$ is an $N_D \times N_R$ Gaussian matrix having i.i.d. circularly symmetric complex entries with zero mean and unit variance, and $\mathbf{\Sigma}$ is an $N_R \times N_R$ covariance matrix of $\mathbf{H}_2$ at the relay side.

At destination node, linear receiver $\mathbf{W}$ is applied to reduce implementation complexity. Hence, the estimated signal at the destination node can be expressed as

$$\tilde{\mathbf{x}} = \mathbf{W}\mathbf{H}\mathbf{x} + \mathbf{W}\mathbf{n}. \tag{4.7}$$

It is assumed that the average power at the source and relay are upper bounded by P_s and P_r. Since the transmitted signal from the relay is $\mathbf{G}\mathbf{y}_1 = \mathbf{G}\mathbf{H}_1\mathbf{F}\mathbf{x} + \mathbf{G}\mathbf{n}_1$, the power constraint on the source and relay can be expressed as

$$\begin{aligned} p(\mathbf{F}) &= \sigma_x^2 tr\left\{\mathbf{F}^H\mathbf{F}\right\} \le P_s \\ p(\mathbf{F},\mathbf{G}) &= tr\left\{\mathbf{G}(\sigma_x^2\mathbf{H}_1\mathbf{F}\mathbf{F}^H\mathbf{H}_1^H + \sigma_1^2\mathbf{I}_{N_R})\mathbf{G}^H\right\} \le P_r. \end{aligned} \tag{4.8}$$

Our goal is to design $\mathbf{F}$, $\mathbf{G}$ and $\mathbf{W}$ so as to obtain the estimated signal which minimizes the following MSE function subject to the power constraints (4.8).

$$J(\mathbf{F},\mathbf{G},\mathbf{W}) = tr\Big\{E\Big\{(\tilde{\mathbf{x}}-\mathbf{x})(\tilde{\mathbf{x}}-\mathbf{x})^H\Big\}\Big\} \tag{4.9}$$

Mathematically, this problem can be formulated as

$$\begin{aligned}(\mathbf{F},\mathbf{G},\mathbf{W}) = &\arg\min_{(\mathbf{F},\mathbf{G},\mathbf{W})} J(\mathbf{F},\mathbf{G},\mathbf{W}),\\ s.t.\ &p(\mathbf{F})\le P_s,\\ &p(\mathbf{F},\mathbf{G})\le P_r.\end{aligned} \tag{4.10}$$

After substituting (4.7) into (4.9), the MSE function (4.9) is simplified to

$$\begin{aligned}J(\mathbf{F},\mathbf{G},\mathbf{W}) = tr\Big\{&\sigma_x^2\Big(\mathbf{WH}-\mathbf{I}_{N_S}\Big)\Big(\mathbf{WH}-\mathbf{I}_{N_S}\Big)^H\\ &+\mathbf{W}\mathbf{R}_n\mathbf{W}^H\Big\}\end{aligned} \tag{4.11}$$

where $\mathbf{R}_n$ is the equivalent noise covariance matrix, given by

$$\begin{aligned}\mathbf{R}_n &= E\Big\{\mathbf{n}\mathbf{n}^H\Big\}\\ &= E\Big\{\big(\mathbf{H}_2\mathbf{G}\mathbf{n}_1+\mathbf{n}_2\big)\big(\mathbf{H}_2\mathbf{G}\mathbf{n}_1+\mathbf{n}_2\big)^H\Big\}\\ &= \sigma_1^2\mathbf{H}_2\mathbf{G}\mathbf{G}^H\mathbf{H}_2^H+\sigma_2^2\mathbf{I}_{N_D}.\end{aligned} \tag{4.12}$$

Note that directly solving the constrained MSE function (4.10) is difficult due to the fact that both the objective function $J(\mathbf{F},\mathbf{G},\mathbf{W})$ and the power constraint $p(\mathbf{F},\mathbf{G})$ are non-linear and non-convex function of $\mathbf{F}$, $\mathbf{G}$ and $\mathbf{W}$.

In the following section a suboptimal approach will be used to tackle the constrained non-linear optimization problem. First, the problem will be solved for the optimal linear receiver $\mathbf{W}$ for any given precoding matrices $\mathbf{F}$ and $\mathbf{G}$ which satisfies the power constraints (4.8). Then, an iterative source and relay precoder design is proposed for obtaining the source and relay precoding matrices $\mathbf{F}$ and $\mathbf{G}$ by solving a closely related constrained optimization problem. In order to reduce computational complexity of the proposed iterative scheme, a suboptimal relay-only precoder design is proposed.

4.3 Proposed Optimal Transceiver Design Algorithms

For any given precoding matrices $\mathbf{F}$ and $\mathbf{G}$ which satisfy the power constraint at the source and relay nodes (4.8), the optimal linear receiver $\mathbf{W}$ that minimizes the MSE

function $J(\mathbf{F},\mathbf{G},\mathbf{W})$ is the same as the MMSE (Wiener filter) receiver [59], which is given by

$$\mathbf{W} = \sigma_x^2\mathbf{H}^H(\sigma_x^2\mathbf{H}\mathbf{H}^H + \mathbf{R}_n)^{-1}. \tag{4.13}$$

After substituting (4.13) into (4.11), the MSE function is obtained as

$$J(\mathbf{F},\mathbf{G}) = \sigma_x^2 tr\Big\{\mathbf{I}_{N_S} - \sigma_x^2\mathbf{H}^H(\sigma_x^2\mathbf{H}\mathbf{H}^H + \mathbf{R}_n)^{-1}\mathbf{H}\Big\}. \tag{4.14}$$

Using the following matrix inversion lemma [60]

$$(\mathbf{A}+\mathbf{BCD})^{-1}=\mathbf{A}^{-1} - \mathbf{A}^{-1}\mathbf{B}(\mathbf{D}\mathbf{A}^{-1}\mathbf{B}+\mathbf{C}^{-1})^{-1}\mathbf{D}\mathbf{A}^{-1}, \tag{4.15}$$

the MSE function (4.14) can be written as

$$J(\mathbf{F},\mathbf{G}) = \sigma_x^2 tr\Big\{\Big[\mathbf{I}_{N_S} + \sigma_x^2\mathbf{H}^H\mathbf{R}_n^{-1}\mathbf{H}\Big]^{-1}\Big\}. \tag{4.16}$$

Substituting (4.3) and (4.12) into (4.16), the MSE function can be expressed as

$$\begin{aligned} J(\mathbf{F},\mathbf{G})=\sigma_x^2 tr\Big\{\Big[&\mathbf{I}_{N_S} + \sigma_x^2\mathbf{F}^H\mathbf{H}_1^H\mathbf{G}^H\mathbf{H}_2^H \\ &\times\Big(\sigma_1^2\mathbf{H}_2\mathbf{G}\mathbf{G}^H\mathbf{H}_2^H + \sigma_2^2\mathbf{I}_{N_D}\Big)^{-1}\mathbf{H}_2\mathbf{G}\mathbf{H}_1\mathbf{F}\Big]^{-1}\Big\}. \end{aligned} \tag{4.17}$$

Using the matrix inversion lemma (4.15), the MSE function (4.17) can be written as

$$\begin{aligned} J(\mathbf{F},\mathbf{G})=\sigma_x^2 tr\Big\{\Big[&\mathbf{I}_{N_S} + \frac{\sigma_x^2}{\sigma_1^2}\mathbf{F}^H\mathbf{H}_1^H\Big[\mathbf{I}_{N_R} \\ &-\Big(\mathbf{I}_{N_R} + \frac{\sigma_1^2}{\sigma_2^2}\mathbf{G}^H\mathbf{H}_2^H\mathbf{H}_2\mathbf{G}\Big)^{-1}\Big]\mathbf{H}_1\mathbf{F}\Big]^{-1}\Big\}. \end{aligned} \tag{4.18}$$

Now the problem is reduced to find the optimal precoder matrices $\mathbf{F}$ and $\mathbf{G}$ that minimize $J(\mathbf{F},\mathbf{G})$ subject to the power constraints (4.8). Observing the MSE function (4.18) and power constraints (4.8), it is readily noticed that the optimization problem is not easy to solve with the current form. Hence, the optimization problem should be converted into scalar-valued optimization problem. The SVD and EVD properties of the matrix is used to simplify the optimization problem into scalar form. Hence, SVD of $\mathbf{H}_1$ can be written as

$$\mathbf{H}_1 = \mathbf{U}_1\mathbf{\Lambda}_1^{1/2}\mathbf{V}_1^H \tag{4.19}$$

where $\mathbf{\Lambda}_1 = \text{diag}\{\Lambda_{1,1}\cdots\Lambda_{1,N_R}\}$ is a diagonal matrix with $\Lambda_{1,1}\geq\cdots\geq\Lambda_{1,N_R}$, $\mathbf{U}_1$ and $\mathbf{V}_1$ are the singular matrices of $\mathbf{H}_1$. To diagonalize (4.18), $\mathbf{F}$ can be selected as [28]

$$\mathbf{F} = \mathbf{V}_1\mathbf{\Lambda}_F^{1/2}\mathbf{U}_F \tag{4.20}$$

where $\mathbf{\Lambda}_F = \text{diag}\{\Lambda_{\text{F},1} \cdots \Lambda_{F,N_R}\}$ is a diagonal matrix with $\Lambda_{\text{F},1} \geq \cdots \geq \Lambda_{F,N_R}$ and $\mathbf{U}_F$ is a unitary matrix. The EVD of $\mathbf{\Sigma}$ can be expressed as

$$\mathbf{\Sigma} = \mathbf{V}_\Sigma \mathbf{\Lambda}_\Sigma \mathbf{V}_\Sigma^H \tag{4.21}$$

where $\mathbf{\Lambda}_\Sigma = \text{diag}\{\Lambda_{\Sigma,1} \cdots \Lambda_{\Sigma,N_S}\}$ with $\Lambda_{\Sigma,1} \geq \cdots \geq \Lambda_{\Sigma,N_S}$. The columns of $\mathbf{V}_\Sigma$ are the eigenvectors of $\mathbf{\Sigma}$ for the corresponding eigenvalues. Substituting (4.21) into (4.6), the channel matrix $\mathbf{H}_2$ can be written as

$$\mathbf{H}_2 \triangleq \bar{\mathbf{H}}_\mu + \widetilde{\mathbf{H}}_\omega \mathbf{\Lambda}_\Sigma^{1/2} \mathbf{V}_\Sigma^H \tag{4.22}$$

where $\widetilde{\mathbf{H}}_\omega \triangleq \mathbf{H}_\omega \mathbf{V}_\Sigma$. Here, $\widetilde{\mathbf{H}}_\omega$ has the same distribution as $\mathbf{H}_\omega$, because the unitary matrix $\mathbf{V}_\Sigma$ does not change the statistical distribution of $\mathbf{H}_\omega$. Due to the similar statistical distribution, the $\widetilde{\mathbf{H}}_\omega$ is an $N_D \times N_R$ Gaussian matrix having i.i.d. circularly symmetric complex entries. Let's assume that the optimal precoding matrix $\mathbf{G}$ which minimizes (4.18) can be expressed as

$$\mathbf{G} = \mathbf{V}_\Sigma \mathbf{\Lambda}_G^{1/2} \mathbf{U}_1^H \tag{4.23}$$

where $\mathbf{\Lambda}_G = \text{diag}\{\Lambda_{G,1} \cdots \Lambda_{G,N_R}\}$. Substituting (4.19) - (4.23) in (4.18), now the MSE function is given by

$$\begin{aligned} J(\mathbf{\Lambda}_F, \mathbf{\Lambda}_G) = \sigma_x^2 tr\Big\{ \Big[\mathbf{I}_{N_S} + \frac{\sigma_x^2}{\sigma_1^2} \mathbf{U}_F^H \mathbf{\Lambda}_F^{1/2} \mathbf{\Lambda}_1^{1/2} \mathbf{U}_1^H \\ \times \Big[\mathbf{I}_{N_R} - \mathbf{D}_1 \Big] \mathbf{U}_1 \mathbf{\Lambda}_1^{1/2} \mathbf{\Lambda}_F^{1/2} \mathbf{U}_F \Big]^{-1} \Big\} \end{aligned} \tag{4.24}$$

where

$$\begin{aligned} \mathbf{D}_1 = \Big(\mathbf{I}_{N_R} + \frac{\sigma_1^2}{\sigma_2^2} \mathbf{U}_1 \mathbf{\Lambda}_G^{1/2} \mathbf{V}_\Sigma^H \Big[\bar{\mathbf{H}}_\mu + \widetilde{\mathbf{H}}_\omega \mathbf{\Lambda}_\Sigma^{1/2} \mathbf{V}_\Sigma^H \Big]^H \\ \times \Big[\bar{\mathbf{H}}_\mu + \widetilde{\mathbf{H}}_\omega \mathbf{\Lambda}_\Sigma^{1/2} \mathbf{V}_\Sigma^H \Big] \mathbf{V}_\Sigma \mathbf{\Lambda}_G^{1/2} \mathbf{U}_1^H \Big)^{-1}. \end{aligned}$$

Using the SVD and trace properties, the MSE function (4.24) can be simplified to

$$J(\mathbf{\Lambda}_F, \mathbf{\Lambda}_G) = \sigma_x^2 tr\Big\{ \Big[\mathbf{I}_{N_S} + \frac{\sigma_x^2}{\sigma_1^2} \mathbf{\Lambda}_F^{1/2} \mathbf{\Lambda}_1^{1/2} \Big[\mathbf{I}_{N_R} - \mathbf{D}_2 \Big] \mathbf{\Lambda}_1^{1/2} \mathbf{\Lambda}_F^{1/2} \Big]^{-1} \Big\} \tag{4.25}$$

where

$$\begin{aligned} \mathbf{D}_2 = \Big(\mathbf{I}_{N_R} + \frac{\sigma_1^2}{\sigma_2^2} \mathbf{\Lambda}_G^{1/2} \mathbf{V}_\Sigma^H \Big[\bar{\mathbf{H}}_\mu^H \bar{\mathbf{H}}_\mu + \bar{\mathbf{H}}_\mu^H \widetilde{\mathbf{H}}_\omega \mathbf{\Lambda}_\Sigma^{1/2} \mathbf{V}_\Sigma^H \\ + \mathbf{V}_\Sigma \mathbf{\Lambda}_\Sigma^{1/2} \widetilde{\mathbf{H}}_\omega^H \bar{\mathbf{H}}_\mu + \mathbf{V}_\Sigma \mathbf{\Lambda}_\Sigma^{1/2} \widetilde{\mathbf{H}}_\omega^H \widetilde{\mathbf{H}}_\omega \mathbf{\Lambda}_\Sigma^{1/2} \mathbf{V}_\Sigma^H \Big] \mathbf{V}_\Sigma \mathbf{\Lambda}_G^{1/2} \Big)^{-1}. \end{aligned}$$

It can be seen from (4.25) that $J(\mathbf{\Lambda}_F, \mathbf{\Lambda}_G)$ depends on $\widetilde{\mathbf{H}}_\omega$, which is random and unknown. In the following, $E_{\widetilde{\mathbf{H}}_\omega}\{J(\mathbf{\Lambda}_F, \mathbf{\Lambda}_G)\}$ is optimized, where $E_{\widetilde{\mathbf{H}}_\omega}\{.\}$ indicates that the expectation is taken with respect to the random matrix $\widetilde{\mathbf{H}}_\omega$. Now $E_{\widetilde{\mathbf{H}}_\omega}\{J(\mathbf{\Lambda}_F, \mathbf{\Lambda}_G)\}$ can be expressed as

$$E_{\widetilde{\mathbf{H}}_\omega}\{J(\mathbf{\Lambda}_F, \mathbf{\Lambda}_G)\}=\sigma_x^2\sigma_1^2 E_{\widetilde{\mathbf{H}}_\omega}\Big[tr\Big\{\Big[\sigma_1^2\mathbf{I}_{N_S}+\sigma_x^2\mathbf{\Lambda}_F^{1/2}\mathbf{\Lambda}_1^{1/2} \times\Big[\mathbf{I}_{N_R}-\mathbf{D}_2\Big]\mathbf{\Lambda}_1^{1/2}\mathbf{\Lambda}_F^{1/2}\Big]^{-1}\Big\}\Big]. \tag{4.26}$$

Now the work is left to determine the diagonal elements $\mathbf{\Lambda}_F$ and $\mathbf{\Lambda}_G$ of precoder matrices $\mathbf{F}$ and $\mathbf{G}$. Direct minimization of (4.26) for the optimal power allocation is difficult. In the following, the lower bound of the MSE is used together with the power constraint (4.8) to derive the suboptimal power allocation for the precoder matrices $\mathbf{F}$ and $\mathbf{G}$. Since $J(\mathbf{\Lambda}_F, \mathbf{\Lambda}_G)$ is convex in $\widetilde{\mathbf{H}}_\omega^H\widetilde{\mathbf{H}}_\omega$, which is proved in Appendix 4.A and has the following lower bound using Jensen's inequality [65]

$$E_{\widetilde{\mathbf{H}}_\omega}\{J_L(\mathbf{\Lambda}_F, \mathbf{\Lambda}_G)\}=\sigma_x^2\sigma_1^2 tr\Big\{\Big[\sigma_1^2\mathbf{I}_{N_S}+\sigma_x^2\mathbf{\Lambda}_F^{1/2}\mathbf{\Lambda}_1^{1/2} \times\Big[\mathbf{I}_{N_R}-\mathbf{D}_3\Big]\mathbf{\Lambda}_1^{1/2}\mathbf{\Lambda}_F^{1/2}\Big]^{-1}\Big\} \tag{4.27}$$

where

$$\mathbf{D}_3=\Big(\mathbf{I}_{N_R}+\frac{\sigma_1^2}{\sigma_2^2}\mathbf{\Lambda}_G^{1/2}\mathbf{V}_\Sigma^H\Big(\bar{\mathbf{H}}_\mu^H\bar{\mathbf{H}}_\mu+E_{\widetilde{\mathbf{H}}_\omega}\{\bar{\mathbf{H}}_\mu^H\widetilde{\mathbf{H}}_\omega\}\mathbf{\Lambda}_\Sigma^{1/2}\mathbf{V}_\Sigma^H +\mathbf{V}_\Sigma\mathbf{\Lambda}_\Sigma^{1/2}E_{\widetilde{\mathbf{H}}_\omega}\{\widetilde{\mathbf{H}}_\omega^H\bar{\mathbf{H}}_\mu\}+\mathbf{V}_\Sigma\mathbf{\Lambda}_\Sigma^{1/2}E_{\widetilde{\mathbf{H}}_\omega}\{\widetilde{\mathbf{H}}_\omega^H\widetilde{\mathbf{H}}_\omega\}\mathbf{\Lambda}_\Sigma^{1/2}\mathbf{V}_\Sigma^H\Big)\mathbf{V}_\Sigma\mathbf{\Lambda}_G^{1/2}\Big)^{-1}.$$

Using the properties of Gaussian random matrices with i.i.d circularly symmetric complex entries, $E_{\widetilde{\mathbf{H}}_\omega}\{\widetilde{\mathbf{H}}_\omega^H\widetilde{\mathbf{H}}_\omega\}=N_D\mathbf{I}_{NR}$, $E_{\widetilde{\mathbf{H}}_\omega}\{\bar{\mathbf{H}}_\mu^H\widetilde{\mathbf{H}}_\omega\}=E_{\widetilde{\mathbf{H}}_\omega}\{\widetilde{\mathbf{H}}_\omega^H\bar{\mathbf{H}}_\mu\}=0$ and taking the expectation on (4.27) with respect to $E_{\widetilde{\mathbf{H}}_\omega}$, the MSE function can be written as

$$J_L(\mathbf{\Lambda}_F, \mathbf{\Lambda}_G)=\sigma_x^2\sigma_1^2 tr\Big\{\Big[\sigma_1^2\mathbf{I}_{N_S}+\sigma_x^2\mathbf{\Lambda}_F^{1/2}\mathbf{\Lambda}_1^{1/2} \times\Big[\mathbf{I}_{N_R}-\mathbf{D}_4\Big]\mathbf{\Lambda}_1^{1/2}\mathbf{\Lambda}_F^{1/2}\Big]^{-1}\Big\} \tag{4.28}$$

where

$$\mathbf{D}_4=\Big(\mathbf{I}_{N_R}+\frac{\sigma_1^2}{\sigma_2^2}\mathbf{\Lambda}_G^{1/2}\mathbf{V}_\Sigma^H\Big[\bar{\mathbf{H}}_\mu^H\bar{\mathbf{H}}_\mu+N_D\mathbf{V}_\Sigma\mathbf{\Lambda}_\Sigma\mathbf{V}_\Sigma^H\Big]\mathbf{V}_\Sigma\mathbf{\Lambda}_G^{1/2}\Big)^{-1}.$$

After using the SVD properties, the MSE function (4.28) can be simplified to

$$J_L(\mathbf{\Lambda}_F, \mathbf{\Lambda}_G)=\sigma_x^2\sigma_1^2 tr\Big\{\Big[\sigma_1^2\mathbf{I}_{N_S}+\sigma_x^2\mathbf{\Lambda}_F^{1/2}\mathbf{\Lambda}_1^{1/2} \times\Big[\mathbf{I}_{N_R}-\mathbf{D}_5\Big]\mathbf{\Lambda}_1^{1/2}\mathbf{\Lambda}_F^{1/2}\Big]^{-1}\Big\} \tag{4.29}$$

where

$$\mathbf{D}_5 = \Big(\mathbf{I}_{N_R} + \frac{\sigma_1^2}{\sigma_2^2}\mathbf{\Lambda}_G^{1/2}(\mathbf{V}_\Sigma^H \bar{\mathbf{H}}_\mu^H \bar{\mathbf{H}}_\mu \mathbf{V}_\Sigma + N_D \mathbf{\Lambda}_\Sigma)\mathbf{\Lambda}_G^{1/2}\Big)^{-1}.$$

To proceed further, using the matrix inversion lemma (4.15), the MSE function (4.29) can be written as

$$\begin{aligned} J_L(\mathbf{\Lambda}_F, \mathbf{\Lambda}_G) = \sigma_x^2\sigma_1^2 tr\Big\{\Big[\sigma_1^2\mathbf{I}_{N_S} + \sigma_x^2\mathbf{\Lambda}_F^{1/2}\mathbf{\Lambda}_1^{1/2}\mathbf{\Lambda}_G^{1/2} \\ \times\Big[\mathbf{\Lambda}_G + \frac{\sigma_2^2}{\sigma_1^2}\Big(\mathbf{V}_\Sigma^H \bar{\mathbf{H}}_\mu^H \bar{\mathbf{H}}_\mu \mathbf{V}_\Sigma + N_D\mathbf{\Lambda}_\Sigma\Big)^{-1}\Big]^{-1}\mathbf{\Lambda}_G^{1/2}\mathbf{\Lambda}_1^{1/2}\mathbf{\Lambda}_F^{1/2}\Big]^{-1}\Big\} \end{aligned} \quad (4.30)$$

Applying the matrix inversion lemma (4.15), the MSE function (4.30) can be written as

$$\begin{aligned} J_L(\mathbf{\Lambda}_F, \mathbf{\Lambda}_G) = \sigma_x^2 tr\Big\{\Big[\mathbf{I}_{N_S} - \frac{1}{\sigma_1^2}\mathbf{\Lambda}_F^{1/2}\mathbf{\Lambda}_1^{1/2}\mathbf{\Lambda}_G^{1/2}\Big(\frac{1}{\sigma_1^2}\mathbf{\Lambda}_G^{1/2}\mathbf{\Lambda}_1^{1/2}\mathbf{\Lambda}_F\mathbf{\Lambda}_1^{1/2}\mathbf{\Lambda}_G^{1/2} + \mathbf{C}\Big)^{-1} \\ \times\mathbf{\Lambda}_G^{1/2}\mathbf{\Lambda}_1^{1/2}\mathbf{\Lambda}_F^{1/2}\Big]\Big\} \end{aligned} \quad (4.31)$$

where

$$\mathbf{C} = \frac{1}{\sigma_x^2}\Big[\mathbf{\Lambda}_G + \frac{\sigma_2^2}{\sigma_1^2}\Big(\mathbf{V}_\Sigma^H \bar{\mathbf{H}}_\mu^H \bar{\mathbf{H}}_\mu \mathbf{V}_\Sigma + N_D\mathbf{\Lambda}_\Sigma\Big)^{-1}\Big].$$

An upper-bound of (4.31) is considered. Hence, the MSE function (4.31) can be rewritten as

$$J_L(\mathbf{\Lambda}_F, \mathbf{\Lambda}_G) = \sigma_x^2\Big[tr\Big(\mathbf{A}^{-1}\Big) - tr\Big(\mathbf{A}^{-1}\mathbf{E}^H\Big(\mathbf{E}\mathbf{A}^{-1}\mathbf{E}^H + \mathbf{C}\Big)^{-1}\mathbf{E}\mathbf{A}^{-1}\Big)\Big] \quad (4.32)$$

where

$$\begin{aligned} \mathbf{A} &= \mathbf{I}_{N_S}, \\ \mathbf{E} &= \frac{1}{\sigma_1}\mathbf{\Lambda}_G^{1/2}\mathbf{\Lambda}_1^{1/2}\mathbf{\Lambda}_F^{1/2}. \end{aligned}$$

By using the following inequality from [28]

$$\begin{aligned} &tr\Big(\mathbf{A}^{-1}\mathbf{E}^H\Big(\mathbf{E}\mathbf{A}^{-1}\mathbf{E}^H + \mathbf{C}\Big)^{-1}\mathbf{E}\mathbf{A}^{-1}\Big) \\ &\geq tr\Big(\mathbf{A}^{-1}\mathbf{E}^H\Big(\mathbf{E}\mathbf{A}^{-1}\mathbf{E}^H + \mathrm{diag}(\mathbf{C})\Big)^{-1}\mathbf{E}\mathbf{A}^{-1}\Big), \end{aligned} \quad (4.33)$$

an upper-bound of $J_L(\mathbf{\Lambda}_F, \mathbf{\Lambda}_G)$ is given by

$$J_U(\mathbf{\Lambda}_F, \mathbf{\Lambda}_G) = \sigma_x^2 tr\Big\{\Big[\mathbf{I}_{N_S} - \Big(\mathbf{\Lambda}_F\mathbf{\Lambda}_1\mathbf{\Lambda}_G + \sigma_1^2\lambda_C\Big)^{-1}\mathbf{\Lambda}_F\mathbf{\Lambda}_1\mathbf{\Lambda}_G\Big]\Big\} \quad (4.34)$$

where

$$\lambda_C = \frac{1}{\sigma_x^2}\mathrm{diag}\Big[\mathbf{\Lambda}_G + \frac{\sigma_2^2}{\sigma_1^2}\Big(\mathbf{V}_\Sigma^H \bar{\mathbf{H}}_\mu^H \bar{\mathbf{H}}_\mu \mathbf{V}_\Sigma + N_D\mathbf{\Lambda}_\Sigma\Big)^{-1}\Big]. \quad (4.35)$$

Inserting (4.20) into (4.8), the power constraint for the source node can be expressed as

$$p(\mathbf{\Lambda}_F) = \sigma_x^2 tr\Big\{\mathbf{\Lambda}_F\Big\} \leq P_s. \tag{4.36}$$

Substituting (4.19) and (4.23) into (4.8), the power constraint for the relay node can be expressed as

$$\begin{aligned} p(\mathbf{\Lambda}_F, \mathbf{\Lambda}_G) = & tr\Big\{\mathbf{V}_\Sigma \mathbf{\Lambda}_G^{1/2} \mathbf{U}_1^H \Big(\sigma_x^2 \mathbf{U}_1 \mathbf{\Lambda}_1^{1/2} \mathbf{\Lambda}_F \mathbf{\Lambda}_1^{1/2} \mathbf{U}_1^H + \sigma_1^2 \mathbf{I}_{N_R}\Big) \\ & \times \mathbf{U}_1 \mathbf{\Lambda}_G^{1/2} \mathbf{V}_\Sigma^H \Big\} \leq P_r. \end{aligned} \tag{4.37}$$

Using the SVD and trace properties, the power constraint (4.37) can be simplified to

$$p(\mathbf{\Lambda}_F, \mathbf{\Lambda}_G) = tr\Big\{\big(\sigma_x^2 \mathbf{\Lambda}_1 \mathbf{\Lambda}_F + \sigma_1^2 \mathbf{I}_{N_R}\big) \mathbf{\Lambda}_G\Big\} \leq P_r. \tag{4.38}$$

4.3.1 Joint Source and Relay Precoder Design

In this section, a joint source and relay procder design is proposed to obtain the diagonal elements of $\mathbf{\Lambda}_F$, $\mathbf{\Lambda}_G$. From (4.34), (4.36) and (4.38), the diagonal elements of $\mathbf{\Lambda}_F$, $\mathbf{\Lambda}_G$ can be obtained by solving the following constrained optimization problem with scalar variables

$$\min J_U(\mathbf{\Lambda}_F, \mathbf{\Lambda}_G) = \sum_{i=1}^{N_S} \frac{\sigma_x^2 \sigma_1^2 \lambda_{C,i}}{\Lambda_{1,i} \Lambda_{F,i} \Lambda_{G,i} + \sigma_1^2 \lambda_{C,i}} \tag{4.39}$$

$$s.t.\ p(\mathbf{\Lambda}_F) = \sigma_x^2 \sum_{i=1}^{N_S} \Lambda_{F,i} \leq P_s, \tag{4.40}$$

$$p(\mathbf{\Lambda}_F, \mathbf{\Lambda}_G) = \sum_{i=1}^{N_S} \big(\sigma_x^2 \Lambda_{1,i} \Lambda_{F,i} + \sigma_1^2\big) \Lambda_{G,i} \leq P_r. \tag{4.41}$$

Using the KKT conditions [61], the optimal diagonal elements of $\Lambda_{F,i}$ and $\Lambda_{G,i}$ are obtained as

$$\Lambda_{F,i} = \frac{1}{\Lambda_{1,i} \Lambda_{G,i}} \left(\sqrt{\frac{\sigma_1^2 \lambda_{C,i} \Lambda_{1,i} \Lambda_{G,i}}{\mu_s + \mu_r \Lambda_{1,i} \Lambda_{G,i}}} - \sigma_1^2 \lambda_{C,i} \right)^+ \tag{4.42}$$

$$\Lambda_{G,i} = \frac{1}{\Lambda_{1,i} \Lambda_{F,i}} \left(\sqrt{\frac{\sigma_x^2 \sigma_1^2 \lambda_{C,i} \Lambda_{1,i} \Lambda_{F,i}}{\mu_r (\sigma_x^2 \Lambda_{1,i} \Lambda_{F,i} + \sigma_1^2)}} - \sigma_1^2 \lambda_{C,i} \right)^+ \tag{4.43}$$

where $(x)^+ = \max(x, 0)$, μ_s and μ_r should be chosen to meet the power constraints (4.40) and (4.41).

It can be seen from (4.42) and (4.43) that the diagonal elements of $\Lambda_{F,i}$, $\Lambda_{G,i}$ matrices are function of each other, so directly solving the diagonal elements of the matrices are

too difficult. To avoid this difficulty, an iterative algorithm is proposed to compute the diagonal elements of $\Lambda_{F,i}$ and $\Lambda_{G,i}$.

In this algorithm, initialize $\mathbf{\Lambda}_F = \mathbf{I}_{N_s}$ and $\mathbf{\Lambda}_G = \mathbf{I}_{N_s}$. Then calculate λ_C with (4.35), and calculate the water filling variables μ_r and μ_s to satisfy the power constraints (4.8) at the source and destination nodes. Update $\mathbf{\Lambda}_F$ and $\mathbf{\Lambda}_G$ according to (4.42) and (4.43) respectively. $\mathbf{\Lambda}_F$ and $\mathbf{\Lambda}_G$ are iteratively updated until $||\mathbf{\Lambda}'_F - \mathbf{\Lambda}_F|| \leq 0.0001$ and $||\mathbf{\Lambda}'_G - \mathbf{\Lambda}_G|| \leq 0.0001$. Here $\mathbf{\Lambda}'_F$ and $\mathbf{\Lambda}'_G$ are the two recent calculated values of $\mathbf{\Lambda}_F$ and $\mathbf{\Lambda}_G$.

4.3.2 Relay-only Precoder Design

In this section, a suboptimal algorithm is proposed to obtain the diagonal elements of $\mathbf{\Lambda}_G$ while fixing $\mathbf{\Lambda}_F$. It is assumed that $\mathbf{\Lambda}_F = \mathbf{I}_{N_S}$, the constrained optimization problem (4.39) to (4.41) can be rewritten in scalar form as

$$\min J_U(\mathbf{\Lambda}_G) = \sum_{i=1}^{N_S} \frac{\sigma_x^2 \sigma_1^2 \lambda_{C,i}}{\Lambda_{1,i}\Lambda_{G,i} + \sigma_1^2 \lambda_{C,i}} \tag{4.44}$$

$$s.t.\ p(\mathbf{\Lambda}_G) = \sum_{i=1}^{N_S} \left(\sigma_x^2 \Lambda_{1,i} + \sigma_1^2\right) \Lambda_{G,i} \leq P_r. \tag{4.45}$$

Using the KKT conditions [61], the optimal diagonal elements of $\Lambda_{G,i}$ are obtained as

$$\Lambda_{G,i} = \frac{1}{\Lambda_{1,i}} \left(\sqrt{\frac{\sigma_x^2 \sigma_1^2 \lambda_{C,i} \Lambda_{1,i}}{\mu_r (\sigma_x^2 \Lambda_{1,i} + \sigma_1^2)}} - \sigma_1^2 \lambda_{C,i} \right)^+ \tag{4.46}$$

where μ_r should be chosen to meet the power constraint (4.45).

4.4 Numerical Examples

In this section, the performance of the proposed algorithms is verified by numerical examples. The unitary matrix, $\mathbf{U}_F$, of the source precoder matrix (4.20) is generated by the N_S-point discrete Fourier-transform matrix. The channel matrices $\mathbf{H}_1$ and $\mathbf{H}_\omega$ are generated as complex Gaussian variables with zero mean and unit variance. The mean, $\bar{\mathbf{H}}_\mu$, of $\mathbf{H}_2$ is randomly generated as

$$\bar{\mathbf{H}}_\mu = \begin{bmatrix} 0.33 + 0.47i, & 1.03 - 0.96i, & 0.88 - 0.17i, & -0.94 + 0.82i \\ 0.58 + 0.01i, & 0.93 - 0.08i, & -0.56 - 0.12i, & 1.02 - 0.32i \\ 0.73 - 0.05i, & 0.49 - 0.56i, & -0.36 - 0.67i, & -0.39 + 0.72i \\ -0.62 - 1.72i, & 0.51 + 0.95i, & 1.00 - 0.88i, & -0.09 - 0.05i \end{bmatrix}$$

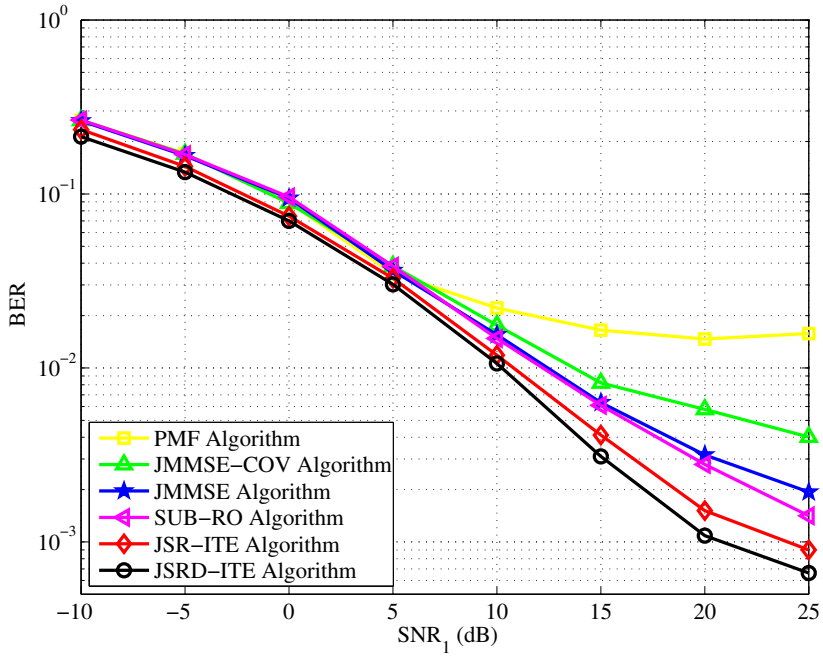

Figure 4.2: BER versus SNR_1 while fixing $\text{SNR}_2 = 20\text{dB}$.

The elements of covariance matrix $\mathbf{\Sigma}$ of $\mathbf{H}_2$ is generated by $\Sigma_{i,j} = J_0(\triangle\pi|i-j|)$ [11], where $J_0(.)$ is the zeroth order Bessel function of the first kind, $\triangle$ the angle of fading spread. The SNRs for the source-relay and relay-destination links are defined as follows $\text{SNR}_1 = \frac{\sigma_x^2}{\sigma_1^2}$, $\text{SNR}_2 = \frac{P_r}{N_R\sigma_1^2}$.

The performance of the proposed schemes is compared with the PMF [22], JMMSE [23], JMMSE-COV [32] algorithms, and the iterative joint source, relay and destination algorithm (JSRD-ITE) [67]. The JSRD-ITE algorithm provides the lower-bound of the proposed schemes.

In the first example, a non-regenerative MIMO relay system is simulated with $N_S = N_R = N_D = 4$. The angle spread is set as $\triangle = 30^o$. The symbols are generated from 1000 QPSK constellation at the source node. The Fig. 4.2 shows the performance of the MSE algorithms in terms of BER versus SNR_1 while fixing SNR_2 = 20dB. The proposed suboptimal relay-only (SUB-RO) algorithm shows better BER performance over all range of SNR_1 than the PMF and JMMSE-COV algorithms. For $\text{SNR}_1 \leq 15dB$, the BER performance of the SUB-RO algorithm is closer to that of the JMMSE algorithm. For $\text{SNR}_1 \geq 15dB$, the proposed SUB-RO algorithm outperforms the JMMSE algorithm. The proposed iterative joint source and relay (JSR-ITE) algorithm outperforms the JMMSE-COV, SUB-RO and JMMSE algorithms over the tested

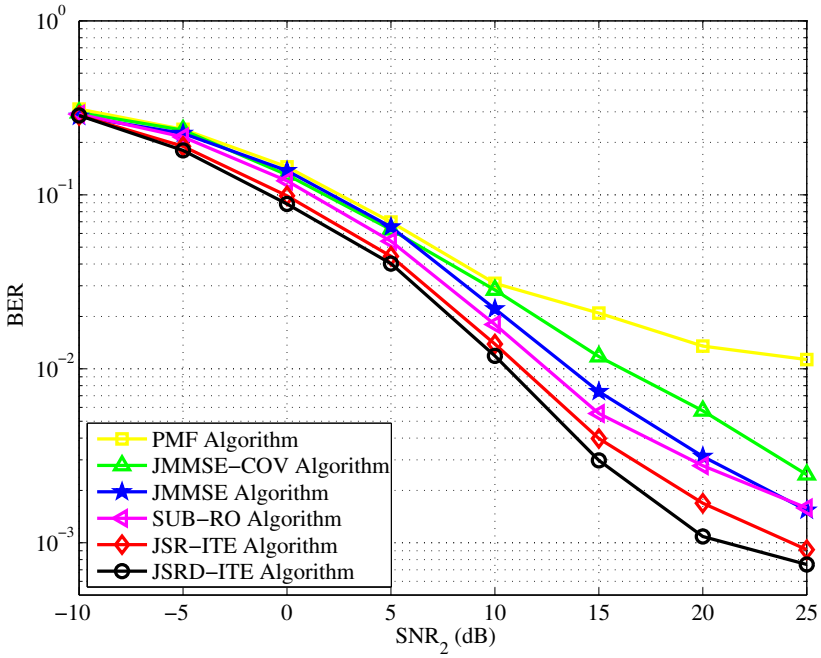

Figure 4.3: BER versus SNR_2 while fixing $\mathrm{SNR}_1 = 20\mathrm{dB}$.

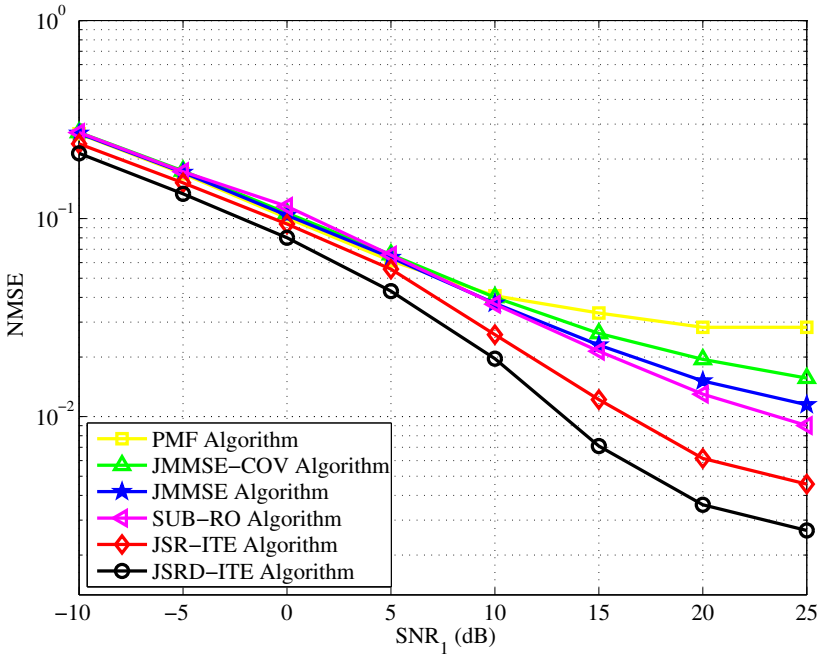

Figure 4.4: NMSE versus SNR_1 while fixing $\mathrm{SNR}_2 = 20\mathrm{dB}$.

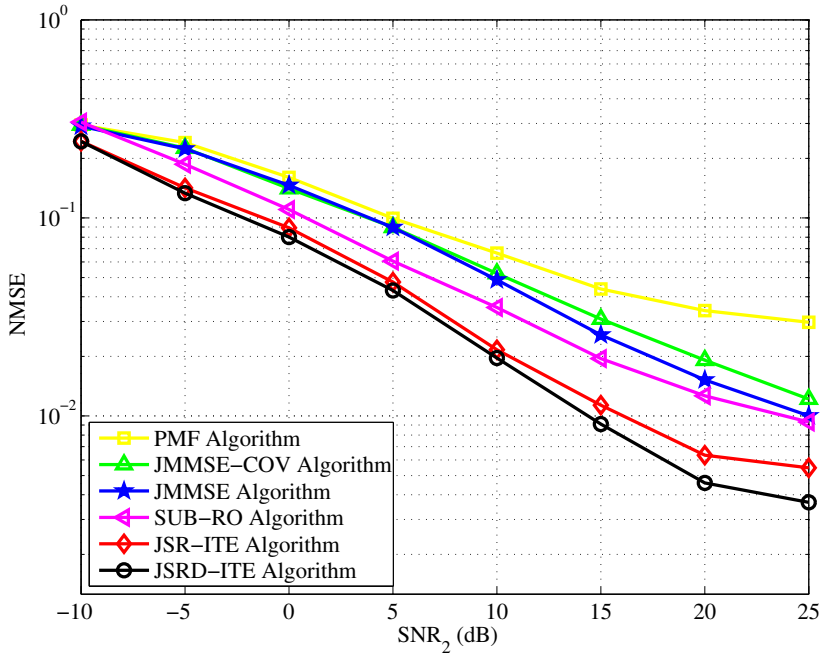

Figure 4.5: NMSE versus SNR_2 while fixing $SNR_1 = 20$dB.

range of SNR_1.

In the second example, the BER performance of the MSE algorithms is compared for various SNR_2 while fixing SNR_1= 20dB and the MIMO relay system is simulated with $N_S = N_R = N_D$=4. The angle of the delay spread is fixed as $\triangle = 30^o$. 1000 randomly generated QPSK constellations are transmitted from source node for each channel realization. It can be noticed from the Fig. 4.3 that the proposed SUB-RO algorithm has better performance than the PMF, JMMSE-COV and JMMSE algorithms. It can be noticed from the Fig. 4.3 that the performance of the proposed JSR-ITE algorithm outshines the JMMSE-COV, SUB-RO and JMMSE algorithms over the tested range of SNR_2.

In the third example, the NMSE performance of the MSE algorithms is investigated for various SNR_1 while fixing $SNR_2 = 20$dB. In the simulation, the delay spread angle is set to $\triangle = 30^o$ and the number of antennas at the source, relay and destination nodes are set as $N_S = N_R = N_D$=4. In the example, 1000 QPSK samples are randomly generated at source node for each channel realization. From Fig. 4.4, it can be concluded that PMF, JMMSE-COV, JMMSE algorithms produce much higher NMSE as compared to the proposed SUB-RO algorithm at high SNR (SNR_1 >10dB). It is clearly shown in Fig. 4.4 that the proposed JSR-ITE algorithm offers improved performance in terms of

NMSE compared to the PMF, JMMSE-COV, SUB-RO and JMMSE algorithms over the entire range of SNR_1.

In the final example, the performance of the MSE algorithms is studied for varying SNR_2 while fixing $\mathrm{SNR}_1 = 20\mathrm{dB}$. In this example, the number of antennas in the source, relay and destination nodes are fixed as $N_S = N_R = N_D = 4$ and the angle of delay spread is set as $\triangle = 30^o$. 1000 QPSK symbols are randomly generated at the source node for each channel realization. It can be observed from the Fig. 4.5 that the proposed SUB-RO algorithm has a better NMSE performance than the PMF, JMMSE-COV, JMMSE algorithms. It can be notice from the Fig. 4.5 that the proposed JSR-ITE algorithm always outperforms the PMF, JMMSE-COV, SUB-RO and JMMSE algorithms over the entire range of SNR_2.

4.5 Chapter Summary

In this chapter, the optimal structure of the source and relay precoder matrices of the non-regenerative MIMO relay system is derived to minimize the MSE of the symbol estimation at the destination node with the assumption that the mean and covariance feedback of the relay-destination link are available at the relay node. It is assumed that the relay knows the full CSI of the source-relay link. Simulation results show that the proposed schemes, which minimize the upper-bound of the MSE is achieved and its demonstrate that the proposed scheme has better performance in terms of NMSE and BER as compared to the conventional full CSI and covariance feedback based MSE schemes.

4.A Appendix

In this section, the convexity of the MSE function (4.26) for $\widetilde{\mathbf{H}}_{\omega}^{H}\widetilde{\mathbf{H}}_{\omega}$ is proved. A set of $N_D \times N_R$ positive definite Hermitian matrix is $\mathbf{Z}$. Using the inversion lemma (4.15), the MSE function (4.26) can be rewritten as

$$E_{\mathbf{Z}}[J(\mathbf{F},\mathbf{G})]=\sigma_x^2\sigma_1^2 E_{\mathbf{Z}}\Big[tr\Big\{\Big[\sigma_1^2\mathbf{I}_{N_S}\sigma_x^2\mathbf{\Lambda}_F^{1/2}\mathbf{\Lambda}_1^{1/2}\mathbf{\Lambda}_G^{1/2}\mathbf{V}_{\Sigma}^{H} \times\Big(\mathbf{V}_{\Sigma}\mathbf{\Lambda}_G\mathbf{V}_{\Sigma}^{H}+\frac{\sigma_2^2}{\sigma_1^2}\Big[\mathbf{Z}^H\mathbf{Z}\Big]^{-1}\Big)^{-1}\mathbf{\Lambda}_1^{1/2}\mathbf{\Lambda}_F^{1/2}\Big]^{-1}\Big\}\Big] \tag{4.47}$$

where

$$\mathbf{Z}=\Big(\bar{\mathbf{H}}_{\mu}^{H}+\widetilde{\mathbf{H}}_{\omega}\mathbf{\Lambda}_{\Sigma}^{1/2}\mathbf{V}_{\Sigma}^{H}\Big).$$

From [65], $f(\mathbf{Z}) = \mathbf{Z}^{-1}$ is a matrix-convex function of $\mathbf{Z}$. Hence, the MSE function (4.47) is a convex function for $\mathbf{Z}^H\mathbf{Z}$.

Chapter 5

Non-linear MIMO Relay Design with Covariance Feedback

In this chapter, the performance of the TH precoder based non-linear transceiver design is investigated for a non-regenerative MIMO relay system assuming that the full CSI of the source-relay link is known, while only the CCI of the relay-destination link is available at the relay node. Overview of the existing work is described in Section 5.1. The system model and problem formulation are presented in Section 5.2. In Section 5.3, the optimal structure of the TH precoding, the source precoding and the relay precoding matrices are derived to minimize the MSE of the signal waveform estimation at the destination node. Numerical examples are shown in Section 5.4 to verify the performance of the proposed algorithms, and chapter summary is drawn in Section 5.5.

5.1 Overview of Existing Techniques

In cooperative communication systems, relay nodes can be deployed between the source and destination nodes to mitigate the channel shadowing effect and provide system spatial diversity. Therefore, cooperative communication has great potential in extending the network coverage and increasing the system throughput with reduced infrastructure cost, and thus, has attracted much research interest recently [19, 50].

Wireless relays can be regenerative or non-regenerative [17, 19, 50, 69]. In the regenerative relay strategy, the relay decodes the received signals from the source node and retransmits the re-encoded information to the destination node. In the non-regenerative

relay strategy [17], the relay node simply amplifies (including a possible linear transformation) the received signals from the source node and retransmits the amplified signals to the destination node. Therefore, the complexity and the processing delay of the non-regenerative strategy are generally much smaller than the regenerative strategies.

On the other hand, MIMO systems can provide spatial diversity and multiplexing gains to wireless communication systems [20]. When nodes in a relay network have multiple transmit/receive dimensions, such a system is called as MIMO relay system. In [21, 22, 51–54], relay precoder designs for a two-hop non-regenerative MIMO relay system have been proposed to maximize the mutual information between the source and destination nodes. In [23–28, 55–57], relay precoding algorithms have been developed to minimize the MSE of the signal waveform estimation at the destination node. The precoder designs in [21–28, 51–53, 55–57] assume that the full CSI of the source-relay and relay-destination links is available at the relay node.

However, in practical relay communication systems, the exact CSI is unknown and therefore, has to be estimated. There is always mismatch between the true and the estimated CSI due to channel noise, quantization errors and outdated channel estimates. A more practical assumption is that only partial information of the relay-destination channel is available at the relay node. In [29–31, 58], relay precoding matrix design has been investigated for maximizing the ergodic capacity of the relay system with the CCI of the relay-destination channel. Robust broadcasting schemes have been developed in [70] to minimize the transmission power necessary to guarantee that the quality-of-service (QoS) requirements are satisfied for all channels within bounded uncertainty regions around the transmitters estimate of each users channel. MMSE based transceiver designs have been addressed in [32–35] with the assumption that the relay knows the CCI of the relay-destination link and the full CSI of the source-relay link.

In the work of [29–35], linear transceiver design has been considered for MIMO relay systems, i.e., linear source/relay precoders and linear MMSE receiver. Compared with linear transceivers, non-linear transceivers have a better BER performance. Recently, non-linear transceiver based non-regenerative MIMO relay system design has been proposed [36, 37]. Non-linear transceiver can be implemented at the receiver as a DFE and/or at the transmitter in the form of a TH precoder. In general, the TH precoding scheme has a better BER performance than the DFE-based transceiver design, as the latter one suffers from error propagation.

The performance of the TH precoding scheme has been well studied for one-hop MIMO systems [38, 39, 71, 72]. In [73], a TH-based pre-filtering algorithm has been designed for multi-antenna multi-user systems where the base station allocates the transmit power according to the QoS requirement of each active user. A unified approach has been developed in [74] for transceiver optimization in MIMO systems with TH precoding at the transmitter and linear equalization at the receiver. In [75], a multiuser MIMO TH precoding algorithm has been proposed based on quantized CSI at the transmitter side. Recently, the TH precoding scheme has been introduced to non-regenerative MIMO relay systems [40] with the assumption that the full CSI of the entire channel is known at the relay node. In [41–43], imperfect CSI has been considered for designing the TH precoding based non-regenerative MIMO relay systems. Due to the nonlinearity nature of the precoding scheme, the TH precoding is highly sensitive to the time-varying nature of the wireless channel [44]. Hence, covariance information based non-linear transceiver design is more appropriate in such scenario.

In this chapter, a TH precoder-based transceiver design is proposed for two-hop non-regenerative MIMO relay systems where the full CSI of the source-relay link is known, while only the CCI of the relay-destination link is available at the relay node. In particular, it is assumed that the channel of the relay-destination link is correlated at the transmit antennas and uncorrelated at the receive antennas. This model is suitable for an environment where the relay is not surrounded by local scatterers [11] and the destination node is located amongst rich scatterers [30, 31]. Similar to [23, 25, 32, 33], it is assumed that there is no direct link between the source and destination nodes. Moreover, a TH precoder is considered at the source node. The relay precoder is assumed as a linear precoder and the destination node is considered as a linear MMSE receiver.

A transceiver design is proposed that minimizes the MSE of the signal waveform estimation at the destination node. First, the structure of the optimal TH precoder is derived and the source precoder is as a function of the relay precoder. Then, an iterative algorithm is proposed to optimize the relay precoding matrix by exploiting the link between the mutual information and the weighted MMSE functions [76, 77]. To reduce the computational complexity of the proposed iterative algorithm, a simplified precoding matrices design algorithm is proposed. Numerical simulations are carried out to compare the performance of the proposed precoding matrices design algorithms with existing schemes. Simulation results show that both proposed algorithms outperform existing TH precoder based MIMO transceiver optimization algorithms in terms of

BER. Moreover, the system BER yielded by the proposed algorithms is very close to that of the system with the perfect CSI. Furthermore, the BER performance of the simplified precoding matrices design algorithm is very close to that of the iterative algorithm. Therefore, the simplified algorithm is very attractive for practical MIMO relay communication systems.

5.2 System Model and Problem Formulation

A two-hop non-regenerative MIMO relay system is considered as shown in Fig. 5.1, where the source, relay, and destination nodes have N_S, N_R, and N_D antennas, respectively. It is assumed that there is no direct link between the source and destination due to the long distance between these two nodes. It is also assumed that $N_S \leq N_R, N_D$, so that N_S independent data streams can be transmitted.

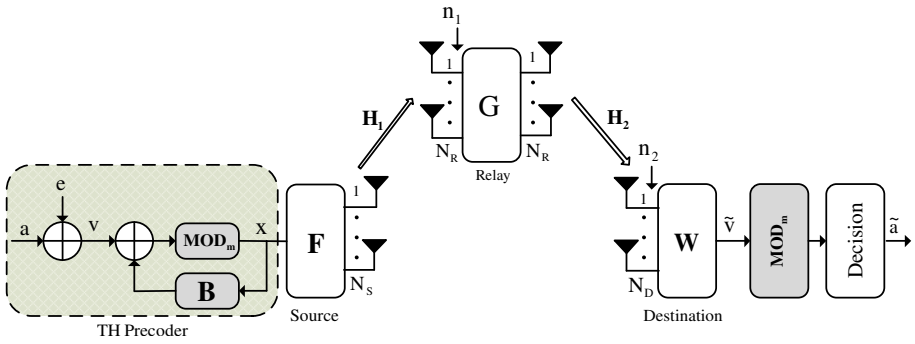

Figure 5.1: Block diagram of a non-regenerative MIMO relay system with TH precoder.

As shown in Fig. 5.1, the non-regenerative MIMO relay system has two precoders, i.e, a TH-based source precoder and a relay precoder. At the receiver, a linear MMSE receiver filter is considered. At the transmitter side, the source signal vector $\mathbf{a} \in \mathbb{C}^{N_S \times 1}$ is first fed into the TH precoder. The TH precoder performs a successive cancelation operation which can be implemented through a feedback matrix $\mathbf{B}$ and a modulo operation $\mathrm{MOD_m}(\cdot)$ expressed as

$$\mathrm{MOD}_m(x) = x - 2\sqrt{m}\left\lfloor \frac{x + \sqrt{m}}{2\sqrt{m}} \right\rfloor. \tag{5.1}$$

Here m is the number of constellation points in the modulation scheme and $\lfloor \cdot \rfloor$ denotes the floor operation. The signal vector after the modulo operation can be denoted as $\mathbf{x}$,

whose nth element can be written as

$$x_n = a_n - \sum_{l=1}^{n-1} [\mathbf{B}]_{k,l} x_l + e_n, \quad n = 1, \cdots, N_S. \tag{5.2}$$

where $[\mathbf{B}]_{k,l}$ is the (k,l)-th element of $\mathbf{B}$, $e_n = 2\sqrt{m}\, q_n$, and q_n is a complex-valued quantity with integer real and imaginary components that reduces x_n within the region of $\mathcal{R} = \{x_R + jx_I | x_R, x_I \in (-\sqrt{m}, \sqrt{m})\}$. By introducing $\mathbf{e} = [e_1, \cdots, e_{N_S}]^T$, (5.2) can be expressed in matrix-vector form as

$$\mathbf{x} = \mathbf{C}^{-1}\mathbf{v} \tag{5.3}$$

where $\mathbf{C} = \mathbf{B} + \mathbf{I}_K$ is a lower triangular matrix with unit diagonal elements, $\mathbf{v} = \mathbf{a} + \mathbf{e}$, and $\mathbf{I}_n$ denotes the $n \times n$ identity matrix, and $\mathbf{x}$ has the covariance matrix of $E\{\mathbf{x}\mathbf{x}^H\} = \sigma_x^2 \mathbf{I}_{N_S}$. The data transmission from source to destination is completed in two time slots. At the first time slot, the source node linearly precodes $\mathbf{x}$ as

$$\mathbf{s} = \mathbf{F}\mathbf{x} \tag{5.4}$$

and transmits $\mathbf{s}$ to the relay node, where $\mathbf{F} \in \mathbb{C}^{N_S \times N_S}$ is the source precoding matrix. The received signal vector at the relay is given by

$$\mathbf{y}_1 = \mathbf{H}_1\mathbf{F}\mathbf{x} + \mathbf{n}_1 \tag{5.5}$$

where $\mathbf{H}_1 \in \mathbb{C}^{N_R \times N_S}$ is the channel matrix of the source-relay link, $\mathbf{n}_1 \in \mathbb{C}^{N_R \times 1}$ is the circularly symmetric complex Gaussian noise vector with zero mean and covariance matrix $E\{\mathbf{n}_1\mathbf{n}_1^H\} = \sigma_1^2 \mathbf{I}_{N_R}$. At the second time slot, the relay linearly precodes $\mathbf{y}_1$ as

$$\mathbf{x}_2 = \mathbf{G}\mathbf{y}_1 = \mathbf{G}\mathbf{H}_1\mathbf{F}\mathbf{x} + \mathbf{G}\mathbf{n}_1 \tag{5.6}$$

and forwards $\mathbf{x}_2$ to the destination, where $\mathbf{G} \in \mathbb{C}^{N_R \times N_R}$ is the relay precoding matrix. The received signal vector at the destination is given by

$$\mathbf{y}_2 = \mathbf{H}_2\mathbf{x}_2 + \mathbf{n}_2 = \mathbf{H}_2\mathbf{G}\mathbf{H}_1\mathbf{F}\mathbf{x} + \mathbf{H}_2\mathbf{G}\mathbf{n}_1 + \mathbf{n}_2 \tag{5.7}$$

where $\mathbf{H}_2 \in \mathbb{C}^{N_D \times N_R}$ is the channel matrix of the relay-destination link, $\mathbf{n}_2 \in \mathbb{C}^{N_D \times 1}$ is the circularly symmetric complex Gaussian noise vector with zero mean and covariance matrix $E\{\mathbf{n}_2\mathbf{n}_2^H\} = \sigma_2^2 \mathbf{I}_{N_D}$. The combined $\mathbf{H}$ and $\mathbf{n}$ matrices can be written as

$$\mathbf{H} = \mathbf{H}_2\mathbf{G}\mathbf{H}_1\mathbf{F}, \quad \mathbf{n} = \mathbf{H}_2\mathbf{G}\mathbf{n}_1 + \mathbf{n}_2 \tag{5.8}$$

where $\mathbf{H} \in \mathbb{C}^{N_D \times N_S}$ is the equivalent MIMO channel matrix between the source and destination nodes, and $\mathbf{n} \in \mathbb{C}^{N_D \times 1}$ represents the equivalent noise vector. Now (5.7) can be rewritten as

$$\mathbf{y}_2 = \mathbf{H}\mathbf{x} + \mathbf{n}. \tag{5.9}$$

It is assumed that the relay node knows the instantaneous CSI of $\mathbf{H}_1$, which can be obtained at the relay node through training sequence from the source node. To obtain the instantaneous CSI of $\mathbf{H}_2$ at the relay node, the channel $\mathbf{H}_2$ must be fed back to the relay node from the destination node. When the relay-destination channel varies rapidly, a large signalling overhead for feedback of $\mathbf{H}_2$ is required and this may not be feasible since the rate of feedback link is often limited in practical wireless communication systems. Hence, in the proposed design, it is assumed that only the covariance information of $\mathbf{H}_2$, which is much more stable than the instantaneous information of $\mathbf{H}_2$, is known at the relay node. In particular, a scenario is considered where the channel of the relay-destination link is correlated at the transmit antennas and uncorrelated at the receive antennas. For example, this scenario can occur in a relay communication system where the relay node is located at the top of a radio mast and a mobile destination node is in an urban area [31]. With this assumption, the channel matrix $\mathbf{H}_2$ can be modelled as

$$\mathbf{H}_2 = \mathbf{H}_\omega \mathbf{\Sigma}^{\frac{1}{2}} \tag{5.10}$$

where $\mathbf{H}_\omega$ is an $N_D \times N_R$ Gaussian matrix having i.i.d. circularly symmetric complex entries with zero mean and unit variance, and $\mathbf{\Sigma}$ is an $N_R \times N_R$ covariance matrix of $\mathbf{H}_2$ at the relay side. Note that the covariance matrix $\mathbf{\Sigma}$ is assumed to be known to the relay node and $\mathbf{H}_\omega$ is unown to the relay node.

At the destination node, a linear receiver with weight matrix $\mathbf{W}$ is applied due to its implementation simplicity. Hence, the estimated signal vector at the destination node can be expressed as

$$\tilde{\mathbf{v}} = \mathbf{W}\mathbf{y}_2 = \mathbf{W}\mathbf{H}\mathbf{x} + \mathbf{W}\mathbf{n}. \tag{5.11}$$

It is assumed that the average transmission power at the source and relay is upper bounded by p_s and p_r, respectively. Based on (5.4) and (5.6), the power constraints at the source and relay nodes can be expressed as

$$P(\mathbf{F}) = \sigma_x^2 tr\{\mathbf{F}\mathbf{F}^H\} \leq p_s \tag{5.12}$$

$$Q_1(\mathbf{F}, \mathbf{G}) = tr\{\mathbf{G}(\sigma_x^2 \mathbf{H}_1 \mathbf{F}\mathbf{F}^H \mathbf{H}_1^H + \sigma_1^2 \mathbf{I}_{N_R})\mathbf{G}^H\} \leq p_r \tag{5.13}$$

Our goal is to design $\mathbf{C}$, $\mathbf{F}$, $\mathbf{G}$, and $\mathbf{W}$ to obtain the estimated signal $\tilde{\mathbf{v}}$ which minimizes the following MSE cost function subjecting to the power constraints (5.12) and (5.13)

$$J_1(\mathbf{C},\mathbf{F},\mathbf{G},\mathbf{W}) = tr\Big\{E\big\{(\tilde{\mathbf{v}}-\mathbf{v})(\tilde{\mathbf{v}}-\mathbf{v})^H\big\}\Big\}. \tag{5.14}$$

Note that once $\tilde{\mathbf{v}}$ is obtained, $\mathbf{a}$ can be recovered from (5.1). After substituting (5.11) into (5.14), the MSE cost function (5.14) can be written as

$$\begin{aligned} J_1(\mathbf{C},\mathbf{F},\mathbf{G},\mathbf{W}) = & tr\big\{\sigma_x^2(\mathbf{WH}-\mathbf{C})(\mathbf{WH}-\mathbf{C})^H \\ & +\mathbf{W}\mathbf{R}_n\mathbf{W}^H\big\} \end{aligned} \tag{5.15}$$

where $\mathbf{R}_n = E\{\mathbf{n}\mathbf{n}^H\}$ is the equivalent noise covariance matrix given by

$$\mathbf{R}_n = \sigma_1^2\mathbf{H}_2\mathbf{G}\mathbf{G}^H\mathbf{H}_2^H + \sigma_2^2\mathbf{I}_{N_D}. \tag{5.16}$$

Based on (5.12), (5.13), and (5.15), the optimal precoding matrices design problem can be formulated as

$$\begin{aligned} \min_{\mathbf{C},\mathbf{F},\mathbf{G},\mathbf{W}} \quad & J_1(\mathbf{C},\mathbf{F},\mathbf{G},\mathbf{W}) \\ s.t. \quad & P(\mathbf{F}) \le p_s \\ & Q_1(\mathbf{F},\mathbf{G}) \le p_r. \end{aligned} \tag{5.17}$$

Directly solving the problem (5.17) is difficult due to the fact that $J_1(\mathbf{C},\mathbf{F},\mathbf{G},\mathbf{W})$ is a non-linear and nonconvex function of $\mathbf{C}$, $\mathbf{F}$, $\mathbf{G}$, and $\mathbf{W}$. In the following section, optimal and suboptimal approaches are proposed to solve the problem (5.17). Firstly, the optimal structure of $\mathbf{C}$ and $\mathbf{F}$ are derived as a function of $\mathbf{G}$. Then an iterative algorithm is proposed to optimize the relay precoding matrix $\mathbf{G}$. Finally, a simplified precoding matrices design is developed to reduce the complexity of the iterative algorithm.

5.3 Proposed Transceiver Design Algorithms

Since concurrently finding the optimum $\mathbf{C}$, $\mathbf{F}$, and $\mathbf{G}$ in (5.17) is not possible, hence the optimization problem in (5.17) is reformulated into three subproblems. In the proposed first subproblem, the lower triangular matrix $\mathbf{C}$ is derived as a function of $\mathbf{F}$, and $\mathbf{G}$, and then, second subproblem optimizes the source precoder matrix $\mathbf{F}$. In the third subproblem, an iterative approach is proposed to obtain the relay precoder matrix $\mathbf{G}$. Due to the computational complexity of the prposed iterative approach, a simplified precoding matrices design is proposed in the subsequent subsection.

5.3.1 Tomlinson-Harashima Precoder Design

For any given precoding matrices $\mathbf{C}$, $\mathbf{F}$, and $\mathbf{G}$ which satisfy the power constraints at the source and relay nodes (5.12) and (5.13), the weight matrix $\mathbf{W}$ of the optimal linear receiver that minimizes the MSE function $J_1(\mathbf{C},\mathbf{F},\mathbf{G},\mathbf{W})$ is the well known MMSE receiver (Wiener filter) which is given by [59]

$$\mathbf{W} = \sigma_x^2\mathbf{C}\mathbf{H}^H(\sigma_x^2\mathbf{H}\mathbf{H}^H + \mathbf{R}_n)^{-1}. \tag{5.18}$$

After substituting (5.18) back into (5.15), the MSE function can be written as

$$\begin{aligned} J_2(\mathbf{C},\mathbf{F},\mathbf{G}) = &\sigma_x^2 tr\Big\{\mathbf{C}\Big(\mathbf{I}_{N_S} - \sigma_x^2\mathbf{H}^H \\ &\times(\sigma_x^2\mathbf{H}\mathbf{H}^H + \mathbf{R}_n)^{-1}\mathbf{H}\Big)\mathbf{C}^H\Big\}. \end{aligned} \tag{5.19}$$

By using the following matrix inversion lemma [60]

$$\begin{aligned} (\mathbf{A}+\mathbf{B}\mathbf{C}\mathbf{D})^{-1} = &\mathbf{A}^{-1} - \mathbf{A}^{-1}\mathbf{B} \\ &\times(\mathbf{D}\mathbf{A}^{-1}\mathbf{B} + \mathbf{C}^{-1})^{-1}\mathbf{D}\mathbf{A}^{-1}, \end{aligned} \tag{5.20}$$

the MSE function (5.19) can be written as

$$\begin{aligned} J_2(\mathbf{C},\mathbf{F},\mathbf{G}) &= tr\Big\{\mathbf{C}\Big(\sigma_x^{-2}\mathbf{I}_{N_S} + \mathbf{H}^H\mathbf{R}_n^{-1}\mathbf{H}\Big)^{-1}\mathbf{C}^H\Big\} \\ &= tr\Big\{\mathbf{C}\Big(\sigma_x^{-2}\mathbf{I}_{N_S} + \mathbf{F}^H\tilde{\mathbf{M}}^H\tilde{\mathbf{M}}\mathbf{F}\Big)^{-1}\mathbf{C}^H\Big\} \end{aligned} \tag{5.21}$$

where

$$\tilde{\mathbf{M}} = \Big(\sigma_1^2\mathbf{H}_2\mathbf{G}\mathbf{G}^H\mathbf{H}_2^H + \sigma_2^2\mathbf{I}_{N_D}\Big)^{-\frac{1}{2}}\mathbf{H}_2\mathbf{G}\mathbf{H}_1. \tag{5.22}$$

To proceed further, the MSE function (5.21) is minimized with respect to the lower triangular and unit diagonal matrix $\mathbf{C}$. The optimum $\mathbf{C}$ is given in [38] and can be written as

$$\mathbf{C}_{opt} = \mathbf{D}\mathbf{L}^{-1} \tag{5.23}$$

where

$$\mathbf{L}\mathbf{L}^H = \Big(\sigma_x^{-2}\mathbf{I}_{N_S} + \mathbf{F}^H\tilde{\mathbf{M}}^H\tilde{\mathbf{M}}\mathbf{F}\Big)^{-1} \tag{5.24}$$

is the Cholesky factorization. Here $\mathbf{L}$ is a lower triangular matrix and $\mathbf{D}$ is a diagonal matrix which scales the diagonal elements of $\mathbf{C}$ to unit, and given by

$$\mathbf{D} = \mathrm{diag}\{[\mathbf{L}]_{1,1}, \cdots, [\mathbf{L}]_{N_S,N_S}\}. \tag{5.25}$$

Substituting (5.23)-(5.25) back into (5.21), the MSE function can be written as

$$J_3(\mathbf{F},\mathbf{G})=\sum_{i=1}^{N_S}[\mathbf{L}]_{i,i}^2 \geq N_S\left(\prod_{i=1}^{N_S}[\mathbf{L}]_{i,i}\right)^{2/N_S}. \tag{5.26}$$

Using the arithmetic-geometric inequality (AGI), the inequality in (5.26) can be obtained and the equality can be achieved when $[\mathbf{L}]_{i,i}=[\mathbf{L}]_{j,j},\ i\neq j$.

5.3.2 Source Precoding Matrix Design

It can be seen from (5.24) that $[\mathbf{L}]_{i,i}$ depends on the source precoding matrix $\mathbf{F}$. Hence, in this subsection, $\mathbf{F}$ is derived which minimizes the objective function (5.26). This problem is solved in [39, 71] and [78]. The EVD of $\tilde{\mathbf{M}}^H\tilde{\mathbf{M}}$ can be defined as

$$\tilde{\mathbf{M}}^H\tilde{\mathbf{M}}=\mathbf{V}_{\tilde{M}}\mathbf{\Lambda}_{\tilde{M}}\mathbf{V}_{\tilde{M}}^H \tag{5.27}$$

where $\mathbf{V}_{\tilde{M}}$ is the eigenvector matrix of $\tilde{\mathbf{M}}$ and $\mathbf{\Lambda}_{\tilde{M}}=\text{diag}\{\Lambda_{\tilde{M},1},\cdots,\Lambda_{\tilde{M},N_S}\}$ is the diagonal eigenvalue matrix with $\Lambda_{\tilde{M},1}\geq\cdots\geq\Lambda_{\tilde{M},N_S}$.

Lemma 5.1 *[40, 79]. The optimal source precoding matrix as the solution to the problem (5.17) can be expressed as*

$$\mathbf{F}_{opt}=\rho\mathbf{V}_{\tilde{M}}\mathbf{\Phi}_F \tag{5.28}$$

where $\mathbf{\Phi}_F$ is a unitary matrix and ρ is chosen to satisfy the power constraint (5.12).

Substituting (5.27) and (5.28) back into (5.24), the Cholesky factorization (5.24) can be written as

$$\mathbf{L}\mathbf{L}^H=\mathbf{\Phi}_F^H\tilde{\mathbf{\Sigma}}^{\frac{1}{2}}\tilde{\mathbf{\Sigma}}^{\frac{1}{2}}\mathbf{\Phi}_F \tag{5.29}$$

where

$$\tilde{\mathbf{\Sigma}}^{\frac{1}{2}}=\left(\sigma_x^{-2}\mathbf{I}_{N_S}+\rho^2\mathbf{\Lambda}_{\tilde{M}}\right)^{-\frac{1}{2}}.$$

Applying the geometric mean decomposition (GMD) [80–82] to $\tilde{\mathbf{\Sigma}}^{\frac{1}{2}}$, $\tilde{\mathbf{\Sigma}}^{\frac{1}{2}}$ can be written as

$$\tilde{\mathbf{\Sigma}}^{\frac{1}{2}}=\mathbf{Q}\mathbf{R}\mathbf{P}^H \tag{5.30}$$

where $\mathbf{Q}$ and $\mathbf{P}$ are semi-unitary matrices and $\mathbf{R}$ is an upper triangular matrix with identical diagonal entries given by

$$[\mathbf{R}]_{ii} = \left(\prod_{k=1}^{N_S} \left(\sigma_x^{-2} + \rho^2 \Lambda_{\tilde{M},k} \right)^{-\frac{1}{2}} \right)^{1/N_S}, \quad i = 1, \cdots, N_S.$$

Substituting (5.30) back into (5.29), $\mathbf{L}\mathbf{L}^H$ can be written as

$$\mathbf{L}\mathbf{L}^H = \mathbf{\Phi}_F^H \mathbf{P} \mathbf{R}^H \mathbf{R} \mathbf{P}^H \mathbf{\Phi}_F. \tag{5.31}$$

$\mathbf{\Phi}_F$ is assumed as $\mathbf{\Phi}_F = \mathbf{P}$ to achieve the lower bound in (5.26), then (5.31) can be simplified as

$$\mathbf{L}\mathbf{L}^H = \mathbf{R}^H \mathbf{R}. \tag{5.32}$$

From (5.32), it can be concluded that $\mathbf{L} = \mathbf{R}^H$. By substituting (5.32) back into (5.26), the MSE function can be depicted as

$$\begin{aligned} J_4(\mathbf{G}) &= \sum_{i=1}^{N_S} [\mathbf{R}]_{i,i}^2 \\ &= N_S \prod_{k=1}^{N_S} \left(\sigma_x^{-2} + \rho^2 \Lambda_{\tilde{M},k} \right)^{-1/N_S}. \end{aligned} \tag{5.33}$$

After substituting (5.28) back into (5.13), the relay power constraint (5.13) can be written as

$$Q_2(\mathbf{G}) = tr\left\{ \mathbf{G} (\sigma_x^2 \rho^2 \mathbf{H}_1 \mathbf{H}_1^H + \sigma_1^2 \mathbf{I}_{N_R}) \mathbf{G}^H \right\} \leq p_r. \tag{5.34}$$

Now the relay precoding matrix optimization problem can be formulated as

$$\min_{\mathbf{G}} \; J_4(\mathbf{G}) \qquad s.t. \; Q_2(\mathbf{G}) \leq p_r. \tag{5.35}$$

5.3.3 Relay Precoding Matrix Design

In this subsection, the optimum $\mathbf{G}$ is derived. It is worth to note that the eigenvalues of (5.22) are a non-linear function of $\mathbf{G}$ and the optimization problem (5.35) is not convex. To solve the problem (5.35), the equivalent MSE function can be considered as

$$\prod_{k=1}^{N_S} \left(\sigma_x^{-2} + \rho^2 \Lambda_{\tilde{M},k} \right) = \left| \sigma_x^{-2} \mathbf{I}_{N_S} + \rho^2 \tilde{\mathbf{M}}^H \tilde{\mathbf{M}} \right|. \tag{5.36}$$

Here $|\cdot|$ denotes the matrix determinant. Substituting (5.36) into (5.35) and taking the log operation to the cost function, the optimization problem (5.35) can be reformulated as

$$\min_{\mathbf{G}} \quad -X \qquad s.t. \;\; Q_2(\mathbf{G}) \leq p_r \tag{5.37}$$

where

$$\begin{aligned} X&=\log|\mathbf{A}^{-1}| \\ \mathbf{A}&=\left(\rho^{-2}\sigma_x^{-2}\mathbf{I}_{N_S}+\mathbf{H}_1^H\mathbf{G}^H\mathbf{H}_2^H\mathbf{R}_n^{-1}\mathbf{H}_2\mathbf{G}\mathbf{H}_1\right)^{-1}. \end{aligned} \tag{5.38}$$

It is worth noting that if $\mathbf{H}_2$ is known at the relay node, (5.37) has a closed-form solution [25]. However, as the exact $\mathbf{H}_2$ is unknown, it is impossible to solve the problem (5.37). To overcome this difficulty, the mean value of $-X$ is consider as given by the following problem

$$\min_{\mathbf{G}} \quad E_{\mathbf{H}_2}\{-X\} \qquad s.t. \;\; Q_2(\mathbf{G}) \leq p_r \tag{5.39}$$

where $E_{\mathbf{H}_2}\{\cdot\}$ denotes the statistical expectation with respect to $\mathbf{H}_2$.

It is noticed that due to the matrix determinant operator in X, the closed-form expression of the objective function in (5.39), if possible to obtain, is a very complicated function of $\mathbf{G}$, which makes the problem (5.39) difficult to solve. To overcome this challenge, the following theorem is applied.

Theorem 5.1 *The problem* (5.37) *has the same Karush-Kuhn-Tucker (KKT) conditions on* $\mathbf{G}$ *as the problem of*

$$\min_{\mathbf{G},\mathbf{\Omega}} \;\; tr\{\mathbf{\Omega}\mathbf{A}\}-\log|\mathbf{\Omega}| \tag{5.40}$$

$$s.t. \;\; Q_2(\mathbf{G}) \leq p_r \tag{5.41}$$

when the Hermitian weight matrix $\mathbf{\Omega}$ *takes value of*

$$\mathbf{\Omega} = \mathbf{A}^{-1}. \tag{5.42}$$

Moreover, with given $\mathbf{G}$*, the weight matrix* $\mathbf{\Omega}$ *minimizing* (5.40) *is given by* (5.42).

Proof: See Appendix 5.A. □

Based on Theorem 5.1, the problem (5.37) can be solved using an iterative approach, where in each iteration, with $\mathbf{\Omega}$ from the previous iteration, first, $\mathbf{G}$ is optimized by solving the problem (5.40)-(5.41). Then $\mathbf{\Omega}$ is updated as (5.42) using $\mathbf{G}$ obtained in the current iteration. Note that the conditional updates of $\mathbf{G}$ and $\mathbf{\Omega}$ may either decrease or maintain but cannot increase the objective function (5.40). Monotonic convergence

of the iterative algorithm towards (at least) a locally optimal solution follows directly from this observation. As $\mathbf{\Omega}$ is unknown due to an unknown $\mathbf{H}_2$. Hence, $\bar{\mathbf{\Omega}}$ is used and it can be expressed as

$$\begin{aligned}\bar{\mathbf{\Omega}}=&E_{\mathbf{H}_2}\{\mathbf{\Omega}\}\\ =&E_{\mathbf{H}_2}\{\mathbf{A}^{-1}\}\\ =&\rho^{-2}\sigma_x^{-2}\mathbf{I}_{N_S}+E_{\mathbf{H}_2}\{\tilde{\mathbf{M}}^H\tilde{\mathbf{M}}\}\end{aligned} \tag{5.43}$$

where

$$\begin{aligned}&E_{\mathbf{H}_2}\{\tilde{\mathbf{M}}^H\tilde{\mathbf{M}}\}\\ =&\mathbf{H}_1^H E_{\mathbf{H}_2}\{\mathbf{G}^H\mathbf{H}_2^H\mathbf{R}_n^{-1}\mathbf{H}_2\mathbf{G}\}\mathbf{H}_1\\ \leq&\sigma_1^{-2}\mathbf{H}_1^H\big[\mathbf{I}_{N_R}-\sigma_2^2(\sigma_1^2\mathbf{G}^H E_{\mathbf{H}_2}\{\mathbf{H}_2^H\mathbf{H}_2\}\mathbf{G}+\sigma_2^2\mathbf{I}_{N_R})^{-1}\big]\mathbf{H}_1\\ =&\sigma_1^{-2}\mathbf{H}_1^H\big[\mathbf{I}_{N_R}-\sigma_2^2(\sigma_1^2 N_D\mathbf{G}^H\mathbf{\Sigma}\mathbf{G}+\sigma_2^2\mathbf{I}_{N_R})^{-1}\big]\mathbf{H}_1.\end{aligned} \tag{5.44}$$

Substituting (5.38) into (5.40), for a given $\bar{\mathbf{\Omega}}$, the objective function of $\mathbf{G}$ can be expressed as

$$\begin{aligned}T_1(\mathbf{G})=&tr\Big\{\bar{\mathbf{\Omega}}\Big[\rho^{-2}\sigma_x^{-2}\mathbf{I}_{N_S}+\mathbf{H}_1^H\mathbf{G}^H\mathbf{H}_2^H\\ &\times\Big(\sigma_1^2\mathbf{H}_2\mathbf{G}\mathbf{G}^H\mathbf{H}_2^H+\sigma_2^2\mathbf{I}_{N_D}\Big)^{-1}\mathbf{H}_2\mathbf{G}\mathbf{H}_1\Big]^{-1}\Big\}.\end{aligned} \tag{5.45}$$

Now the problem is reduced to find the optimal $\mathbf{G}$ that minimizes $T_1(\mathbf{G})$ subjecting to the relay power constraint (5.34). Using the matrix inversion lemma (5.20), (5.45) can be rewritten as

$$\begin{aligned}T_1(\mathbf{G})=&tr\Big\{\bar{\mathbf{\Omega}}\Big[\rho^{-2}\sigma_x^{-2}\mathbf{I}_{N_S}+\sigma_1^{-2}\mathbf{H}_1^H\Big[\mathbf{I}_{N_R}\\ &-\Big(\mathbf{I}_{N_R}+\frac{\sigma_1^2}{\sigma_2^2}\mathbf{G}^H\mathbf{H}_2^H\mathbf{H}_2\mathbf{G}\Big)^{-1}\Big]\mathbf{H}_1\Big]^{-1}\Big\}.\end{aligned} \tag{5.46}$$

The SVD of $\mathbf{H}_1$ can be introduced as

$$\mathbf{H}_1=\mathbf{U}_1\mathbf{\Lambda}_1^{\frac{1}{2}}\mathbf{V}_1^H \tag{5.47}$$

where $\mathbf{\Lambda}_1=\mathrm{diag}\{\Lambda_{1,1},\cdots,\Lambda_{1,N_S}\}$ is a diagonal matrix with $\Lambda_{1,1}\geq\cdots\geq\Lambda_{1,N_S}$, $\mathbf{U}_1\in\mathbb{C}^{N_R\times N_S}$ and $\mathbf{V}_1\in\mathbb{C}^{N_S\times N_S}$ are the singularvector matrices of $\mathbf{H}_1$. The EVD of $\mathbf{\Sigma}$ can written as

$$\mathbf{\Sigma}=\mathbf{V}_\Sigma\mathbf{\Lambda}_\Sigma\mathbf{V}_\Sigma^H \tag{5.48}$$

where $\mathbf{\Lambda}_\Sigma = \text{diag}\{\Lambda_{\Sigma,1}, \cdots, \Lambda_{\Sigma,N_R}\}$ with $\Lambda_{\Sigma,1} \geq \cdots \geq \Lambda_{\Sigma,N_R}$. Substituting (5.48) back into (5.10), the channel matrix $\mathbf{H}_2$ can be written as

$$\mathbf{H}_2 = \widetilde{\mathbf{H}}_\omega \mathbf{\Lambda}_\Sigma^{\frac{1}{2}} \mathbf{V}_\Sigma^H \tag{5.49}$$

where $\widetilde{\mathbf{H}}_\omega \triangleq \mathbf{H}_\omega \mathbf{V}_\Sigma$ has the same distribution as $\mathbf{H}_\omega$, as the unitary matrix $\mathbf{V}_\Sigma$ does not change the statistical distribution of $\mathbf{H}_\omega$. Thus, $\widetilde{\mathbf{H}}_\omega$ is an $N_D \times N_R$ complex Gaussian matrix having i.i.d. circularly symmetric entries. It can be shown that the optimal $\mathbf{G}$ minimizing (5.46) can be expressed as

$$\mathbf{G} = \mathbf{V}_\Sigma \widetilde{\mathbf{G}} \mathbf{U}_1^H. \tag{5.50}$$

It can be seen from (5.50) that the optimal $\mathbf{G}$ allocates power according to the eigenmodes of $\mathbf{H}_1\mathbf{H}_1^H$ and $\mathbf{\Sigma}$, and $\widetilde{\mathbf{G}}$ is needed to be determined.

Substituting (5.47)-(5.50) back into (5.46), (5.46) can be obtained as

$$\begin{aligned} T_1(\widetilde{\mathbf{G}}) = tr\Big\{ \bar{\mathbf{\Omega}} \Big[\rho^{-2}\sigma_x^{-2}\mathbf{I}_{N_S} + \sigma_1^{-2}\mathbf{V}_1 \mathbf{\Lambda}_1^{\frac{1}{2}} \mathbf{U}_1^H \\ \times (\mathbf{I}_{N_R} - \mathbf{D}_1)\mathbf{U}_1 \mathbf{\Lambda}_1^{\frac{1}{2}} \mathbf{V}_1^H \Big]^{-1} \Big\} \end{aligned} \tag{5.51}$$

where

$$\mathbf{D}_1 = \left(\mathbf{I}_{N_R} + \frac{\sigma_1^2}{\sigma_2^2} \mathbf{U}_1 \widetilde{\mathbf{G}}^H \mathbf{\Lambda}_\Sigma^{\frac{1}{2}} \widetilde{\mathbf{H}}_\omega^H \widetilde{\mathbf{H}}_\omega \mathbf{\Lambda}_\Sigma^{\frac{1}{2}} \widetilde{\mathbf{G}} \mathbf{U}_1^H \right)^{-1}.$$

Using $\mathbf{U}_1^H \mathbf{U}_1 = \mathbf{I}_{N_S}$, (5.51) can be simplified to

$$\begin{aligned} T_1(\widetilde{\mathbf{G}}) = tr\Big\{ \bar{\mathbf{\Omega}} \Big[\rho^{-2}\sigma_x^{-2}\mathbf{I}_{N_S} + \sigma_1^{-2}\mathbf{V}_1 \mathbf{\Lambda}_1^{\frac{1}{2}} \\ \times (\mathbf{I}_{N_R} - \mathbf{D}_2)\mathbf{\Lambda}_1^{\frac{1}{2}} \mathbf{V}_1^H \Big]^{-1} \Big\} \end{aligned} \tag{5.52}$$

where

$$\mathbf{D}_2 = \left(\mathbf{I}_{N_R} + \frac{\sigma_1^2}{\sigma_2^2} \widetilde{\mathbf{G}}^H \mathbf{\Lambda}_\Sigma^{\frac{1}{2}} \widetilde{\mathbf{H}}_\omega^H \widetilde{\mathbf{H}}_\omega \mathbf{\Lambda}_\Sigma^{\frac{1}{2}} \widetilde{\mathbf{G}} \right)^{-1}.$$

It can be seen from (5.52) that $T_1(\widetilde{\mathbf{G}})$ depends on $\widetilde{\mathbf{H}}_\omega$, which is random and unknown. In the following, $E_{\widetilde{\mathbf{H}}_\omega}\{T_1(\widetilde{\mathbf{G}})\}$ is optimized, where $E_{\widetilde{\mathbf{H}}_\omega}\{\cdot\}$ indicates that the expectation is taken with respect to the random matrix $\widetilde{\mathbf{H}}_\omega$. Now $E_{\widetilde{\mathbf{H}}_\omega}\{T_1(\widetilde{\mathbf{G}})\}$ can be expressed as

$$\begin{aligned} E_{\widetilde{\mathbf{H}}_\omega}\{T_1(\widetilde{\mathbf{G}})\} = E_{\widetilde{\mathbf{H}}_\omega}\Big\{ tr\Big\{ \bar{\mathbf{\Omega}} \Big[\rho^{-2}\sigma_x^{-2}\mathbf{I}_{N_S} + \sigma_1^{-2}\mathbf{V}_1 \mathbf{\Lambda}_1^{\frac{1}{2}} \\ \times (\mathbf{I}_{N_R} - \mathbf{D}_2)\mathbf{\Lambda}_1^{\frac{1}{2}} \mathbf{V}_1^H \Big]^{-1} \Big\} \Big\}. \end{aligned} \tag{5.53}$$

Direct minimization of (5.53) over $\widetilde{\mathbf{G}}$ is difficult due to the expectation operation. In the following, a lower bound of (5.53) is exploited together with the power constraint (5.34) to derive the suboptimal $\widetilde{\mathbf{G}}$ for the precoding matrix $\mathbf{G}$.

Theorem 5.2 *A lower bound of (5.53) is given by*

$$T_2(\widetilde{\mathbf{G}})=tr\Big\{\bar{\mathbf{\Omega}}\Big[\rho^{-2}\sigma_x^{-2}\mathbf{I}_{N_S}+\sigma_1^{-2}\mathbf{V}_1\mathbf{\Lambda}_1^{\frac{1}{2}}\Big[\mathbf{I}_{N_R} -\Big(\mathbf{I}_{N_R}+\frac{\sigma_1^2N_D}{\sigma_2^2}\widetilde{\mathbf{G}}^H\mathbf{\Lambda}_\Sigma\widetilde{\mathbf{G}}\Big)^{-1}\Big]\mathbf{\Lambda}_1^{\frac{1}{2}}\mathbf{V}_1^H\Big]^{-1}\Big\}. \tag{5.54}$$

PROOF: See Appendix 5.B. □

Substituting (5.47) and (5.50) back into (5.34), the power constraint at the relay node can be simplified to

$$Q_3(\widetilde{\mathbf{G}})=tr\Big\{\widetilde{\mathbf{G}}(\rho^2\sigma_x^2\mathbf{\Lambda}_1+\sigma_1^2\mathbf{I}_{N_R})\widetilde{\mathbf{G}}^H\Big\}\leq p_r. \tag{5.55}$$

From (5.54) and (5.55), the problem of optimizing $\widetilde{\mathbf{G}}$ can be written as

$$\min_{\widetilde{\mathbf{G}}}\ T_2(\widetilde{\mathbf{G}}) \qquad s.t.\ Q_3(\widetilde{\mathbf{G}})\leq p_r. \tag{5.56}$$

The problem (5.56) does not have a closed-form solution due to the presence of $\mathbf{\Omega}$ in the objective function. The problem (5.56) can be solved by resorting to numerical methods, such as the projected gradient algorithm [61]. By introducing

$$\begin{aligned}\mathbf{B}&=\sigma_1^2\mathbf{I}_{N_S}+\rho^2\sigma_x^2\mathbf{V}_1\mathbf{\Lambda}_1\mathbf{V}_1^H\\ \mathbf{K}&=\rho^2\sigma_x^2\mathbf{V}_1\mathbf{\Lambda}_1^{\frac{1}{2}}\\ \mathbf{D}_4&=\Big(\mathbf{I}_{N_R}+\frac{\sigma_1^2N_D}{\sigma_2^2}\widetilde{\mathbf{G}}^H\mathbf{\Lambda}_\Sigma\widetilde{\mathbf{G}}\Big)^{-1}\end{aligned}$$

$T_2(\widetilde{\mathbf{G}})$ can be rewritten as

$$T_2(\widetilde{\mathbf{G}})\triangleq\rho^2\sigma_x^2\sigma_1^2tr\big\{\bar{\mathbf{\Omega}}(\mathbf{B}-\mathbf{K}\mathbf{D}_4\mathbf{K}^H)^{-1}\big\}. \tag{5.57}$$

The gradient of (5.57) is given by

$$\nabla_{\tilde{G}}T_2=\frac{-2\sigma_1^4\sigma_x^2\rho^2N_D}{\sigma_2^2}\Big(\mathbf{D}_4\mathbf{K}^H\big(\mathbf{B}-\mathbf{K}\mathbf{D}_4\mathbf{K}^H\big)^{-1}\bar{\mathbf{\Omega}} \times\big(\mathbf{B}-\mathbf{K}\mathbf{D}_4\mathbf{K}^H\big)^{-1}\mathbf{K}\mathbf{D}_4\widetilde{\mathbf{G}}^H\mathbf{\Lambda}_\Sigma\Big)^H. \tag{5.58}$$

The procedure of applying the projected gradient algorithm to solve the problem (5.56) is summarized in Table 5.1, where the superscript (n) denotes the variables at the nth iteration, t_n and γ_n are the step size parameters at the nth iteration, $\max\text{abs}(\cdot)$ denotes the maximum among the absolute value of all elements in a matrix, and ε is a positive constant close to 0. The step size parameters t_n and γ_n are chosen by the Armijo

Table 5.1: Procedure of solving the problem (5.56) using the projected gradient algorithm

1. Initialize the algorithm at a feasible $\widetilde{\mathbf{G}}^{(0)}$; Set $n = 0$.

2. Compute the gradient of $T_2(\widetilde{\mathbf{G}}^{(n)})$ as (5.58);
   Project $(\breve{\mathbf{G}}^{(n)}) = \widetilde{\mathbf{G}}^{(n)} - t_n \nabla_{\tilde{G}^{(n)}} T_2$ to the set of $Q_3(\bar{\mathbf{G}}^{(n)}) = p_r$ to obtain $\bar{\mathbf{G}}^{(n)}$;
   Update $\widetilde{\mathbf{G}}$ with $\widetilde{\mathbf{G}}^{(n+1)} = \widetilde{\mathbf{G}}^{(n)} + \gamma_n(\bar{\mathbf{G}}^{(n)} - \widetilde{\mathbf{G}}^{(n)})$.

3. If $\max \mathrm{abs}(\widetilde{\mathbf{G}}^{(n+1)} - \widetilde{\mathbf{G}}^{(n)}) \leq \varepsilon$, then end.
   Otherwise, let $n := n + 1$ and go to Step 2).

rule [83], i.e., $t_n = t$ is a constant through all iterations, while at the nth iteration, γ_n is set to be β^{m_n}. Here m_n is the minimal nonnegative integer that satisfies the inequality of $T_2(\widetilde{\mathbf{G}}^{(n+1)}) - T_2(\widetilde{\mathbf{G}}^{(n)}) \leq \alpha\beta^{m_n} \mathrm{tr}\Big(\big(\nabla_{\tilde{G}^{(n)}} T_2\big)^H \big(\bar{\mathbf{G}}^{(n)} - \widetilde{\mathbf{G}}^{(n)}\big)\Big)$, α and β are constants. According to [83], usually α is chosen close to 0, for example $\alpha \in [10^{-5}, 10^{-1}]$, and a proper choice of β is normally from 0.1 to 0.5.

The procedure of the iterative precoding matrices design algorithm developed in Sections 5.3.1–5.3.3 are summarized in Table 5.2, where the superscript (m) denotes the variables at the mth iteration.

Table 5.2: Procedure of the proposed iterative precoding matrices design algorithm

1. Initialize the algorithm with $\bar{\mathbf{\Omega}}^{(0)} = \sqrt{p_s/N_S}\mathbf{I}_{N_S}$; Set $m = 0$.

2. Update $\widetilde{\mathbf{G}}^{(m)}$ by solving the problem (5.56) using the projected gradient algorithm listed in Table 5.1.

3. Update $\bar{\mathbf{\Omega}}^{(m+1)}$ by (5.43); If $\max \mathrm{abs}(\bar{\mathbf{\Omega}}^{(m+1)} - \bar{\mathbf{\Omega}}^{(m)}) \leq \varepsilon$, then go to Step 4).
   Otherwise, let $m := m + 1$ and go to Step 2).

4. Obtain $\mathbf{F}_{opt}$ as (5.28), and $\mathbf{C}_{opt}$ by (5.23) with $\tilde{\mathbf{M}}^H\tilde{\mathbf{M}}$ replaced by $E_{\mathbf{H}_2}\{\tilde{\mathbf{M}}^H\tilde{\mathbf{M}}\}$ in (5.44).

5.3.4 Simplified Precoding Matrices Design

In this subsection, a precoding matrices design algorithm is proposed which has a significant computational complexity reduction compared with the iterative algorithm in Table 5.2. In this algorithm, a lower bound of the MSE function is obtained by using the arithmetic-geometric mean inequality [60], which is given by the following lemma.

Lemma 5.2 *For a positive semidefinite (PSD) matrix* $\mathbf{A} \in \mathbb{C}^{N\times N}$*, there is*

$$|\mathbf{A}|^{1/N} \leq tr(\mathbf{A})/N \tag{5.59}$$

where the equality is achieved when $\mathbf{A}$ is a diagonal matrix with equal diagonal elements. Using Lemma 5.2, a lower bound of the MSE function (5.21) can be written as

$$\begin{aligned}&\left|\sigma_x^{-2}\mathbf{I}_{N_S} + \mathbf{F}^H\tilde{\mathbf{M}}^H\tilde{\mathbf{M}}\mathbf{F}\right|^{-1/N_S}\\ &\leq tr\left\{\mathbf{C}(\sigma_x^{-2}\mathbf{I}_{N_S} + \mathbf{F}^H\tilde{\mathbf{M}}^H\tilde{\mathbf{M}}\mathbf{F})^{-1}\mathbf{C}^H\right\}/N_S.\end{aligned} \tag{5.60}$$

Since minimizing $|\mathbf{A}|^{-1}$ is equivalent to maximizing $|\mathbf{A}|$ [60], the source and relay precoding matrices design problem can be reformulated as

$$\begin{aligned}\max_{\mathbf{F},\mathbf{G}}\ & X(\mathbf{F},\mathbf{G})\\ s.t.\ & P(\mathbf{F}) \leq p_s\\ & Q_1(\mathbf{F},\mathbf{G}) \leq p_r\end{aligned} \tag{5.61}$$

where the objective function $X(\mathbf{F},\mathbf{G})$ can be expressed as

$$\begin{aligned}X(\mathbf{F},\mathbf{G}) =& \log\left|\sigma_x^{-2}\mathbf{I}_{N_S} + \mathbf{F}^H\tilde{\mathbf{M}}^H\tilde{\mathbf{M}}\mathbf{F}\right|\\ =& \log\left|\sigma_x^{-2}\mathbf{I}_{N_S} + \mathbf{F}^H\mathbf{H}_1^H\mathbf{G}^H\mathbf{H}_2^H\right.\\ & \left.\times\left(\sigma_1^2\mathbf{H}_2\mathbf{G}\mathbf{G}^H\mathbf{H}_2^H + \sigma_2^2\mathbf{I}_{N_D}\right)^{-1}\mathbf{H}_2\mathbf{G}\mathbf{H}_1\mathbf{F}\right|\\ =& \log\left|\sigma_x^{-2}\mathbf{I}_{N_S} + \sigma_1^{-2}\mathbf{F}^H\mathbf{H}_1^H\left[\mathbf{I}_{N_R}\right.\right.\\ & \left.\left.-\left(\mathbf{I}_{N_R} + \frac{\sigma_1^2}{\sigma_2^2}\mathbf{G}^H\mathbf{H}_2^H\mathbf{H}_2\mathbf{G}\right)^{-1}\right]\mathbf{H}_1\mathbf{F}\right|.\end{aligned} \tag{5.62}$$

Here the matrix inversion lemma (5.20) is applied to obtain the last equation. From [84], it can be defined that if the matrix is diagonal, then the determinant of a positive definite matrix is maximized. Hence, without loss of generality, the source precoding matrix $\mathbf{F}$ can be expressed in terms of the following decomposition

$$\mathbf{F} = \mathbf{V}_1\mathbf{\Lambda}_F^{\frac{1}{2}}\mathbf{\Phi}_F \tag{5.63}$$

where $\mathbf{\Lambda}_F = \text{diag}\{\Lambda_{F,1} \cdots \Lambda_{F,N_S}\}$, and $\mathbf{\Phi}_F$ is a unitary matrix defined later. It can be assumed that the matrix $\mathbf{G}$ which maximizes (5.62) can be expressed as

$$\mathbf{G} = \mathbf{V}_{\Sigma,1}\mathbf{\Lambda}_G^{\frac{1}{2}}\mathbf{U}_1^H \tag{5.64}$$

where $\mathbf{V}_{\Sigma,1}$ contains N_S columns of $\mathbf{V}_\Sigma$ associated with the largest N_S eigenvalues of $\mathbf{\Sigma}$, and $\mathbf{\Lambda}_G = \text{diag}\{\Lambda_{G,1}, \cdots, \Lambda_{G,N_S}\}$. Substituting (5.47), (5.49), (5.63) and (5.64) in (5.62), $X(\mathbf{F}, \mathbf{G})$ can be written as

$$X(\mathbf{F}, \mathbf{G}) = \log \left| \sigma_x^{-2}\mathbf{I}_{N_S} + \sigma_1^{-2}\mathbf{\Lambda}_F^{\frac{1}{2}}\mathbf{\Lambda}_1^{\frac{1}{2}}(\mathbf{I}_{N_S} - \mathbf{D}_5)\mathbf{\Lambda}_1^{\frac{1}{2}}\mathbf{\Lambda}_F^{\frac{1}{2}} \right| \tag{5.65}$$

where

$$\mathbf{D}_5 = \left(\mathbf{I}_{N_S} + \frac{\sigma_1^2}{\sigma_2^2}\mathbf{\Lambda}_G^{\frac{1}{2}}\mathbf{\Lambda}_{\Sigma,1}^{\frac{1}{2}}\widetilde{\mathbf{H}}_{\omega,1}^H\widetilde{\mathbf{H}}_{\omega,1}\mathbf{\Lambda}_{\Sigma,1}^{\frac{1}{2}}\mathbf{\Lambda}_G^{\frac{1}{2}} \right)^{-1}$$

and $\widetilde{\mathbf{H}}_{\omega,1}$ is a matrix containing the left-most N_S columns of $\widetilde{\mathbf{H}}_\omega$. It can be seen from (5.65) that $X(\mathbf{F}, \mathbf{G})$ depends on $\widetilde{\mathbf{H}}_{\omega,1}$, which is random and unknown. In the following, $E_{\widetilde{\mathbf{H}}_{\omega,1}}\{X(\mathbf{F}, \mathbf{G})\}$ is optimized which is given by

$$\begin{aligned} E_{\widetilde{\mathbf{H}}_{\omega,1}}\{X(\mathbf{F}, \mathbf{G})\} = E_{\widetilde{\mathbf{H}}_{\omega,1}}\Big\{ \log \Big| & \sigma_x^{-2}\mathbf{I}_{N_S} + \sigma_1^{-2}\mathbf{\Lambda}_F^{\frac{1}{2}}\mathbf{\Lambda}_1^{\frac{1}{2}} \\ & \times (\mathbf{I}_{N_S} - \mathbf{D}_5)\mathbf{\Lambda}_1^{\frac{1}{2}}\mathbf{\Lambda}_F^{\frac{1}{2}} \Big| \Big\}. \end{aligned} \tag{5.66}$$

Due to the expectation operation, maximizing (5.66) with respect to $\mathbf{\Lambda}_F$ and $\mathbf{\Lambda}_G$ is difficult. In the following, an upper bound of $E_{\widetilde{\mathbf{H}}_{\omega,1}}\{X(\mathbf{F}, \mathbf{G})\}$ is used together with the power constraints (5.12) and (5.13) to derive the suboptimal power allocation for the precoding matrices $\mathbf{F}$ and $\mathbf{G}$.

Theorem 5.3 *The function*

$$\begin{aligned} f(\mathbf{Z}) = \log \Big| & \mathbf{I}_{N_S} + \sigma_x^2\sigma_1^{-2}\mathbf{\Lambda}_F^{\frac{1}{2}}\mathbf{\Lambda}_1^{\frac{1}{2}} \Big[\mathbf{I}_{N_S} \\ & - \left(\mathbf{I}_{N_S} + \frac{\sigma_1^2}{\sigma_2^2}\mathbf{\Lambda}_G^{\frac{1}{2}}\mathbf{\Lambda}_{\Sigma,1}^{\frac{1}{2}}\mathbf{Z}\mathbf{\Lambda}_{\Sigma,1}^{\frac{1}{2}}\mathbf{\Lambda}_G^{\frac{1}{2}} \right)^{-1} \Big] \mathbf{\Lambda}_1^{\frac{1}{2}}\mathbf{\Lambda}_F^{\frac{1}{2}} \Big| \end{aligned} \tag{5.67}$$

is concave with respect to a PSD $\mathbf{Z}$.

PROOF: See Appendix 5.C. □

According to Theorem 5.3, $X(\mathbf{F}, \mathbf{G})$ is concave in $\widetilde{\mathbf{H}}_{\omega,1}^H\widetilde{\mathbf{H}}_{\omega,1}$. Hence, $E_{\widetilde{\mathbf{H}}_{\omega,1}}\{X(\mathbf{F}, \mathbf{G})\}$ has the following upper bound by using the Jensen's inequality [65]

$$X_U = \log \left| \sigma_x^{-2}\mathbf{I}_{N_S} + \sigma_1^{-2}\mathbf{\Lambda}_F^{\frac{1}{2}}\mathbf{\Lambda}_1^{\frac{1}{2}}(\mathbf{I}_{N_S} - \mathbf{D}_6)\mathbf{\Lambda}_1^{\frac{1}{2}}\mathbf{\Lambda}_F^{\frac{1}{2}} \right| \tag{5.68}$$

where

$$\mathbf{D}_6 = \left(\mathbf{I}_{N_S} + \frac{\sigma_1^2}{\sigma_2^2}\mathbf{\Lambda}_G^{\frac{1}{2}}\mathbf{\Lambda}_\Sigma^{\frac{1}{2}} E_{\widetilde{\mathbf{H}}_{\omega,1}}\{\widetilde{\mathbf{H}}_{\omega,1}^H \widetilde{\mathbf{H}}_{\omega,1}\}\mathbf{\Lambda}_\Sigma^{\frac{1}{2}}\mathbf{\Lambda}_G^{\frac{1}{2}}\right)^{-1}.$$

Using the property of Gaussian random matrices with i.i.d. circularly symmetric complex entries, it is assumed that $E_{\widetilde{\mathbf{H}}_{\omega,1}}\{\widetilde{\mathbf{H}}_{\omega,1}^H \widetilde{\mathbf{H}}_{\omega,1}\} = N_D\mathbf{I}_{N_S}$, and (5.68) can be simplified to

$$X_U \triangleq \log\left|\sigma_x^{-2}\mathbf{I}_{N_S} + \sigma_1^{-2}\mathbf{\Lambda}_F\mathbf{\Lambda}_1(\mathbf{I}_{N_S} - \mathbf{D}_7)\right| \tag{5.69}$$

where

$$\mathbf{D}_7 = \left(\mathbf{I}_{N_S} + \frac{\sigma_1^2 N_D}{\sigma_2^2}\mathbf{\Lambda}_G\mathbf{\Lambda}_\Sigma\right)^{-1}.$$

By substituting (5.47), (5.63), and (5.64) back into (5.12) and (5.13), the power constraints at source and relay nodes can be simplified to

$$\sigma_x^2 tr\{\mathbf{\Lambda}_F\} \leq p_s \tag{5.70}$$

$$tr\{(\sigma_x^2\mathbf{\Lambda}_F\mathbf{\Lambda}_1 + \sigma_1^2\mathbf{I}_{N_S})\mathbf{\Lambda}_G\} \leq p_r. \tag{5.71}$$

Based on (5.69)-(5.71), the diagonal elements of $\mathbf{\Lambda}_F$ and $\mathbf{\Lambda}_G$ can be obtained by solving the following constrained optimization problem with scalar variables

$$\max_{\{\Lambda_{F,i}\},\{\Lambda_{G,i}\}} \sum_{i=1}^{N_S} \log\left(\sigma_x^{-2} + \frac{N_D\Lambda_{F,i}\Lambda_{1,i}\Lambda_{G,i}\Lambda_{\Sigma,i}}{\sigma_1^2 N_D\Lambda_{G,i}\Lambda_{\Sigma,i} + \sigma_2^2}\right) \tag{5.72}$$

$$s.t. \sum_{i=1}^{N_S} \sigma_x^2\Lambda_{F,i} \leq p_s \tag{5.73}$$

$$\sum_{i=1}^{N_S} \left(\sigma_x^2\Lambda_{F,i}\Lambda_{1,i} + \sigma_1^2\right)\Lambda_{G,i} \leq p_r \tag{5.74}$$

where $\{\Lambda_{F,i}\} \triangleq \Lambda_{F,1}, \cdots, \Lambda_{F,N_S}$, $\{\Lambda_{G,i}\} \triangleq \Lambda_{G,1}, \cdots, \Lambda_{G,N_S}$. Two new variables, a_i and b_i, are introduced which can be defined as

$$a_i \triangleq \sigma_x^2\Lambda_{F,i}, \quad i = 1, \cdots, N_S \tag{5.75}$$

$$b_i \triangleq \left(\sigma_x^2\Lambda_{F,i}\Lambda_{1,i} + \sigma_1^2\right)\Lambda_{G,i}, \quad i = 1, \cdots, N_S. \tag{5.76}$$

Substituting (5.75) and (5.76) back into (5.72)-(5.74), the problem (5.72)-(5.74) can be rewritten as

$$\max_{\{a_i\},\{b_i\}} \sum_{i=1}^{N_S} \log \frac{(a_i\Lambda_{1,i}+\sigma_1^2)(N_D b_i \Lambda_{\Sigma,i}+\sigma_2^2)}{\sigma_x^2(\sigma_1^2 N_D \Lambda_{\Sigma,i} b_i + a_i \Lambda_{1,i}\sigma_2^2 + \sigma_2^2\sigma_1^2)} \tag{5.77}$$

$$s.t. \sum_{i=1}^{N_S} a_i \le p_s, \quad a_i \ge 0, \quad i=1,\cdots,N_S \tag{5.78}$$

$$\sum_{i=1}^{N_S} b_i \le p_r, \quad b_i \ge 0, \quad i=1,\cdots,N_S \tag{5.79}$$

where $\{a_i\} \triangleq a_1,\cdots,a_{N_S}$ and $\{b_i\} \triangleq b_1,\cdots,b_{N_S}$.

Using the KKT conditions, the solution to the problem (5.77)-(5.79) is given by

$$a_i = \varphi_{a_i}\left[\sqrt{\frac{b_i^2\Lambda_{\Sigma,i}^2}{\sigma_2^4} + \frac{4b_i\Lambda_{1,i}\Lambda_{\Sigma,i}}{\mu_s N_D \sigma_1^2\sigma_2^2}} - \frac{b_i\Lambda_{\Sigma,i}}{\sigma_2^2} - \frac{2}{N_D}\right]^+ \tag{5.80}$$

$$b_i = \varphi_{b_i}\left[\sqrt{\frac{a_i^2\Lambda_{1,i}^2}{\sigma_1^4} + \frac{4N_D a_i\Lambda_{1,i}\Lambda_{\Sigma,i}}{\mu_r \sigma_1^2\sigma_2^2}} - \frac{a_i\Lambda_{1,i}}{\sigma_1^2} - 2\right]^+ \tag{5.81}$$
$$i=1,\cdots,N_S$$

where $[x]^+ = \max(x,0)$, μ_s and μ_r are the Lagrangian multipliers chosen to meet the power constraints (5.78) and (5.79), and

$$\varphi_{a_i} = \frac{\sigma_1^2 N_D}{2\Lambda_{1,i}}, \quad \varphi_{b_i} = \frac{\sigma_2^2}{2N_D\Lambda_{\Sigma,i}}, \quad i=1,\cdots,N_S. \tag{5.82}$$

The detailed derivation of (5.80) and (5.81) is shown in Appendix 5.D.

It can be seen from (5.80) and (5.81) that $\{a_i\}$ and $\{b_i\}$ are functions of each other. Thus, directly solving (5.80) and (5.81) is difficult. To avoid this difficulty, an iterative algorithm is proposed to compute $\{a_i\}$ and $\{b_i\}$. This algorithm is initialized with $a_i = \sqrt{p_s/N_S}$, $i=1,\cdots,N_S$. At each iteration, first $\{b_i\}$ is optimized according to (5.81) based on the initial value of $\{a_i\}$. Then $\{a_i\}$ is optimized following (5.80) using $\{b_i\}$. $\{a_i\}$ and $\{b_i\}$ are updated iteratively until convergence. Finally, the diagonal elements of $\mathbf{\Lambda}_F$ and $\mathbf{\Lambda}_G$ can be obtained by from (5.75) and (5.76).

After obtaining the optimal source and relay precoding matrices, the structure of the unitary matrix $\mathbf{\Phi}_F$ and the lower triangular matrix $\mathbf{C}$ are determined. The optimal $\mathbf{C}$ is given in (5.23). Substituting (5.47), (5.49), (5.63), and (5.64) back into (5.24), the Cholesky factorization (5.24) can be written as

$$\mathbf{L}\mathbf{L}^H = \mathbf{\Phi}_F^H \tilde{\mathbf{\Psi}}^{\frac{1}{2}} \tilde{\mathbf{\Psi}}^{\frac{1}{2}} \mathbf{\Phi}_F \tag{5.83}$$

where

$$\tilde{\mathbf{\Psi}}^{\frac{1}{2}} = \left(\sigma_x^{-2}\mathbf{I}_{N_S} + \sigma_1^{-2}\mathbf{\Lambda}_F\mathbf{\Lambda}_1(\mathbf{I}_{N_R} - \mathbf{D}_7)\right)^{-\frac{1}{2}}. \tag{5.84}$$

The proof of (5.84) can be found in [32]. Applying the GMD [81] to $\tilde{\mathbf{\Psi}}^{\frac{1}{2}}$, $\tilde{\mathbf{\Psi}}^{\frac{1}{2}}$ can be written as

$$\left(\sigma_x^{-2}\mathbf{I}_{N_S} + \sigma_1^{-2}\mathbf{\Lambda}_F\mathbf{\Lambda}_1(\mathbf{I}_{N_R} - \mathbf{D}_7)\right)^{-\frac{1}{2}} = \mathbf{Q}_2\mathbf{R}_2\mathbf{P}_2^H. \tag{5.85}$$

Substituting (5.85) back into (5.83), the Cholesky factorization (5.83) can be written as $\mathbf{L}\mathbf{L}^H = \mathbf{\Phi}_F^H\mathbf{P}_2\mathbf{R}_2^H\mathbf{R}_2\mathbf{P}_2^H\mathbf{\Phi}_F$. Similar to (5.31) and (5.32), the unitary matrix $\mathbf{\Phi}_F$ can be chosen as $\mathbf{\Phi}_F = \mathbf{P}_2$.

5.4 Numerical Examples

In this section, the performance of the proposed precoder design algorithms is investigated through numerical simulations. The channel matrices $\mathbf{H}_1$ and $\mathbf{H}_\omega$ have complex Gaussian entries with zero mean and unit variance.

The elements of the covariance matrix $\mathbf{\Sigma}$ of $\mathbf{H}_2$ is generated by $[\mathbf{\Sigma}]_{i,j} = J_0(2\pi|i-j| \triangle d_t/\lambda_c)$ [11], where $J_0(\cdot)$ is the zeroth order Bessel function of the first kind, $\triangle$ is the angle of fading spread, λ_c is the wavelength at the center frequency, and d_t is the spacing of transmit antennas. k is defined as $k = \lambda_c/\triangle d_t$. Unless explicitly mentioned, the N and k are set as $N = 4$ and $k = 3$ in the simulations. The signal-to-noise ratios (SNRs) for the source-relay and relay-destination links are defined as $\text{SNR}_1 = \frac{\sigma_x^2}{\sigma_1^2}$ and $\text{SNR}_2 = \frac{P_r}{N_R\sigma_2^2}$, respectively. The signal-to-noise ratios (SNRs) for the source-relay and relay-destination links are defined as $\text{SNR}_1 = \frac{\sigma_x^2}{\sigma_1^2}$ and $\text{SNR}_2 = \frac{P_r}{N_R\sigma_2^2}$, respectively.

First, the impact of initialization to the performance of the proposed algorithms is studied. The following three initializations are tried for the optimal precoder design (OPT-TH-cov) algorithm in Table 5.2: Initialization 1 is given in Table 5.2. In Initialization 2, $\bar{\mathbf{\Omega}} = c_1\mathbf{D}$, where $c_1 = \sqrt{p_s/N_S}$ and $\mathbf{D}$ is a 4×4 diagonal matrix whose main diagonal elements are $[\sqrt{2}, 1, \sqrt{0.5}, \sqrt{0.5}]$. For Initialization 3, $\bar{\mathbf{\Omega}}$ is set as $\bar{\mathbf{\Omega}} = c_1\mathbf{U}$, where $\mathbf{U}$ is a 4×4 random Hermitian matrix. For the suboptimal precoder design (SUB-TH-cov) algorithm in Section III.D, the following two starting points are attempted: Initialization 1 as given after (5.82) and Initialization 2 where $a_1 = a_2 = \sqrt{2p_s/N_S}$ and $a_3 = a_4 = 0$. It is observed that the proposed algorithms converge for the various initialization methods tested. Fig. 5.2 shows the BER performance of the two proposed algorithms using the initialization points tested. It can be seen from Fig. 5.2 that the

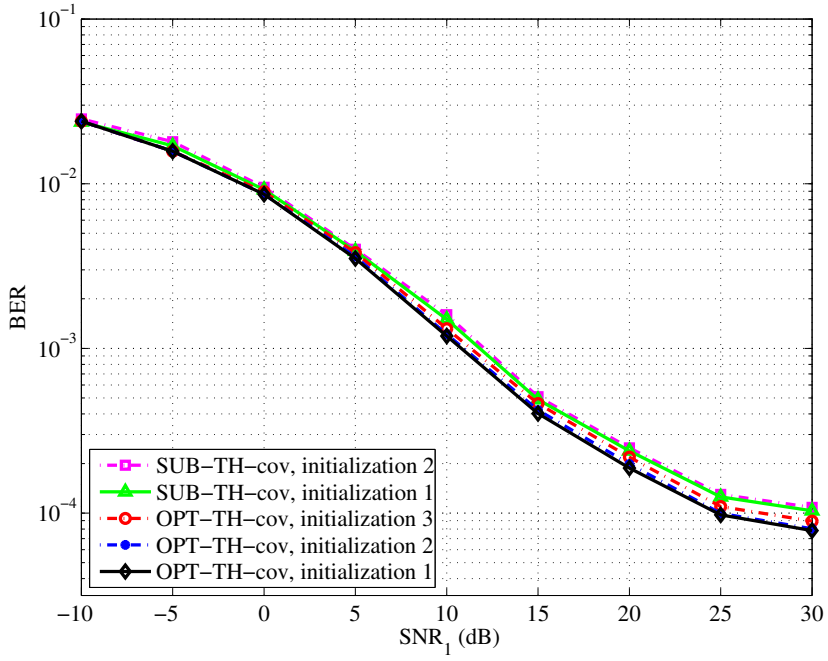

Figure 5.2: BER versus SNR_1 at different number of initialization points while fixing $\text{SNR}_2 = 20\text{dB}$.

system BER yielded by different starting points is quite small, and Initialization 1 has the lowest BER. Therefore, for the rest of simulations, Initialization 1 is used for both proposed algorithms.

In the following simulations, the performance of two proposed algorithms is compared with the linear transceiver-based precoding scheme such as the joint MMSE (JMMSE) scheme [23], the TH precoding based scheme with the full CSI (TH-FCSI) [40], TH-robust [85], TH-L-robust [43], and M-Schur-convex [41] schemes. Note that in contrast to other algorithms, the JMMSE and TH-FCSI schemes require the full CSI of the relay-destination link.

In the second example, a two-hop non-regenerative MIMO relay system is simulated with $N_S = N_R = N_D = 4$ and the information-carrying symbols are generated from 16-QAM constellations. In the example, the angle of correlation coefficient is set as $k = 3$. Fig. 5.3 shows the BER performance of all algorithms tested versus SNR_1 while fixing $\text{SNR}_2 = 20\text{dB}$. It can be seen from Fig. 5.3 that as expected, the TH-FCSI scheme has the lowest system BER. It can also be observed that over the whole range of SNR_1, the two proposed algorithms significantly outperform the JMMSE, TH-robust, TH-L-robust, and M-Schur-convex schemes in terms of BER. Moreover, for the whole range

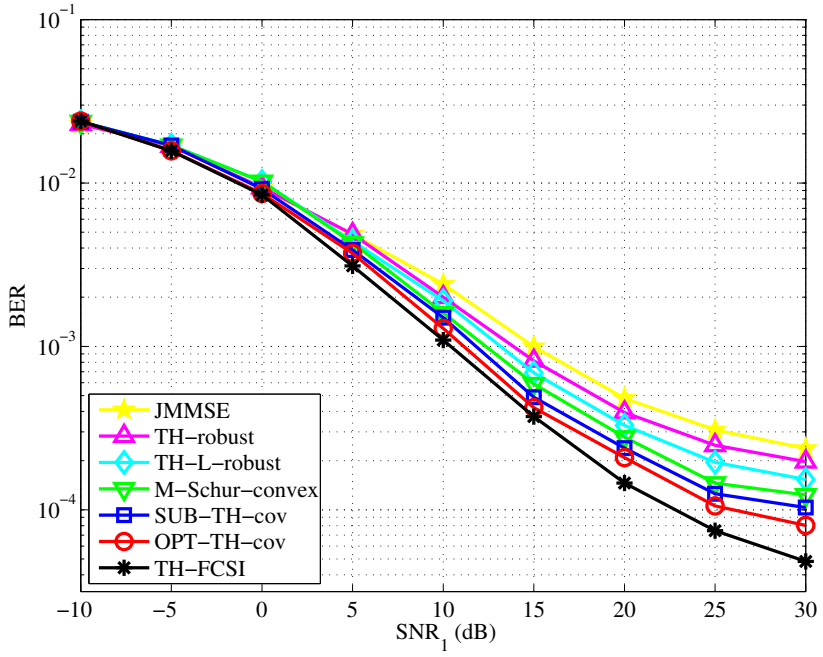

Figure 5.3: BER versus SNR_1 while fixing $\mathrm{SNR}_2 = 20\mathrm{dB}$.

of SNR_1, the BER performance of the SUB-TH-cov algorithm is very close to that of the OPT-TH-cov algorithm.

In the third example, the performance of the proposed two MSE algorithms is investigated in terms of BER performance. In the example, a two-hop non-regenerative MIMO relay system with $N_S = N_R = N_D = 4$ is considered and the information-carrying symbols are generated from 16-QAM constellations for each channel realization. The correlated coefficient is chosen as $k = 3$. Fig. 5.4 shows the performance of seven algorithms in terms of BER versus SNR_2 while fixing $\mathrm{SNR}_1 = 20\mathrm{dB}$. It can be noted from Fig. 5.4 that the proposed OPT-TH-cov and SUB-TH-cov algorithms show better BER performance over the whole range of SNR_2 than the existing schemes. Moreover, the system BER yielded by the proposed algorithms is very close to that of the system with the perfect CSI (TH-FCSI scheme).

In the fourth example, a two-hop non-regenerative MIMO relay system is considered with $N_S = N_R = N_D = 4$ and the 1000 symbols are generated from 16-QAM constellations at the source node. Fig. 5.5 shows the BER performance comparison of the algorithms tested versus SNR_1 for $k = 3$ and $k = 10$ when SNR_2 is fixed at 20dB. It can be seen from Fig. 5.5 that for both value of k, the proposed OPT-TH-cov and SUB-TH-cov algorithms show better BER performance over the whole range of SNR_1

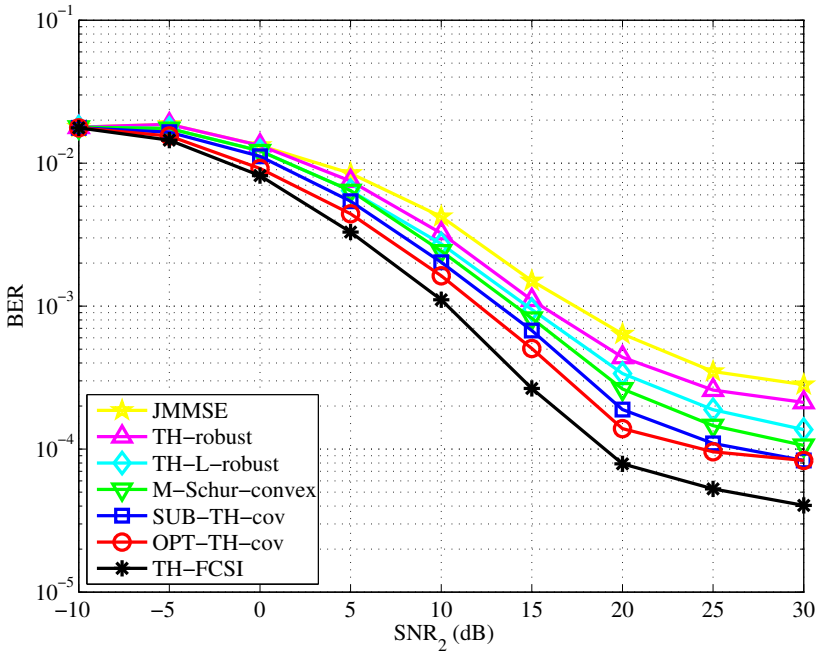

Figure 5.4: BER versus SNR_2 while fixing $\mathrm{SNR}_1 = 20\mathrm{dB}$.

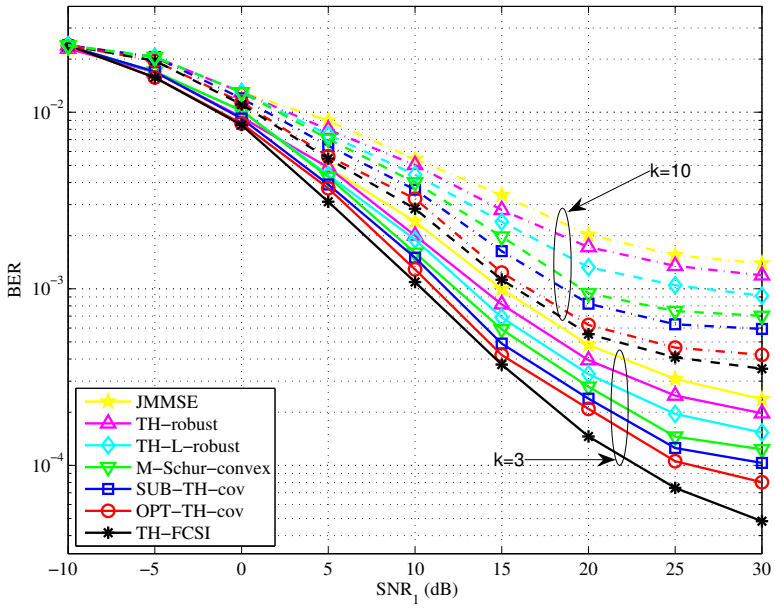

Figure 5.5: BER versus SNR_2 at different correlation coefficient k while fixing $\mathrm{SNR}_2 = 20\mathrm{dB}$.

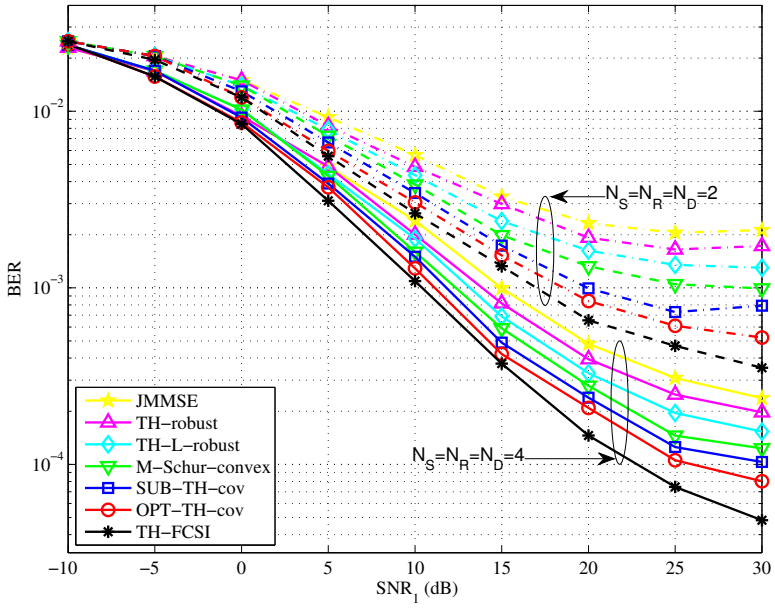

Figure 5.6: BER versus SNR_1 at different number of antennas while fixing $\text{SNR}_2 = 20\text{dB}$.

than the JMMSE, TH-robust, TH-L-robust, and M-Schur-convex schemes in terms of BER. The BER performance of the proposed OPT-TH-cov and SUB-TH-cov scheme is closer to that of the TH-FSCI scheme when k is large (i.e., the elements of $\mathbf{H}_2$ are highly correlated).

In the last example, a non-regenerative MIMO relay system is simulated and randomly 1000 16-QAM symbols are generated at the source node for each channel realization. The correlated coefficient at the relay-destination link is chosen as $k = 3$. Fig. 5.6 shows the performance of all algorithms in terms of BER versus SNR_1 for $N = 2$ and $N = 4$, while fixing $\text{SNR}_2 = 20\text{dB}$. It can be observed that the proposed OPT-TH-cov and SUB-TH-cov algorithms outperform the JMMSE, TH-robust, TH-L-robust, and M-Schur-convex schemes over the whole range of SNR_1. It can also be seen from Fig. 5.6 that with increasing number of antennas at the source, relay, and destination nodes, the BER performance of all algorithms improve. Finally, computational complexity of the proposed SUB-TH-cov and OPT-TH-cov algorithms is compared. In the SUB-TH-cov algorithm, the complexity order of matrix inversion, matrix GMD, and matrix SVD is $\mathcal{O}(N^3)$. Since the complexity of solving the problem (5.77)-(5.79) is much lower than the matrix operations mentioned above, the complexity order of the SUB-TH-cov algorithm is $\mathcal{O}(N^3)$. In each iteration of the proposed OPT-TH-cov algorithm, the major oper-

Table 5.3: Average Number of Iterations Required by the OPT-TH-cov Algorithm Till Convergence

SNR_1(dB)	0	5	10	15	20	25	30
Number of Iterations	3	4	6	8	10	12	12

ation is to update the relay matrix using the projected gradient method, which has a complexity order of $\mathcal{O}(I_1 N^3)$. Here I_1 is the number of projected gradient steps required to reach a stationary point. The overall computational complexity of the OPT-TH-cov algorithm also depends on the number of iterations required till convergence, which is shown in Table 5.3. Obviously, the SUB-TH-cov algorithm has a much lower overall computational complexity than the OPT-TH-cov algorithm. Thus, the SUB-TH-cov algorithm is very attractive for practical MIMO relay communication systems.

5.5 Chapter Summary

In this chapter, the challenging issue of precoding matrices optimization problem is addressed for a TH-based two-hop MIMO relay system where the full CSI of the source-relay link is known, while only the CCI of the relay-destination link is available at the relay node. The structure of the optimal TH precoding matrix and the source precoding matrix are derived that minimize the MSE of the signal waveform estimation at the destination. Then an iterative algorithm is developed to optimize the relay precoding matrix. A simplified precoding matrices design algorithm is proposed which has lower computational complexity than the iterative algorithm. Numerical results show that the proposed precoding matrices design schemes outperform existing algorithms.

5.A Proof of Theorem 5.1

The Lagrangian function associated with the problem (5.37) can be written as

$$\mathcal{L}_1 = -X + \mu(Q_2(\mathbf{G}) - p_r) \tag{5.86}$$

where μ is the Lagrangian multiplier. $\nabla_G \mathcal{L}_1 = 2(\frac{\partial \mathcal{L}_1}{\partial \mathbf{G}})^*$ is denoted as the gradient of (5.86). The KKT conditions [61] of the problem (5.37) on $\mathbf{G}$ are given by

$$\nabla_G \mathcal{L}_1 = 0 \tag{5.87}$$

$$\mu(Q_2(\mathbf{G}) - p_r) = 0 \tag{5.88}$$

$$Q_2(\mathbf{G}) \leq p_r. \tag{5.89}$$

Using $\frac{\partial \ln|\mathbf{X}|}{\partial \mathbf{X}} = \mathbf{X}^{-T}$, $\frac{\partial tr(\mathbf{A}\mathbf{X}^{-1})}{\partial \mathbf{X}} = -(\mathbf{X}^{-1}\mathbf{A}\mathbf{X}^{-1})^T$, and $\frac{\partial tr(\mathbf{X}\mathbf{A})}{\partial \mathbf{X}} = \mathbf{A}^T$, $\nabla_G \mathcal{L}_1$ can be written as

$$\begin{aligned}\nabla_G \mathcal{L}_1 = & -2\mathbf{H}_2^H \mathbf{R}_n^{-1} \mathbf{H}_2 \mathbf{G} \mathbf{H}_1 \mathbf{A} \mathbf{H}_1^H \\ & + 2\sigma_1^2 \mathbf{H}_2^H \mathbf{R}_n^{-1} \mathbf{H}_2 \mathbf{G} \mathbf{H}_1 \mathbf{A} \mathbf{H}_1^H \mathbf{G}^H \mathbf{H}_2^H \mathbf{R}_n^{-1} \mathbf{H}_2 \mathbf{G} \\ & + 2\mu\sigma_x^2 \mathbf{G} \mathbf{H}_1 \mathbf{F} \mathbf{F}^H \mathbf{H}_1^H.\end{aligned} \tag{5.90}$$

The Lagrangian function of the problem (5.40)-(5.41) associated with $\mathbf{G}$ can be written as

$$\mathcal{L}_2 = tr\{\mathbf{\Omega}\mathbf{A}\} + \mu(Q_2(\mathbf{G}) - p_r). \tag{5.91}$$

The KKT conditions of the problem (5.40)-(5.41) on $\mathbf{G}$ are given by

$$\nabla_G \mathcal{L}_2 = 0 \tag{5.92}$$

$$\mu(Q_2(\mathbf{G}) - p_r) = 0 \tag{5.93}$$

$$Q_2(\mathbf{G}) \leq p_r. \tag{5.94}$$

The gradient $\nabla_G \mathcal{L}_2$ of the Lagrangian function (5.91) can be derived as

$$\begin{aligned}\nabla_G \mathcal{L}_2 = & -2\mathbf{H}_2^H \mathbf{R}_n^{-1} \mathbf{H}_2 \mathbf{G} \mathbf{H}_1 \mathbf{A} \mathbf{\Omega} \mathbf{A} \mathbf{H}_1^H \\ & + 2\sigma_1^2 \mathbf{H}_2^H \mathbf{R}_n^{-1} \mathbf{H}_2 \mathbf{G} \mathbf{H}_1 \mathbf{A} \mathbf{\Omega} \mathbf{A} \mathbf{H}_1^H \mathbf{G}^H \mathbf{H}_2^H \mathbf{R}_n^{-1} \mathbf{H}_2 \mathbf{G} \\ & + 2\mu\sigma_x^2 \mathbf{G} \mathbf{H}_1 \mathbf{F} \mathbf{F}^H \mathbf{H}_1^H.\end{aligned} \tag{5.95}$$

By comparing (5.87)-(5.90) with (5.92)-(5.95), it can be observed that the KKT conditions of the problem (5.40)-(5.41) are equal to those of the problem (5.37) when (5.42) holds. The derivative of (5.40) with respect to $\mathbf{\Omega}$ can be written as

$$\frac{\partial(tr\{\mathbf{\Omega}\mathbf{A}\} - \log|\mathbf{\Omega}|)}{\partial \mathbf{\Omega}} = \mathbf{A}^T - (\mathbf{\Omega}^{-1})^T \tag{5.96}$$

By equating (5.96) to zero, (5.42) is obtained. Thus with given $\mathbf{G}$, the weight matrix $\mathbf{\Omega}$ minimizing (5.40) is given by (5.42).

5.B Proof of Theorem 5.2

First, the following definition and lemma are introduced.

Definition 5.1 *[65]. Let $\mathbf{\Phi}$ be a matrix-convex function. The Jensen's inequality for matrix valued functions is given by $E\{\mathbf{\Phi}(\mathbf{X})\} \geq \mathbf{\Phi}(E\{\mathbf{X}\})$, where $E\{\cdot\}$ is expectation on the random matrix $\mathbf{X}$.*

Lemma 5.3 *[86]. For positive definite Hermitian matrix $\mathbf{X}$, the matrix-valued function $\mathbf{\Phi}(\mathbf{X}) = \mathbf{X}^{-1}$ is matrix-convex. Therefore, from Definition 1, there is $E\{\mathbf{X}^{-1}\} \geq (E\{\mathbf{X}\})^{-1}$.*

The Theorem 5.2 is proved as follows. By using the matrix inversion lemma (5.20), (5.53) can be written as

$$\begin{aligned} E_{\widetilde{\mathbf{H}}_\omega}\{T_1(\widetilde{\mathbf{G}})\} = & E_{\widetilde{\mathbf{H}}_\omega}\Big\{tr\Big\{\bar{\mathbf{\Omega}}\Big[\rho^{-2}\sigma_x^{-2}\mathbf{I}_{N_S} + \sigma_1^{-2}\mathbf{V}_1\mathbf{\Lambda}_1^{\frac{1}{2}}\widetilde{\mathbf{G}}^H \\ & \times\mathbf{\Lambda}_\Sigma^{\frac{1}{2}}\Big(\mathbf{\Lambda}_\Sigma^{\frac{1}{2}}\widetilde{\mathbf{G}}\widetilde{\mathbf{G}}^H\mathbf{\Lambda}_\Sigma^{\frac{1}{2}} + \frac{\sigma_2^2}{\sigma_1^2}\big[\widetilde{\mathbf{H}}_\omega^H\widetilde{\mathbf{H}}_\omega\big]^{-1}\Big)^{-1} \\ & \times\mathbf{\Lambda}_\Sigma^{\frac{1}{2}}\widetilde{\mathbf{G}}\mathbf{\Lambda}_1^{\frac{1}{2}}\mathbf{V}_1^H\Big]^{-1}\Big\}\Big\}. \end{aligned} \tag{5.97}$$

By applying Lemma 5.3 to (5.97), (5.97) can be rewritten as

$$\begin{aligned} E_{\widetilde{\mathbf{H}}_\omega}\{T_1(\widetilde{\mathbf{G}})\} \geq & tr\Big\{\bar{\mathbf{\Omega}}\Big[\rho^{-2}\sigma_x^{-2}\mathbf{I}_{N_S} + \sigma_1^{-2}\mathbf{V}_1\mathbf{\Lambda}_1^{\frac{1}{2}}\widetilde{\mathbf{G}}^H\mathbf{\Lambda}_\Sigma^{\frac{1}{2}} \\ & \times\Big(\mathbf{\Lambda}_\Sigma^{\frac{1}{2}}\widetilde{\mathbf{G}}\widetilde{\mathbf{G}}^H\mathbf{\Lambda}_\Sigma^{\frac{1}{2}} + \frac{\sigma_2^2}{\sigma_1^2}E_{\widetilde{\mathbf{H}}_\omega}\Big\{\widetilde{\mathbf{H}}_\omega^H\widetilde{\mathbf{H}}_\omega\Big\}^{-1}\Big)^{-1} \\ & \times\mathbf{\Lambda}_\Sigma^{\frac{1}{2}}\widetilde{\mathbf{G}}\mathbf{\Lambda}_1^{\frac{1}{2}}\mathbf{V}_1^H\Big]^{-1}\Big\} \\ = & tr\Big\{\bar{\mathbf{\Omega}}\Big[\rho^{-2}\sigma_x^{-2}\mathbf{I}_{N_S} + \sigma_1^{-2}\mathbf{V}_1\mathbf{\Lambda}_1^{\frac{1}{2}} \\ & \times(\mathbf{I}_{N_R} - \mathbf{D}_3)\mathbf{\Lambda}_1^{\frac{1}{2}}\mathbf{V}_1^H\Big]^{-1}\Big\} \end{aligned} \tag{5.98}$$

where

$$\mathbf{D}_3 = \Big(\mathbf{I}_{N_R} + \frac{\sigma_1^2}{\sigma_2^2}\widetilde{\mathbf{G}}^H\mathbf{\Lambda}_\Sigma^{\frac{1}{2}}E_{\widetilde{\mathbf{H}}_\omega}\{\widetilde{\mathbf{H}}_\omega^H\widetilde{\mathbf{H}}_\omega\}\mathbf{\Lambda}_\Sigma^{\frac{1}{2}}\widetilde{\mathbf{G}}\Big)^{-1}.$$

Using $E_{\widetilde{\mathbf{H}}_\omega}\{\widetilde{\mathbf{H}}_\omega^H\widetilde{\mathbf{H}}_\omega\} = N_D\mathbf{I}_{N_R}$, $E_{\widetilde{\mathbf{H}}_\omega}\{T_1(\widetilde{\mathbf{G}})\}$ is obtained as $E_{\widetilde{\mathbf{H}}_\omega}\{T_1(\widetilde{\mathbf{G}})\} \geq T_2(\widetilde{\mathbf{G}})$.

5.C Proof of Theorem 5.3

For the sake of notational simplicity, let introduce $\mathbf{T}_1^{\frac{1}{2}} \triangleq \frac{\sigma_x}{\sigma_1}\mathbf{\Lambda}_F^{\frac{1}{2}}\mathbf{\Lambda}_1^{\frac{1}{2}}$ and $\mathbf{T}_2^{\frac{1}{2}} \triangleq \frac{\sigma_1}{\sigma_2}\mathbf{\Lambda}_G^{\frac{1}{2}}\mathbf{\Lambda}_{\Sigma,1}^{\frac{1}{2}}$. Then (5.67) can be written as

$$\begin{aligned} f(\mathbf{Z}) =& \log\left|\mathbf{I}_{N_S} + \mathbf{T}_1^{\frac{1}{2}}\left(\mathbf{I}_{N_S} - \left(\mathbf{I}_{N_S} + \mathbf{T}_2^{\frac{1}{2}}\mathbf{Z}\mathbf{T}_2^{\frac{1}{2}}\right)^{-1}\right)\mathbf{T}_1^{\frac{1}{2}}\right| \\ =& \log\left|\mathbf{I}_{N_S} + \mathbf{T}_1^{\frac{1}{2}}\mathbf{T}_2^{\frac{1}{2}}(\mathbf{T}_2 + \mathbf{Z}^{-1})^{-1}\mathbf{T}_2^{\frac{1}{2}}\mathbf{T}_1^{\frac{1}{2}}\right| \\ =& \log\left|\mathbf{T}_1\mathbf{T}_2 + \mathbf{T}_2 + \mathbf{Z}^{-1}\right| - \log\left|\mathbf{T}_2 + \mathbf{Z}^{-1}\right| \\ =& \log\left|\mathbf{I}_{N_S} + \mathbf{T}_3\mathbf{Z}\right| - \log\left|\mathbf{I}_{N_S} + \mathbf{T}_2\mathbf{Z}\right| \end{aligned} \tag{5.99}$$

where $\mathbf{T}_3 \triangleq \mathbf{T}_1\mathbf{T}_2 + \mathbf{T}_2$. The concavity of (5.C) can be proven by considering an arbitrary line [87] given by $\mathbf{Z} = \mathbf{X} + t\mathbf{Y} \geq 0$. Then can be rewritten as

$$\begin{aligned} g(t) =& \log\left|\mathbf{I}_{N_S} + \mathbf{T}_3(\mathbf{X} + t\mathbf{Y})\right| - \log\left|\mathbf{I}_{N_S} + \mathbf{T}_2(\mathbf{X} + t\mathbf{Y})\right| \\ =& \log\left|\mathbf{I}_{N_S} + \mathbf{T}_3^{\frac{1}{2}}(\mathbf{X} + t\mathbf{Y})\mathbf{T}_3^{\frac{1}{2}}\right| \\ & - \log\left|\mathbf{I}_{N_S} + \mathbf{T}_2^{\frac{1}{2}}(\mathbf{X} + t\mathbf{Y})\mathbf{T}_2^{\frac{1}{2}}\right| \\ =& \log\left|\mathbf{I}_{N_S} + t\mathbf{P}_3\right| - \log\left|\mathbf{I}_{N_S} + t\mathbf{P}_2\right| + \xi \\ =& \sum_{n=1}^{N_S}\left(\log(1 + t\lambda_{3,n}) - \log(1 + t\lambda_{2,n})\right) + \xi \end{aligned} \tag{5.100}$$

where $\xi \triangleq \log\left|\mathbf{I}_{N_S} + \mathbf{T}_3\mathbf{X}\right| - \log\left|\mathbf{I}_{N_S} + \mathbf{T}_2\mathbf{X}\right|$, $\lambda_{i,n}$, $i = 2, 3$, $n = 1, \cdots, N_S$, are the eigenvalues of $\mathbf{P}_i$, and for $i = 2, 3$,

$$\mathbf{P}_i = \left(\mathbf{I}_{N_S} + \mathbf{T}_i^{\frac{1}{2}}\mathbf{X}\mathbf{T}_i^{\frac{1}{2}}\right)^{-\frac{1}{2}}\mathbf{T}_i^{\frac{1}{2}}\mathbf{Y}\mathbf{T}_i^{\frac{1}{2}}\left(\mathbf{I}_{N_S} + \mathbf{T}_i^{\frac{1}{2}}\mathbf{X}\mathbf{T}_i^{\frac{1}{2}}\right)^{-\frac{1}{2}}.$$

The second-order derivative of (5.100) is

$$\begin{aligned} g''(t) =& \sum_{n=1}^{N_S}\left(\frac{\lambda_{2,n}^2}{(1 + t\lambda_{2,n})^2} - \frac{\lambda_{3,n}^2}{(1 + t\lambda_{3,n})^2}\right) \\ =& \sum_{n=1}^{N_S}\frac{(\lambda_{2,n} - \lambda_{3,n})(\lambda_{2,n} + \lambda_{3,n} + 2t\lambda_{2,n}\lambda_{2,n})}{(1 + t\lambda_{2,n})^2(1 + t\lambda_{3,n})^2}. \end{aligned} \tag{5.101}$$

Let introduce $\lambda(\mathbf{X})$ as the eigenvalue of $\mathbf{X}$. Using the property of $\lambda(\mathbf{AB}) = \lambda(\mathbf{BA})$, $\lambda(\mathbf{P}_i)$ can be written as

$$\begin{aligned} \lambda(\mathbf{P}_i) =& \lambda\left(\mathbf{T}_i^{\frac{1}{2}}\left(\mathbf{I}_{N_S} + \mathbf{T}_i^{\frac{1}{2}}\mathbf{X}\mathbf{T}_i^{\frac{1}{2}}\right)^{-1}\mathbf{T}_i^{\frac{1}{2}}\mathbf{Y}\right) \\ =& \lambda\left(\mathbf{Y}^{\frac{1}{2}}\left(\mathbf{T}_i^{-1} + \mathbf{X}\right)^{-1}\mathbf{Y}^{\frac{1}{2}}\right), \quad i = 1, 2. \end{aligned} \tag{5.102}$$

Since $\mathbf{T}_3 \geq \mathbf{T}_2$, it can be seen from (5.102) that $\lambda(\mathbf{P}_3) \geq \lambda(\mathbf{P}_2)$, i.e., $\lambda_{3,n} \geq \lambda_{2,n}$, $n = 1, \cdots, N_S$. As a result, from (5.101), $g''(t)$ can be defined as $g''(t) \leq 0$. Therefore, it can be concluded that $f(\mathbf{Z})$ is concave.

5.D Derivation of (5.80) and (5.81)

The Lagrangian function of (5.77) can be written as

$$\begin{aligned} L=&-\sum_{i=1}^{N_S}\log\frac{(a_i\Lambda_{1,i}+\sigma_1^2)(N_D b_i\Lambda_{\Sigma,i}+\sigma_2^2)}{\sigma_x^2(\sigma_1^2 N_D\Lambda_{\Sigma,i}b_i+a_i\Lambda_{1,i}\sigma_2^2+\sigma_2^2\sigma_1^2)} \\ &+\mu_s\left(\sum_{i=1}^{N_S}a_i-p_s\right)+\mu_r\left(\sum_{i=1}^{N_S}b_i-p_r\right) \end{aligned} \tag{5.103}$$

where $\mu_s \geq 0$ and $\mu_r \geq 0$ are the Lagrangian multipliers. The KKT conditions of the Lagrangian function (5.103) can be written as

$$\begin{aligned} \frac{\partial L}{\partial a_i}=&-\frac{\sigma_1^2 N_D b_i\Lambda_{\Sigma,i}\Lambda_{1,i}}{(a_i\Lambda_{1,i}+\sigma_1^2)(\sigma_1^2 N_D b_i\Lambda_{\Sigma,i}+\sigma_2^2 a_i\Lambda_{1,i}+\sigma_2^2\sigma_1^2)} \\ &+\mu_s=0 \end{aligned} \tag{5.104}$$

$$\begin{aligned} \frac{\partial L}{\partial b_i}=&-\frac{\sigma_2^2 N_D a_i\Lambda_{\Sigma,i}\Lambda_{1,i}}{(N_D b_i\Lambda_{\Sigma,i}+\sigma_2^2)(\sigma_1^2 N_D b_i\Lambda_{\Sigma,i}+\sigma_2^2 a_i\Lambda_{1,i}+\sigma_2^2\sigma_1^2)} \\ &+\mu_r=0 \end{aligned} \tag{5.105}$$

$$\mu_s\left(\sum_{i=1}^{N_S}a_i-p_s\right)=0,\quad \mu_s\geq 0,\quad a_i\geq 0, i=1,\cdots,N_S$$

$$\mu_r\left(\sum_{i=1}^{N_S}b_i-p_r\right)=0,\quad \mu_r\geq 0,\quad b_i\geq 0, i=1,\cdots,N_S.$$

Using (5.104) and (5.105) and after some manipulations, the optimum a_i and b_i can be obtained as given by (5.80) and (5.81).

Chapter 6

Robust Design for Multicasting MIMO Relay Systems

In this chapter, the transceiver design is investigated for non-regenerative multicasting MIMO relay systems, where one transmitter broadcasts common message to multiple receivers with the aid of a relay node. The transmitter, relay, and receivers are all equipped with multiple antennas. It is assumed that the true (unknown) channel matrices have Gaussian distribution, with the estimated channels as the mean value, and the channel estimation errors follow the well-known Kronecker model. In Section 6.1, overview of the existing multicasting techniques is introduced. The system model of the proposed non-regenerative multicasting MIMO relay networks is described in Section 6.2. In Section 6.3, an optimal robust transceiver design algorithm is proposed to jointly design the transmitter, relay, and receiver matrices to minimize the maximal MSE of the signal waveform estimation among all receivers. In Section 6.4, an alternative suboptimal transceiver design algorithm is developed with low computational complexity. Section 6.5 shows the numerical simulations which demonstrate the improved robustness of the proposed transceiver design algorithm against the mismatch between the true and estimated channels. Finally, the chapter is briefly summarized in Section 6.6.

6.1 Overview of Existing Techniques

In many practical communication systems, one source node transmits common information to multiple receivers simultaneously. These systems are referred to as multicast broadcasting or multicasting systems. Recently, multicasting systems have attracted much research interest, due to the increasing demand for mobile applications such as location based video broadcasting and streaming media.

The wireless channel has the multicast broadcasting nature, making it suitable for multicasting applications. However, the wireless system performance may be degraded due to the channel fading and shadowing effects. By deploying multi-antenna and beamforming techniques at the transmitter and receivers, the channel shadowing effect can be mitigated [7]. Next generation wireless standards such as WiMAX 802.16m and 3GPP LTE-Advanced have already included technologies which enable better multicasting solutions based on multi-antenna and beamforming techniques [88].

Due to the nonconvex nature of the problem, designing the optimal transmit beamforming vector for multicasting is difficult in general. Capacity limits of multi-antenna multicasting channel have been studied in [89], and the channel spatial correlation effect on the channel capacity has been investigated in [90]. In [91], transmit beamforming vectors for physical layer multicasting have been designed with the assumption that the CSI is available at the transmitter. In the multicasting systems [88–93], single-antenna has been assumed at the receivers. Recently multicasting systems with multi-antenna receivers have been investigated in [94–98].

In the case of long distance between the transmitter and receivers, relay node is necessary to efficiently mitigate the pathloss of wireless channel. In [99], a cooperative protocol for multicasting systems with multiple transmit antenna is proposed with the assumption that the users are equipped with single antenna. A two-hop MIMO relay multicasting system has been proposed in [45, 46] where one transmitter multicasts common message to multiple receivers with the aid of a relay node, and the transmitter, relay, and receivers are all equipped with multiple antennas. It is also assumed in [45, 46] that the full CSI of all channels is available at the relay node. However, in practical communication systems, the exact CSI is not available, and therefore, has to be estimated. There is always mismatch between the true and estimated CSI. Hence, the performance of the algorithm in [45, 46] will degrade due to such CSI mismatch.

In this chapter, transceiver design algorithms are proposed for multicasting MIMO relay systems which are robust against the CSI mismatch. Similar to [45, 46], the

transmitter, relay, and receivers in the system are all equipped with multiple antennas. However, different to [45, 46], the true channel matrices have Gaussian distribution, with the estimated channels as the mean value, and the channel estimation errors follow the well-known Kronecker model [85, 100–105]. An optimal robust transceiver design algorithm is developed to jointly design the transmitter, relay, and receiver matrices to minimize the maximal MSE of the signal waveform estimation among all receivers. It can be mentioned that although robust transceiver design has been studied for single-user MIMO relay systems [40, 101, 102, 106, 107], and multiuser MIMO relay systems [108]. Due to the computational complexity of the proposed optimal robust transceiver design algorithm, an alternative computationally reduced suboptimal robust transceiver design algorithm is proposed.

In the proposed two algorithms, it is proved that the MSE at each receiver can be decomposed into the sum of the MSEs of the first-hop and second-hop channels, which extends the result of MSE decomposition [109] from MIMO relay systems with perfect CSI to practical MIMO relay systems such as imperfect CSI. Based on this MSE decomposition, transceiver design algorithms are developed with low computational complexity. It is shown that under some mild condition, the transmitter and relay precoding matrices can be optimized separately. In particular, the transmitter precoding matrix optimization problem has a closed-form solution, while the relay precoding matrix can be optimized through solving a convex semidefinite programming (SDP) problem [87]. Numerical simulations demonstrate the improved robustness of the proposed algorithms against the CSI mismatch.

6.2 System Model

A two-hop non-regenerative MIMO relay multicasting system is considered with L receivers as shown in Fig. 6.1, where the transmitter and relay have N_S and N_R antennas, respectively. For simplicity, it is assumed that each receiver has N_D antennas. It is assumed that due to severe pathloss, there is no direct link between the transmitter and receivers. The data transmission takes place over two time slots. The received signal at the relay during the first time slot is given by

$$\mathbf{y}_r = \mathbf{H}_1\mathbf{F}\mathbf{x} + \mathbf{n}_1 \tag{6.1}$$

where $\mathbf{x} \in \mathbb{C}^{N_B \times 1}$ is the source signal vector satisfying $E\{\mathbf{x}\mathbf{x}^H\} = \mathbf{I}_{N_B}$, N_B is chosen to satisfy $N_B \leq \min(N_S, N_R, N_D)$, $\mathbf{H}_1 \in \mathbb{C}^{N_R \times N_S}$ is the MIMO channel matrix between

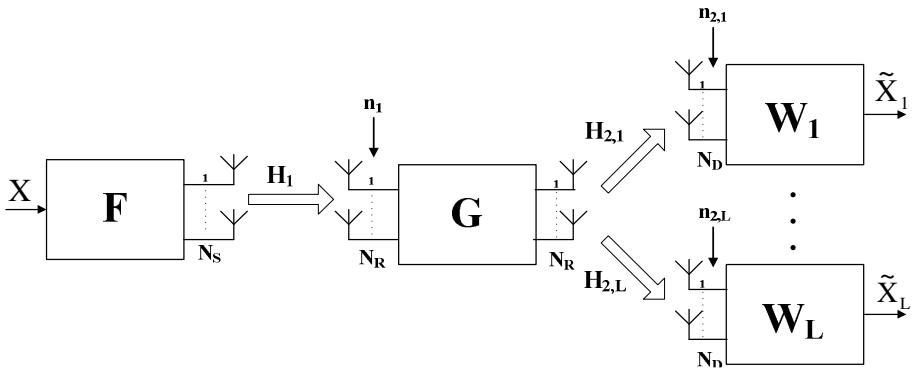

Figure 6.1: Block diagram of a two-hop non-regenerative multicasting MIMO relay system.

the transmitter and relay, $\mathbf{F} \in \mathbb{C}^{N_S \times N_B}$ is the transmitter precoding matrix, and $\mathbf{n}_1 \in \mathbb{C}^{N_R \times 1}$ is the additive noise vector at the relay. Here $\mathbf{I}_n$ represents the $n \times n$ identity matrix. At the second time slot, the relay node linear precodes $\mathbf{y}_r$ with the relay precoding matrix $\mathbf{G} \in \mathbb{C}^{N_R \times N_R}$, and broadcasts the linearly precoded signal vector

$$\mathbf{x}_r = \mathbf{G}\mathbf{y}_r \tag{6.2}$$

to all receivers. The received signal at the ith receiver can be written as

$$\mathbf{y}_{d,i} = \mathbf{H}_{2,i}\mathbf{G}\mathbf{H}_1\mathbf{F}\mathbf{x} + \mathbf{H}_{2,i}\mathbf{G}\mathbf{n}_1 + \mathbf{n}_{2,i}, \quad i = 1, \cdots, L \tag{6.3}$$

where $\mathbf{H}_{2,i} \in \mathbb{C}^{N_D \times N_R}$ is the MIMO channel matrix between the relay and the ith receiver, $\mathbf{n}_{2,i} \in \mathbb{C}^{N_D \times 1}$ is the additive noise vector at the ith receiver. It is assumed that all noises are i.i.d. with zero mean and unit variance.

In general, the instantaneous CSI is required for the optimal design of the precoding matrices $\mathbf{F}$ and $\mathbf{G}$. However, in practice, the exact CSI is not available due to channel estimation errors. In fact, the exact CSI $\mathbf{H}_1$ and $\mathbf{H}_{2,i}$ can be modeled as [102, 103, 110, 111]

$$\mathbf{H}_1 = \widehat{\mathbf{H}}_1 + \mathbf{\Delta}_1 \tag{6.4}$$

$$\mathbf{H}_{2,i} = \widehat{\mathbf{H}}_{2,i} + \mathbf{\Delta}_{2,i}, \quad i = 1, \cdots, L \tag{6.5}$$

where $\widehat{\mathbf{H}}_1$ and $\widehat{\mathbf{H}}_{2,i}$ are the estimated transmitter-relay and relay-ith receiver channel matrices, respectively, $\mathbf{\Delta}_1$ and $\mathbf{\Delta}_{2,i}$ are the corresponding channel estimation error matrices. It is assumed that $\mathbf{\Delta}_1$ and $\mathbf{\Delta}_{2,i}$ satisfy the Gaussian-Kronecker model as

[102, 103, 112–115]

$$\mathbf{\Delta}_1 \sim \mathcal{CN}\Big(\mathbf{0}, \mathbf{\Sigma}_1 \otimes \mathbf{\Psi}_1^T\Big) \tag{6.6}$$

$$\mathbf{\Delta}_{2,i} \sim \mathcal{CN}\Big(\mathbf{0}, \mathbf{\Sigma}_{2,i} \otimes \mathbf{\Psi}_{2,i}^T\Big), \quad i = 1, \cdots, L \tag{6.7}$$

where $\mathbf{\Sigma}_1$ and $\mathbf{\Psi}_1^T$ are the row and column covariance matrices of $\mathbf{\Delta}_1$, respectively, and similarly, $\mathbf{\Sigma}_{2,i}$ and $\mathbf{\Psi}_{2,i}^T$ are the row and column covariance matrices of $\mathbf{\Delta}_{2,i}$, respectively. From (6.4)-(6.7), the channel matrices $\mathbf{H}_1$ and $\mathbf{H}_{2,i}$ can be modeled as [102]

$$\mathbf{H}_1 = \widehat{\mathbf{H}}_1 + \mathbf{\Sigma}_1^{\frac{1}{2}} \mathbf{H}_{\omega_1} \mathbf{\Psi}_1^{\frac{1}{2}} \tag{6.8}$$

$$\mathbf{H}_{2,i} = \widehat{\mathbf{H}}_{2,i} + \mathbf{\Sigma}_{2,i}^{\frac{1}{2}} \mathbf{H}_{\omega_{2,i}} \mathbf{\Psi}_{2,i}^{\frac{1}{2}}, \quad i = 1, \cdots, L \tag{6.9}$$

where $\mathbf{H}_{\omega_1}$ and $\mathbf{H}_{\omega_{2,i}}$ are complex Gaussian random matrices whose entries are i.i.d. with zero mean and unit variance.

At the ith receiver, a linear receiver with the weight matrix $\mathbf{W}_i$ is applied to retrieve the source signal vector $\mathbf{x}$. Hence, the estimated signal at the ith receiver can be expressed as

$$\tilde{\mathbf{x}}_i = \mathbf{W}_i \, \mathbf{y}_{d,i}, \quad i = 1, \cdots, L. \tag{6.10}$$

Using (6.3) and (6.10), the MSE of the signal waveform estimation at the ith receiver is given by

$$\begin{aligned} M_i(\mathbf{W}_i, \mathbf{G}, \mathbf{F}) &= E\big\{ tr\big\{ (\mathbf{W}_i \mathbf{y}_{d,i} - \mathbf{x})(\mathbf{W}_i \mathbf{y}_{d,i} - \mathbf{x})^H \big\} \big\} \\ &= tr\big\{ \big(\mathbf{W}_i \mathbf{H}_{2,i} \mathbf{G} \mathbf{H}_1 \mathbf{F} - \mathbf{I}_{N_B} \big) \\ &\quad \times \big(\mathbf{W}_i \mathbf{H}_{2,i} \mathbf{G} \mathbf{H}_1 \mathbf{F} - \mathbf{I}_{N_B} \big)^H + \mathbf{W}_i \mathbf{R}_{n,i} \mathbf{W}_i^H \big\} \end{aligned} \tag{6.11}$$

where $\mathbf{R}_{n,i}$ is the equivalent noise covariance matrix given by

$$\mathbf{R}_{n,i} = \mathbf{H}_{2,i} \mathbf{G} \mathbf{G}^H \mathbf{H}_{2,i}^H + \mathbf{I}_{N_D}.$$

The power constraints on the transmitter can be written as

$$P(\mathbf{F}) = tr\{\mathbf{F}\mathbf{F}^H\} \leq P_s. \tag{6.12}$$

From (6.2), the transmission power consumed by the relay node can be written as

$$\begin{aligned} P(\mathbf{G}) &= E\{tr\{\mathbf{x}_r \mathbf{x}_r^H\}\} \\ &= tr\{\mathbf{G}(\mathbf{H}_1 \mathbf{F} \mathbf{F}^H \mathbf{H}_1^H + \mathbf{I}_{N_R}) \mathbf{G}^H\} \leq P_r. \end{aligned} \tag{6.13}$$

6.3 Proposed Optimal Robust Transceiver Design Algorithm

It can be seen from (6.11) that if the exact $\mathbf{H}_1$ and $\mathbf{H}_{2,i}$ are unavailable at the receivers, it is impossible to design $\mathbf{W}_i$ that optimizes $M_i(\mathbf{W}_i, \mathbf{G}, \mathbf{F})$ in (6.11). If $\mathbf{W}_i$ is designed, $\mathbf{F}$, and $\mathbf{G}$ based only on $\widehat{\mathbf{H}}_1$ and $\widehat{\mathbf{H}}_{2,i}$, there can be a great performance degradation due to the mismatch between $\mathbf{H}_1$, $\mathbf{H}_{2,i}$ and $\widehat{\mathbf{H}}_1$, $\widehat{\mathbf{H}}_{2,i}$. Instead of optimizing (6.11), $\mathbf{W}_i$, $\mathbf{F}$, and $\mathbf{G}$ are designed to minimize

$$J_i(\mathbf{W}_i, \mathbf{G}, \mathbf{F}) \triangleq E_{H_1, H_{2,i}}\{M_i(\mathbf{W}_i, \mathbf{G}, \mathbf{F})\}$$

where the statistical expectation is carried out with respect to $\mathbf{H}_1$ and $\mathbf{H}_{2,i}$, with the distribution given in (6.8) and (6.9).

Lemma 6.1 *[116] For* $\mathbf{H} \sim \mathcal{CN}(\widehat{\mathbf{H}}, \mathbf{\Sigma} \otimes \mathbf{\Psi}^T)$ *and any constant matrix* $\mathbf{A}$*, there is*

$$E_H\{\mathbf{HAH}^H\} = \widehat{\mathbf{H}}\mathbf{A}\widehat{\mathbf{H}}^H + tr\{\mathbf{A\Psi}\}\mathbf{\Sigma} \tag{6.14}$$

By applying Lemma 6.1 in (6.14) to (6.11), $J_i(\mathbf{W}_i, \mathbf{G}, \mathbf{F})$ can obtained as

$$\begin{aligned} J_i(\mathbf{W}_i, \mathbf{G}, \mathbf{F}) = tr\big\{&\mathbf{I}_{N_B} + \mathbf{W}_i\big(\widehat{\mathbf{H}}_{2,i}\mathbf{G\Xi G}^H\widehat{\mathbf{H}}_{2,i}^H + tr\big\{\mathbf{G\Xi G}^H\mathbf{\Psi}_{2,i}\big\}\mathbf{\Sigma}_{2,i} \\ &+\mathbf{I}_{N_D}\big)\mathbf{W}_i^H - \mathbf{W}_i\widehat{\mathbf{H}}_{2,i}\mathbf{G}\widehat{\mathbf{H}}_1\mathbf{F} - \mathbf{F}^H\widehat{\mathbf{H}}_1^H\mathbf{G}^H\widehat{\mathbf{H}}_{2,i}^H\mathbf{W}_i^H\big\} \end{aligned} \tag{6.15}$$

where

$$\mathbf{\Xi} = \widehat{\mathbf{H}}_1\mathbf{F}\mathbf{F}^H\widehat{\mathbf{H}}_1^H + tr\{\mathbf{F}\mathbf{F}^H\mathbf{\Psi}_1\}\mathbf{\Sigma}_1 + \mathbf{I}_{N_R}.$$

For any given $\mathbf{F}$ and $\mathbf{G}$, the optimal $\mathbf{W}_i$ that minimizes the MSE function (6.15) is the well known MMSE receiver (Wiener filter) which is given by [59]

$$\begin{aligned} \mathbf{W}_i = \mathbf{F}^H\widehat{\mathbf{H}}_1^H\mathbf{G}^H\widehat{\mathbf{H}}_{2,i}^H\big(&\widehat{\mathbf{H}}_{2,i}\mathbf{G\Xi G}^H\widehat{\mathbf{H}}_{2,i}^H \\ &+tr\{\mathbf{G\Xi G}^H\mathbf{\Psi}_{2,i}\}\mathbf{\Sigma}_{2,i} + \mathbf{I}_{N_D}\big)^{-1} \end{aligned} \tag{6.16}$$

By substituting (6.16) back into (6.15), the objective function (6.15) can be written as

$$\begin{aligned} J_i(\mathbf{G}, \mathbf{F}) = tr\big\{&\mathbf{I}_{N_B} - \mathbf{F}^H\widehat{\mathbf{H}}_1^H\mathbf{G}^H\widehat{\mathbf{H}}_{2,i}^H\big(\widehat{\mathbf{H}}_{2,i}\mathbf{G\Xi G}^H\widehat{\mathbf{H}}_{2,i}^H \\ &+tr\{\mathbf{G\Xi G}^H\mathbf{\Psi}_{2,i}\}\mathbf{\Sigma}_{2,i} + \mathbf{I}_{N_D}\big)^{-1}\widehat{\mathbf{H}}_{2,i}\mathbf{G}\widehat{\mathbf{H}}_1\mathbf{F}\big\}. \end{aligned} \tag{6.17}$$

Since the true $\mathbf{H}_1$ is unknown, the averaged transmission power is considered at the relay node, which can be calculated from (6.13) as

$$\begin{aligned} E_{H_1}\{P(\mathbf{G})\} &= E_{H_1}\{tr\{\mathbf{G}(\mathbf{H}_1\mathbf{F}\mathbf{F}^H\mathbf{H}_1^H + \mathbf{I}_{N_R})\mathbf{G}^H\}\} \\ &= tr\{\mathbf{G\Xi G}^H\}. \end{aligned} \tag{6.18}$$

In the proposed transceiver design, the main aim is to minimize the maximum of (6.17) among all receivers subjecting to the transmitter and relay power constraints, which can be written as the following optimization problem.

$$\min_{\mathbf{F},\mathbf{G}} \ \max_{i} \ J_i(\mathbf{G},\mathbf{F}) \tag{6.19}$$

$$s.t. \ \ tr\{\mathbf{G}\boldsymbol{\Xi}\mathbf{G}^H\} \leq P_r \tag{6.20}$$

$$tr\{\mathbf{F}\mathbf{F}^H\} \leq P_s \tag{6.21}$$

where (6.20) and (6.21) are the transmission power constraints at the relay node and the transmitter, respectively, and $P_r > 0$, $P_s > 0$ are the corresponding power budgets. The min-max problem (6.19)-(6.21) is very hard to solve due to the complicated objective function (6.19). In the following, a low computational complexity approach is proposed to optimize $\mathbf{F}$ and $\mathbf{G}$. The following theorem shows the optimal structure of $\mathbf{G}$ as the solution to the problem (6.19)-(6.21).

Theorem 6.1 *The optimal relay precoding matrix* $\mathbf{G}$ *for each transmitter-relay-receiver link can be expressed as*

$$\mathbf{G} = \mathbf{T}\mathbf{W}_r = \mathbf{T}\mathbf{F}^H\widehat{\mathbf{H}}_1^H\boldsymbol{\Xi}^{-1} \tag{6.22}$$

where $\mathbf{W}_r \triangleq \mathbf{F}^H\widehat{\mathbf{H}}_1^H\boldsymbol{\Xi}^{-1}$ can be viewed as the linear MMSE receiver at the relay node, and $\mathbf{T}$ is unknown and can be viewed as the precoding matrix at the transmit side of the second-hop MIMO multicasting channel. Using $\mathbf{G}$ in (6.22), the MSE of the estimated signal at the ith receiver (6.17) can be reformulated as the sum of two MSE functions

$$\begin{aligned} J_i(\mathbf{T},\mathbf{F}) = & tr\big\{(\mathbf{I}_{N_B}+\mathbf{F}^H\widehat{\mathbf{H}}_1^H\boldsymbol{\Upsilon}^{-1}\widehat{\mathbf{H}}_1\mathbf{F})^{-1}\big\} + tr\Big\{\Big[\mathbf{R}^{-1}+\mathbf{T}^H\widehat{\mathbf{H}}_{2,i}^H \\ & \times\big(tr\{\mathbf{T}\mathbf{R}\mathbf{T}^H\boldsymbol{\Psi}_{2,i}\}\boldsymbol{\Sigma}_{2,i}+\mathbf{I}_{N_D}\big)^{-1}\widehat{\mathbf{H}}_{2,i}\mathbf{T}\Big]^{-1}\Big\} \end{aligned} \tag{6.23}$$

where

$$\boldsymbol{\Upsilon} = tr\{\mathbf{F}\mathbf{F}^H\boldsymbol{\Psi}_1\}\boldsymbol{\Sigma}_1 + \mathbf{I}_{N_R} \tag{6.24}$$

$$\mathbf{R} = \mathbf{F}^H\widehat{\mathbf{H}}_1^H\big(\widehat{\mathbf{H}}_1\mathbf{F}\mathbf{F}^H\widehat{\mathbf{H}}_1^H + \boldsymbol{\Upsilon}\big)^{-1}\widehat{\mathbf{H}}_1\mathbf{F}. \tag{6.25}$$

Proof: See Appendix 6.A. □

Interestingly, Theorem 6.1 extends the MSE matrix decomposition from relay systems with perfect CSI to two-hop relay systems with imperfect CSI. In fact, the first

term in (6.23) is the MSE of the first-hop signal waveform estimation at the relay node given by

$$\begin{aligned}
&E_{H_1}\{E\{tr\{(\mathbf{W}_r\mathbf{y}_r-\mathbf{x})(\mathbf{W}_r\mathbf{y}_r-\mathbf{x})^H\}\}\}\\
=&E_{H_1}\{tr\{(\mathbf{W}_r\mathbf{H}_1\mathbf{F}-\mathbf{I}_{N_B})(\mathbf{W}_r\mathbf{H}_1\mathbf{F}-\mathbf{I}_{N_B})^H+\mathbf{W}_r\mathbf{W}_r^H\}\}\\
=&tr\{\mathbf{W}_r\mathbf{\Xi}\mathbf{W}_r^H-\mathbf{W}_r\widehat{\mathbf{H}}_1\mathbf{F}-\mathbf{F}^H\widehat{\mathbf{H}}_1^H\mathbf{W}_r^H+\mathbf{I}_{N_B}\}\\
=&tr\big\{(\mathbf{I}_{N_B}+\mathbf{F}^H\widehat{\mathbf{H}}_1^H\mathbf{\Upsilon}^{-1}\widehat{\mathbf{H}}_1\mathbf{F})^{-1}\big\}
\end{aligned}$$

while the second term in (6.23) can be viewed as the increment of the MSE introduced by the second-hop.

Using (6.22), the power consumption at the relay node (6.18) can be rewritten as $tr(\mathbf{T}\mathbf{R}\mathbf{T}^H)$. Hence, the problem (6.19)-(6.21) can be rewritten as

$$\min_{\mathbf{F},\mathbf{T}} \ \max_i \ J_i(\mathbf{T},\mathbf{F}) \tag{6.26}$$

$$s.t. \ \ tr\{\mathbf{T}\mathbf{R}\mathbf{T}^H\}\le P_r \tag{6.27}$$

$$tr\{\mathbf{F}\mathbf{F}^H\}\le P_s. \tag{6.28}$$

Using the matrix inversion lemma [60]

$$(\mathbf{A}+\mathbf{B}\mathbf{C}\mathbf{D})^{-1}=\mathbf{A}^{-1}-\mathbf{A}^{-1}\mathbf{B}(\mathbf{D}\mathbf{A}^{-1}\mathbf{B}+\mathbf{C}^{-1})^{-1}\mathbf{D}\mathbf{A}^{-1} \tag{6.29}$$

$\mathbf{R}$ in (6.25) can be expressed as

$$\begin{aligned}
\mathbf{R}=&\mathbf{F}^H\widehat{\mathbf{H}}_1^H\big(\mathbf{\Upsilon}^{-1}-\mathbf{\Upsilon}^{-1}\widehat{\mathbf{H}}_1\mathbf{F}\\
&\times\big(\mathbf{F}^H\widehat{\mathbf{H}}_1^H\mathbf{\Upsilon}^{-1}\widehat{\mathbf{H}}_1\mathbf{F}+\mathbf{I}_{N_B}\big)^{-1}\mathbf{F}^H\widehat{\mathbf{H}}_1^H\mathbf{\Upsilon}^{-1}\big)\widehat{\mathbf{H}}_1\mathbf{F}\\
=&\mathbf{F}^H\widehat{\mathbf{H}}_1^H\mathbf{\Upsilon}^{-1}\widehat{\mathbf{H}}_1\mathbf{F}\big(\mathbf{F}^H\widehat{\mathbf{H}}_1^H\mathbf{\Upsilon}^{-1}\widehat{\mathbf{H}}_1\mathbf{F}+\mathbf{I}_{N_B}\big)^{-1}.
\end{aligned} \tag{6.30}$$

In the case of small CSI mismatch, i.e., $tr\{\mathbf{F}\mathbf{F}^H\mathbf{\Psi}_1\}\mathbf{\Sigma}_1$ is much smaller compared with $\mathbf{I}_{N_R}$, $\mathbf{\Upsilon}$ can be approximated as $\mathbf{I}_{N_R}$. Consequently it can be seen from (6.30) that $\mathbf{R}$ can be approximated as $\mathbf{I}_{N_B}$ when $\mathbf{F}^H\widehat{\mathbf{H}}_1^H\widehat{\mathbf{H}}_1\mathbf{F}$ is much greater than $\mathbf{I}_{N_B}$. Therefore, the problem (6.26)-(6.28) can be approximated as

$$\begin{aligned}
\min_{\mathbf{F},\mathbf{T}} \ \max_i \ &tr\{(\mathbf{I}_{N_B}+\mathbf{F}^H\widehat{\mathbf{H}}_1^H\mathbf{\Upsilon}^{-1}\widehat{\mathbf{H}}_1\mathbf{F})^{-1}\}\\
&+tr\{(\mathbf{I}_{N_B}+\mathbf{T}^H\widehat{\mathbf{H}}_{2,i}^H\mathbf{K}_i^{-1}\widehat{\mathbf{H}}_{2,i}\mathbf{T})^{-1}\}
\end{aligned} \tag{6.31}$$

$$s.t. \ \ tr\{\mathbf{T}\mathbf{T}^H\}\le P_r \tag{6.32}$$

$$tr\{\mathbf{F}\mathbf{F}^H\}\le P_s \tag{6.33}$$

where $\mathbf{K}_i = tr\{\mathbf{T}\mathbf{T}^H\mathbf{\Psi}_{2,i}\}\mathbf{\Sigma}_{2,i} + \mathbf{I}_{N_D}$, $i = 1, \cdots, L$.

It can be observed from the problem (6.31)-(6.33) that the first trace term in the objective function (6.31) does not depend on $\mathbf{T}$, while the value of the second trace term in (6.31) is not affected by $\mathbf{F}$. Therefore, the problem (6.31)-(6.33) can be decomposed into the problem of optimizing $\mathbf{F}$ as

$$\min_{\mathbf{F}} \; tr\{(\mathbf{I}_{N_B} + \mathbf{F}^H\widehat{\mathbf{H}}_1^H\mathbf{\Upsilon}^{-1}\widehat{\mathbf{H}}_1\mathbf{F})^{-1}\} \tag{6.34}$$

$$s.t. \; tr\{\mathbf{F}\mathbf{F}^H\} \leq P_s \tag{6.35}$$

and the problem which optimizes $\mathbf{T}$ as

$$\min_{\mathbf{T}} \; \max_{i} \; tr\{(\mathbf{I}_{N_B} + \mathbf{T}^H\widehat{\mathbf{H}}_{2,i}^H\mathbf{K}_i^{-1}\widehat{\mathbf{H}}_{2,i}\mathbf{T})^{-1}\} \tag{6.36}$$

$$s.t. \; tr\{\mathbf{T}\mathbf{T}^H\} \leq P_r. \tag{6.37}$$

6.3.1 Optimization of F

When $\mathbf{\Psi}_1 = \mathbf{I}_{N_S}$, i.e., the columns of $\mathbf{\Delta}_1$ are uncorrelated, from (6.24) $\mathbf{\Upsilon}$ can be defined as $\mathbf{\Upsilon} = tr\{\mathbf{F}\mathbf{F}^H\}\mathbf{\Sigma}_1 + \mathbf{I}_{N_R}$. It can be easily shown that the optimal solution of the problem (6.34)-(6.35) must meet equality at constraint (6.35), i.e., the optimal $\mathbf{F}$ should satisfy $tr\{\mathbf{F}\mathbf{F}^H\} = P_s$. In this case, $\mathbf{\Upsilon} = P_s\mathbf{\Sigma}_1 + \mathbf{I}_{N_R}$ does not depend on $\mathbf{F}$, and the problem (6.34)-(6.35) has a closed-form solution as shown later.

However, for the general case of $\mathbf{\Psi}_1 \neq \mathbf{I}_{N_S}$, $\mathbf{\Upsilon}$ is a function of $\mathbf{F}$, which makes the problem (6.34)-(6.35) difficult to solve. To overcome this challenge, the following inequality [102] is applied

$$tr\{\mathbf{F}\mathbf{F}^H\mathbf{\Psi}_1\} \leq P_s\lambda_{\mathrm{M}}(\mathbf{\Psi}_1) \tag{6.38}$$

where $\lambda_{\mathrm{M}}(\cdot)$ stands for the maximal eigenvalue of a matrix. From (6.38), an upper-bound of (6.34) is given by

$$\begin{aligned} &tr\{(\mathbf{I}_{N_B} + \mathbf{F}^H\widehat{\mathbf{H}}_1^H\mathbf{\Upsilon}^{-1}\widehat{\mathbf{H}}_1\mathbf{F})^{-1}\} \\ &\leq tr\{(\mathbf{I}_{N_B} + \mathbf{F}^H\widehat{\mathbf{H}}_1^H(P_s\lambda_{\mathrm{M}}(\mathbf{\Psi}_1)\mathbf{\Sigma}_1 + \mathbf{I}_{N_R})^{-1}\widehat{\mathbf{H}}_1\mathbf{F})^{-1}\}. \end{aligned} \tag{6.39}$$

Interestingly, the equality in (6.39) holds when $\mathbf{\Psi}_1 = \mathbf{I}_{N_S}$, as in this case $\lambda_{\mathrm{M}}(\mathbf{\Psi}_1) = 1$. Based on the discussion above, let introduce

$$\mathbf{A} \triangleq \widehat{\mathbf{H}}_1^H(P_s\lambda_{\mathrm{M}}(\mathbf{\Psi}_1)\mathbf{\Sigma}_1 + \mathbf{I}_{N_R})^{-1}\widehat{\mathbf{H}}_1.$$

The problem (6.34)-(6.35) is modified to the following transmitter precoding matrix optimization problem

$$\min_{\mathbf{F}} \; tr\{(\mathbf{I}_{N_B} + \mathbf{F}^H \mathbf{A} \mathbf{F})^{-1}\} \tag{6.40}$$

$$s.t. \; tr\{\mathbf{F}\mathbf{F}^H\} \leq P_s. \tag{6.41}$$

Let introduce the EVD of $\mathbf{A}$ as $\mathbf{A} = \mathbf{U}_A \mathbf{\Lambda}_A \mathbf{U}_A^H$, where the diagonal elements of $\mathbf{\Lambda}_A$ are sorted in a decreasing order. It can be shown that the solution to the problem (6.40)-(6.41) is given by

$$\mathbf{F} = \mathbf{U}_{A,1} \mathbf{\Lambda}_F^{\frac{1}{2}} \tag{6.42}$$

where $\mathbf{U}_{A,1}$ contains the leftmost N_B columns of $\mathbf{U}_A$ associated with the largest N_B eigenvalues and $\mathbf{\Lambda}_F$ is a diagonal matrix. Using (6.42), the problem (6.40)-(6.41) can be written as the following constrained optimization problem with scalar variables

$$\min_{\{\lambda_{F,i}\}} \; \sum_{i=1}^{N_B} \frac{1}{1 + \lambda_{F,i}\lambda_{A,i}} \tag{6.43}$$

$$s.t. \; \sum_{i=1}^{N_B} \lambda_{F,i} \leq P_s \tag{6.44}$$

$$\lambda_{F,i} \geq 0, \qquad i = 1, \cdots, N_B \tag{6.45}$$

where $\lambda_{F,i}$ and $\lambda_{A,i}$, $i = 1, \cdots, N_B$, are the ith diagonal elements of $\mathbf{\Lambda}_F$ and $\mathbf{\Lambda}_A$, respectively, and $\{\lambda_{F,i}\} = \{\lambda_{F,1}, \cdots, \lambda_{F,N_B}\}$. The problem (6.43)-(6.45) has the well-known water-filling solution as

$$\lambda_{F,i} = \frac{1}{\lambda_{A,i}} \left(\sqrt{\frac{\lambda_{A,i}}{\mu}} - 1 \right)^+, \qquad i = 1, \cdots, N_B$$

where $(x)^+ = \max(x, 0)$, and $\mu > 0$ satisfies the nonlinear equation of $\sum_{i=1}^{N_B} \frac{1}{\lambda_{A,i}} \big(\sqrt{\frac{\lambda_{A,i}}{\mu}} - 1 \big)^+ = P_s$.

6.3.2 Optimization of T

Similar to the technique used in optimizing $\mathbf{F}$, the $tr\big\{\mathbf{T}\mathbf{T}^H \mathbf{\Psi}_{2,i}\big\}$ can be defined as $tr\big\{\mathbf{T}\mathbf{T}^H \mathbf{\Psi}_{2,i}\big\} \leq P_r \lambda_{\mathrm{M}}(\mathbf{\Psi}_{2,i})$. Let introduce

$$\mathbf{B}_i \triangleq \widehat{\mathbf{H}}_{2,i}^H (P_r \lambda_{\mathrm{M}}(\mathbf{\Psi}_{2,i}) \mathbf{\Sigma}_{2,i} + \mathbf{I}_{N_D})^{-1} \widehat{\mathbf{H}}_{2,i}, \;\; i = 1, \cdots, L.$$

The problem (6.36)-(6.37) can be modified to the following problem

$$\min_{\mathbf{T}} \ \max_{i} \ tr\{(\mathbf{I}_{N_B} + \mathbf{T}^H \mathbf{B}_i \mathbf{T})^{-1}\} \tag{6.46}$$

$$s.t. \ tr\{\mathbf{T}\mathbf{T}^H\} \leq P_r. \tag{6.47}$$

Using the matrix identity of $tr\{(\mathbf{I}_m + \mathbf{A}_{m\times n}\mathbf{B}_{n\times m})^{-1}\} = tr\{(\mathbf{I}_n + \mathbf{B}_{n\times m}\mathbf{A}_{m\times n})^{-1}\} + m - n$, the min-max problem ((6.46))-(6.47) can be written as

$$\min_{\mathbf{Q}} \ \max_{i} \ tr\left\{\left(\mathbf{I}_{N_D} + \mathbf{B}_i^{\frac{1}{2}}\mathbf{Q}\mathbf{B}_i^{\frac{H}{2}}\right)^{-1}\right\} + N_B - N_D \tag{6.48}$$

$$s.t. \ tr\big(\mathbf{Q}\big) \leq P_r \tag{6.49}$$

$$\mathbf{Q} \succeq 0 \tag{6.50}$$

where $\mathbf{Q} = \mathbf{T}\mathbf{T}^H$ and $\mathbf{Q} \succeq 0$ denotes that $\mathbf{Q}$ is a PSD matrix. Let introduce a real valued slack variable ρ and PSD matrices $\mathbf{Z}_i$ with $\left(\mathbf{I}_{N_D} + \mathbf{B}_i^{\frac{1}{2}}\mathbf{Q}\mathbf{B}_i^{\frac{H}{2}}\right)^{-1} \preceq \mathbf{Z}_i, i = 1, \cdots, L$, where $\mathbf{A} \preceq \mathbf{B}$ means that $\mathbf{B} - \mathbf{A}$ is PSD. By using the Schur complement [87], the problem (6.48)-(6.50) can be equivalently rewritten as

$$\min_{\rho, \mathbf{Q}, \{\mathbf{Z}_i\}} \ \rho \tag{6.51}$$

$$s.t. \ tr(\mathbf{Z}_i) \leq \rho, \qquad i = 1, \cdots, L \tag{6.52}$$

$$tr\big(\mathbf{Q}\big) \leq P_r \tag{6.53}$$

$$\begin{pmatrix} \mathbf{Z}_i & \mathbf{I}_{N_D} \\ \mathbf{I}_{N_D} & \mathbf{I}_{N_D} + \mathbf{B}_i^{\frac{1}{2}}\mathbf{Q}\mathbf{B}_i^{\frac{H}{2}} \end{pmatrix} \succeq 0, \quad i = 1, \cdots, L \tag{6.54}$$

$$\mathbf{Q} \succeq 0 \tag{6.55}$$

where $\{\mathbf{Z}_i\} = \{\mathbf{Z}_1, \cdots, \mathbf{Z}_L\}$. The problem (6.51)-(6.55) is a convex SDP problem and can be solved by the convex programming toolbox CVX [117].

6.4 Proposed Suboptimal Robust Transceiver Design Algorithm

For any given precoding matrices $\mathbf{F}$ and $\mathbf{G}$ which satisfy the power constraints at the transmitter and relay node (6.12) and (6.13), the weight matrix $\mathbf{W}_i$ minimizing (6.11) is the well known MMSE filter which is given by [59]

$$\begin{aligned}\mathbf{W}_i = &\mathbf{F}^H \mathbf{H}_1^H \mathbf{G}^H \mathbf{H}_{2,i}^H \\ &\times (\mathbf{H}_{2,i}\mathbf{G}\mathbf{H}_1\mathbf{F}\mathbf{F}^H\mathbf{H}_1^H\mathbf{G}^H\mathbf{H}_{2,i}^H + \mathbf{R}_{n,i})^{-1}.\end{aligned} \tag{6.56}$$

After substituting (6.56) into (6.11) and using the matrix inversion lemma (6.29) the MSE of the signal waveform estimation at the ith receiver is given by

$$J_i(\mathbf{G},\mathbf{F}) = tr\Big\{\Big[\mathbf{I}_{N_B} + \bar{\mathbf{H}}_i^H \mathbf{R}_{n,i}^{-1}\bar{\mathbf{H}}_i\Big]^{-1}\Big\} \tag{6.57}$$

where $\bar{\mathbf{H}}_i = \mathbf{H}_{2,i}\mathbf{G}\mathbf{H}_1\mathbf{F}$.

From (6.12), (6.13), and (6.57), the linear transceiver design problem can be formulated as

$$\begin{aligned} \min_{\mathbf{G},\mathbf{F}} \ \max_i \ & J_i(\mathbf{G},\mathbf{F}) \\ s.t. \ & tr\Big\{\mathbf{G}(\mathbf{H}_1\mathbf{F}\mathbf{F}^H\mathbf{H}_1^H + \mathbf{I}_{N_R})\mathbf{G}^H\Big\} \le P_r \\ & tr\Big\{\mathbf{F}\mathbf{F}^H\Big\} \le P_s \end{aligned} \tag{6.58}$$

Note that directly solving the min-max problem (6.58) is difficult due to the complicated function of $J_i(\mathbf{G},\mathbf{F})$. In the following, a low computational complexity approach is proposed to solve the problem (6.58).

It can be shown similar to [109] that the optimal relay precoding matrix $\mathbf{G}$ for each link can be expressed as

$$\mathbf{G} = \mathbf{T}\mathbf{D}^H \tag{6.59}$$

where $\mathbf{D} = (\mathbf{H}_1\mathbf{F}\mathbf{F}^H\mathbf{H}_1 + \mathbf{I}_{N_R})^{-1}\mathbf{H}_1\mathbf{F}$ and $\mathbf{T}$ can be considered as the precoding matrix at the transmit side of the second-hop MIMO multicasting channel.

Using the relay precoding matrix $\mathbf{G}$ (6.59), the MSE of the estimated signal at the ith receiver can be reformulated as the sum of two individual MSE [109] functions

$$\begin{aligned} J_i(\mathbf{T},\mathbf{F}) = & tr\Big\{\Big[\mathbf{I}_{N_B} + \mathbf{F}^H\mathbf{H}_1^H\mathbf{H}_1\mathbf{F}\Big]^{-1}\Big\} \\ & + tr\Big\{\Big[\mathbf{R}^{-1} + \mathbf{T}^H\mathbf{H}_{2,i}^H\mathbf{H}_{2,i}\mathbf{T}\Big]^{-1}\Big\}, i = 1,\cdots,L \end{aligned}$$

where

$$\mathbf{R} = \mathbf{F}^H\mathbf{H}_1^H\big(\mathbf{H}_1\mathbf{F}\mathbf{F}^H\mathbf{H}_1^H + \mathbf{I}_{N_R}\big)^{-1}\mathbf{H}_1\mathbf{F}. \tag{6.60}$$

Interestingly, the first term in (6.60) is the MSE of estimating $\mathbf{x}$ from the signal vector (6.1) received at the relay node using the MMSE receiver with the weight matrix $\mathbf{D}$, while the second term in (6.60) can be viewed as the increment of the MSE introduced by the second-hop.

Using the relay precoding matrix $\mathbf{G}$ in (6.59), the power consumption at the relay power can be rewritten as $tr(\mathbf{T}\mathbf{R}\mathbf{T}^H)$. Hence, the problem (6.58) can be equivalently rewritten as the following problem

$$\begin{aligned} \min_{\mathbf{F},\mathbf{T}} \ \max_i \ & J_i(\mathbf{T},\mathbf{F}) \\ s.t. \ & tr\Big\{\mathbf{T}\mathbf{R}\mathbf{T}^H\Big\} \le P_r \\ & tr\Big\{\mathbf{F}\mathbf{F}^H\Big\} \le P_s. \end{aligned} \tag{6.61}$$

Using the matrix inversion lemma (6.29), the matrix $\mathbf{R}$ (6.60) can be expressed as

$$\begin{aligned} \mathbf{R}=&\mathbf{F}^H\mathbf{H}_1^H\Big(\mathbf{I}_{N_R}-\mathbf{H}_1\mathbf{F} \\ &\times\Big(\mathbf{F}^H\mathbf{H}_1^H\mathbf{H}_1\mathbf{F}+\mathbf{I}_{N_B}\Big)^{-1}\mathbf{F}^H\mathbf{H}_1^H\Big)\mathbf{H}_1\mathbf{F} \\ =&\mathbf{F}^H\mathbf{H}_1^H\mathbf{H}_1\mathbf{F}\Big(\mathbf{F}^H\mathbf{H}_1^H\mathbf{H}_1\mathbf{F}+\mathbf{I}_{N_B}\Big)^{-1} \end{aligned} \tag{6.62}$$

It can observed from (6.62) that with increase in the transmitter power P_s, $\mathbf{F}^H\mathbf{H}_1^H\mathbf{H}_1\mathbf{F}$ approaches infinity and for large P_s value, $\mathbf{F}^H\mathbf{H}_1^H\mathbf{H}_1\mathbf{F} \gg \mathbf{I}_{N_B}$. Hence, $\mathbf{R}$ can be approximated as $\mathbf{I}_{N_B}$ for large P_s value [109]. Therefore, the problem (6.61) can be formulated as

$$\begin{aligned} \min_{\mathbf{F},\mathbf{T}} \ \max_i \ & tr\Big\{\Big[\mathbf{I}_{N_B}+\mathbf{F}^H\mathbf{H}_1^H\mathbf{H}_1\mathbf{F}\Big]^{-1}\Big\} \\ & +tr\Big\{\Big[\mathbf{I}_{N_B}+\mathbf{T}^H\mathbf{H}_{2,i}^H\mathbf{H}_{2,i}\mathbf{T}\Big]^{-1}\Big\} \\ s.t. \ & tr\Big\{\mathbf{T}\mathbf{T}^H\Big\} \le P_r, \\ & tr\Big\{\mathbf{F}\mathbf{F}^H\Big\} \le P_s \end{aligned} \tag{6.63}$$

It can be noticed from (6.63) that $\mathbf{T}$ has no influence on the first term of the objective function (6.63) and $\mathbf{F}$ has no influence on the second term as well. Hence, the optimization problem (6.63) can be divided into the following transmitter precoding matrix optimization problem

$$\begin{aligned} \min_{\mathbf{F}} \ & tr\Big\{\Big[\mathbf{I}_{N_B}+\mathbf{F}^H\mathbf{H}_1^H\mathbf{H}_1\mathbf{F}\Big]^{-1}\Big\} \\ s.t. \ & tr\big\{\mathbf{F}\mathbf{F}^H\big\} \le P_s \end{aligned} \tag{6.64}$$

and the relay precoding matrix optimization problem can be expressed as

$$\begin{aligned} \min_{\mathbf{T}} \ \max_i \ & tr\Big\{\Big[\mathbf{I}_{N_B}+\mathbf{T}^H\mathbf{H}_{2,i}^H\mathbf{H}_{2,i}\mathbf{T}\Big]^{-1}\Big\} \\ s.t. \ & tr\big\{\mathbf{T}\mathbf{T}^H\big\} \le P_r. \end{aligned} \tag{6.65}$$

Lemma 6.2 *Let $f(\mathbf{X})$ be a function of random matrix $\mathbf{X}$ having finite expectation $E(\mathbf{X})$. If f is a matrix-convex function, then $E[f(\mathbf{X})] \succeq f(E[\mathbf{X}])$ [87].*

6.4.1 Optimization of F

It can be noticed from (6.64) that the problem is reduced to find the optimal precoding matrix $\mathbf{F}$ to minimize the MSE of the received signal at the relay node. However, as the exact $\mathbf{H}_1$ is unknown, the problem (6.64) cannot be solved. If $\mathbf{F}$ is optimized based on $\widehat{\mathbf{H}}_1$, there might be great performance degradation due to the mismatch between $\mathbf{H}_1$ and $\widehat{\mathbf{H}}_1$. Thus, instead of minimizing $M(\mathbf{F}) = tr\{(\mathbf{I}_{N_B} + \mathbf{F}^H\mathbf{H}_1^H\mathbf{H}_1\mathbf{F})^{-1}\}$, $E_{\Delta_1}\{M(\mathbf{F})\}$ is minimized, where the expectation is over the distribution of $\mathbf{\Delta}_1$.

However, the exact expression of $E_{\Delta_1}\{M(\mathbf{F})\}$ is difficult to obtain. Using the channel estimation error model (6.4) and Lemma 6.2, the lower bound of $E_{\Delta_1}\{M(\mathbf{F})\}$ can be written as

$$\begin{aligned} E_{\Delta_1}\{M(\mathbf{F})\} \succeq & tr\Big\{\big(\mathbf{I}_{N_B} + \mathbf{F}^H E_{\Delta_1}\{\mathbf{H}_1^H\mathbf{H}_1\}\mathbf{F}\big)^{-1}\Big\} \\ = & tr\Big\{\big(\mathbf{I}_{N_B} + \mathbf{F}^H\mathbf{A}\mathbf{F}\big)^{-1}\Big\} \end{aligned} \tag{6.66}$$

where $\mathbf{A} = \widehat{\mathbf{H}}_1^H\widehat{\mathbf{H}}_1 + tr\big\{\mathbf{\Sigma}_1\big\}\mathbf{\Psi}_1$. Using (6.66), the source precoding matrix optimization problem can be written as

$$\begin{aligned} \min_{\mathbf{F}} \;\; & tr\Big\{\big(\mathbf{I}_{N_B} + \mathbf{F}^H\mathbf{A}\mathbf{F}\big)^{-1}\Big\} \\ s.t. \;\; & tr\big\{\mathbf{F}\mathbf{F}^H\big\} \leq P_s. \end{aligned} \tag{6.67}$$

Let introduce the EVD of the matrix $\mathbf{A}$

$$\mathbf{A} = \mathbf{U}_A\mathbf{\Lambda}_A\mathbf{U}_A^H \tag{6.68}$$

where the diagonal elements of $\mathbf{A}$ are sorted in a decreasing order. It can be shown that the solution to the problem (6.67) is given by

$$\mathbf{F} = \mathbf{U}_{A,1}\mathbf{\Lambda}_F^{\frac{1}{2}} \tag{6.69}$$

where $\mathbf{U}_{A,1}$ contains the leftmost N_B columns of $\mathbf{U}_A$ associated with the largest N_B eigenvalues and $\mathbf{\Lambda}_F$ is a diagonal matrix. After substituting (6.68) and (6.69) into (6.67), the problem (6.67) can be written as the following optimization problem with

scalar variables

$$\min_{\{\lambda_{F,i}\}} \sum_{i=1}^{N_B} \frac{1}{1+\lambda_{F,i}\lambda_{A,i}} \tag{6.70}$$

$$s.t. \sum_{i=1}^{N_B} \lambda_{F,i} \le P_s \tag{6.71}$$

$$\lambda_{F,i} \ge 0, \qquad i = 1, \cdots, N_B \tag{6.72}$$

where $\lambda_{F,i}$ and $\lambda_{A,i}$, $i = 1, \cdots, N_B$, are the ith diagonal elements of $\mathbf{\Lambda}_F$ and $\mathbf{\Lambda}_A$, respectively, and $\{\lambda_{F,i}\} = \{\lambda_{F,1}, \cdots, \lambda_{F,N_B}\}$. The problem (6.70)-(6.72) has the well-known water-filling solution as [61]

$$\lambda_{F,i} = \frac{1}{\lambda_{A,i}} \left(\sqrt{\frac{\lambda_{A,i}}{\mu}} - 1 \right)^+, \qquad i = 1, \cdots, N_B$$

where $(x)^+ = \max(x, 0)$, and $\mu > 0$ satisfies the nonlinear equation of $\sum_{i=1}^{N_B} \frac{1}{\lambda_{A,i}} \big(\sqrt{\frac{\lambda_{A,i}}{\mu}} - 1 \big)^+ = P_s$.

6.4.2 Optimization of T

It can be seen from (6.65) that the problem is reduced to find the optimal precoding matrix $\mathbf{T}$ to minimize the maximal MSE of the received signal at the receiver. Similar to the approach for optimizing $\mathbf{F}$, using the channel estimation error model (6.5) and Lemma 6.2, the objective function can be written as

$$\begin{aligned} & E_{\Delta_{2,i}}\{tr\{(\mathbf{I}_{N_B} + \mathbf{T}^H \mathbf{H}_{2,i}^H \mathbf{H}_{2,i} \mathbf{T})^{-1}\}\} \\ & \succeq tr\Big\{ \Big[\mathbf{I}_{N_B} + \mathbf{T}^H E_{\Delta_{2,i}}\{\mathbf{H}_{2,i}^H \mathbf{H}_{2,i}\} \mathbf{T} \Big]^{-1} \Big\} \\ & = tr\{(\mathbf{I}_{N_B} + \mathbf{T}^H \mathbf{B}_i \mathbf{T})^{-1}\} \end{aligned} \tag{6.73}$$

where $\mathbf{B}_i = \widehat{\mathbf{H}}_{2,i}^H \widehat{\mathbf{H}}_{2,i} + tr\big\{\mathbf{\Sigma}_{2,i}\big\}\mathbf{\Psi}_{2,i}$. Using (6.73), the problem of optimizing $\mathbf{T}$ can be written as

$$\begin{aligned} \min_{\mathbf{T}} \ \max_i \ & tr\Big\{ \Big[\mathbf{I}_{N_B} + \mathbf{T}^H \mathbf{B}_i \mathbf{T} \Big]^{-1} \Big\} \\ s.t. \ & tr\big(\mathbf{T}\mathbf{T}^H\big) \le P_r. \end{aligned} \tag{6.74}$$

Using the matrix identity $tr\big\{\big[\mathbf{I}_m + \mathbf{A}_{m\times n}\mathbf{B}_{n\times m}\big]^{-1}\big\} = tr\big\{\big[\mathbf{I}_n + \mathbf{B}_{n\times m}\mathbf{A}_{m\times n}\big]^{-1}\big\} +$

$m - n$ the min-max problem (6.74) can be written as

$$\begin{aligned} \min_{\mathbf{Q}} \ \max_{i} \ & tr\Big\{\Big[\mathbf{I}_{N_D} + \mathbf{B}_i^{\frac{1}{2}}\mathbf{Q}\mathbf{B}_i^{\frac{1}{2}}\Big]^{-1}\Big\} + N_B - N_D \\ s.t. \ & tr\big(\mathbf{Q}\big) \leq P_r \\ & \mathbf{Q} \succeq 0 \end{aligned} \tag{6.75}$$

where $\mathbf{Q} = \mathbf{T}\mathbf{T}^H$ and $\mathbf{Q} \succeq 0$ denotes that $\mathbf{Q}$ is a PSD matrix. Let introduce a PSD matrix $\mathbf{Z}_i$ with $\big[\mathbf{I}_{N_D} + \mathbf{B}_i^{\frac{1}{2}}\mathbf{Q}\mathbf{B}_i^{\frac{1}{2}}\big]^{-1} \preceq \mathbf{Z}_i, i = 1, \cdots, L$ and a real valued slack variable ρ. By using the Schur complement [87], the optimization problem (6.75) can be reformulated as

$$\begin{aligned} \min_{\rho,\, \mathbf{Q},\, \mathbf{Z}_i} \ & \rho \\ s.t. \ & tr\big(\mathbf{Z}_i\big) \leq \rho, \quad i = 1, \cdots, L \\ & tr\big(\mathbf{Q}\big) \leq P_r \\ & \begin{pmatrix} \mathbf{Z}_i & \mathbf{I}_{N_D} \\ \mathbf{I}_{N_D} & \mathbf{I}_{N_D} + \mathbf{B}_i^{\frac{1}{2}}\mathbf{Q}\mathbf{B}_i^{\frac{1}{2}} \end{pmatrix} \succeq 0, \quad i = 1, \cdots, L \\ & \mathbf{Q} \succeq 0. \end{aligned} \tag{6.76}$$

The optimization problem (6.76) is a convex SDP problem and the convex programming toolbox CVX [117] can be used to solve the SDP problem.

6.5 Numerical Examples

In this section, the performance of the proposed two robust transceiver design algorithms is investigated for multicasting MIMO relay systems through numerical simulations. A two-hop non-regenerative multicasting MIMO relay system is simulated with $N_B = N_S = N_R = N_D = 4$. The information-carrying symbols are modulated using the QPSK constellations. The SNRs of the first-hop and second-hop channels are defined as $\text{SNR}_1 = P_s/N_S$ and $\text{SNR}_2 = P_r/N_R$, respectively. SNR_1 is set as $\text{SNR}_1 = 30\text{dB}$. In the simulations, the correlation matrices of the channel estimation errors are modeled

as [102, 118]

$$\mathbf{\Psi}_1{=}\mathbf{\Psi}_{2,i} = \begin{pmatrix} 1 & \alpha & \alpha^2 & \alpha^3 \\ \alpha & 1 & \alpha & \alpha^2 \\ \alpha^2 & \alpha & 1 & \alpha \\ \alpha^3 & \alpha^2 & \alpha & 1 \end{pmatrix}, \quad i = 1, \cdots, L$$

$$\mathbf{\Sigma}_1{=}\mathbf{\Sigma}_{2,i} = \sigma_e^2 \begin{pmatrix} 1 & \beta & \beta^2 & \beta^3 \\ \beta & 1 & \beta & \beta^2 \\ \beta^2 & \beta & 1 & \beta \\ \beta^3 & \beta^2 & \beta & 1 \end{pmatrix}, \; i = 1, \cdots, L$$

where $0 \leq \alpha,\ \beta \leq 1$ are correlation coefficients, and σ_e^2 measures the variance of the estimated error. The estimated channel matrices $\widehat{\mathbf{H}}_1$ and $\widehat{\mathbf{H}}_{2,i}$ are generated based on the following distributions

$$\widehat{\mathbf{H}}_1 \sim \mathcal{CN}\Big(\mathbf{0}, \frac{1-\sigma_e^2}{\sigma_e^2}\mathbf{\Sigma}_1 \otimes \mathbf{\Psi}_1^T\Big)$$

$$\widehat{\mathbf{H}}_{2,i} \sim \mathcal{CN}\Big(\mathbf{0}, \frac{1-\sigma_e^2}{\sigma_e^2}\mathbf{\Sigma}_{2,i} \otimes \mathbf{\Psi}_{2,i}^T\Big), \quad i = 1, \cdots, L.$$

The performance of the proposed robust transceiver design algorithms is compared namely, optimal robust (opt-robust) and suboptimal robust (sub-opt-robust), with the non-robust algorithm developed in [45] in terms of both MSE and BER.

In the first simulation example, the performance of the proposed algorithms is studied at different level of σ_e^2. Fig. 6.2 shows the NMSE performance of the MSE algorithms versus SNR_2 with $L = 2$ and $\alpha = \beta = 0$. It can be depicted from Fig. 6.2 that the proposed sub-opt-robust algorithm outperforms the non-robust algorithm in terms of MSE. It can be observed from Fig. 6.2 that over the whole range of SNR_2, the proposed opt-robust algorithm significantly outperforms the sub-opt-robust and non-robust algorithms in terms of MSE. As expected, for all algorithms, the system MSE decreases when σ_e^2 is reduced.

For this example, the BER yielded by all algorithms versus SNR_2 is shown in Fig. 6.3. It can be clearly noticed from Fig. 6.3 that the proposed sub-opt-robust transceiver design algorithm produces much lower BER compared with the non-robust algorithm. It can be concluded from Fig. 6.3 that the proposed opt-robust transceiver design algorithm yields much lower BER compared with the sub-opt-robust and non-robust algorithms.

In the second example, the performance of the proposed algorithms is investigated at different α or β. Fig. 6.4 demonstrates the NMSE of all algorithms versus SNR_2 at

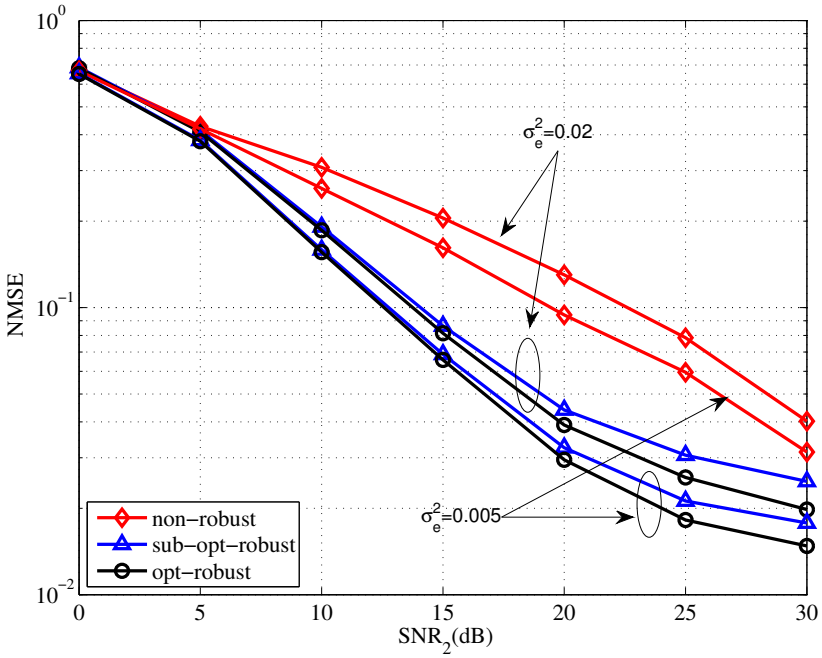

Figure 6.2: NMSE versus SNR_2 at different σ_e^2. $L = 2$ and $\alpha = \beta = 0$.

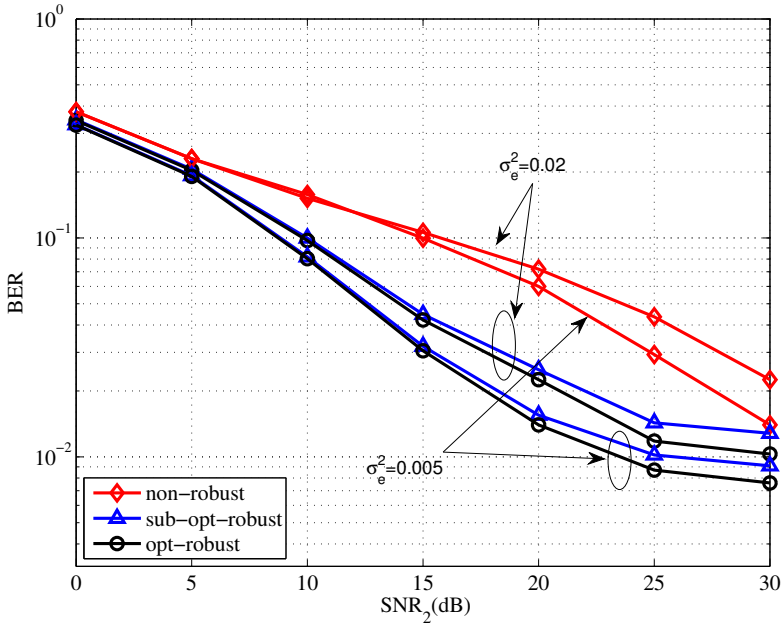

Figure 6.3: BER versus SNR_2 at different σ_e^2. $L = 2$ and $\alpha = \beta = 0$.

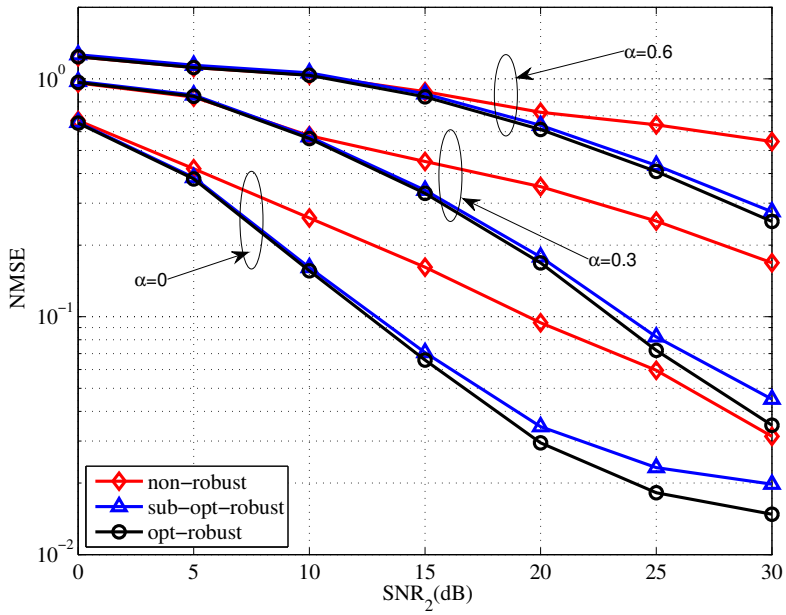

Figure 6.4: NMSE versus SNR_2 at different α. $L = 2$, $\sigma_e^2 = 0.005$, and $\beta = 0$.

different α with $L = 2$, $\sigma_e^2 = 0.005$, and $\beta = 0$. From Fig. 6.4, it can be noticed that the proposed sub-opt-robust algorithm has a comparable performance than the non-robust algorithm. It can be seen from Fig. 6.4 that the proposed opt-robust algorithm provides a better MSE performance than the sub-opt-robust and non-robust algorithms for all the α tested. Moreover, the MSE yielded by all algorithms increases with α. This is due to the fact that as α increases, the correlation among the elements of channel matrices increase, leading to the loss of spatial diversity.

For this example, the NMSE performance of all algorithms is shown in Fig. 6.5 for different β with $L = 2$, $\sigma_e^2 = 0.005$, and $\alpha = 0$. Similar to Fig. 6.4, It can be seen from Fig. 6.5 that the proposed opt-robust algorithm outperforms the sub-opt-robust and non-robust designs, and the NMSE of all algorithms increases with β.

In the third simulation example, the performance of the proposed algorithms is studied with different number of receivers L. In Fig. 6.6, the NMSE performance of the proposed robust transceiver designs is compared at different L as a function of SNR_2 with $\sigma_e^2 = 0.005$ and $\alpha = \beta = 0$. It can be seen from Fig. 6.6 that the NMSE of the proposed sub-opt-robust algorithm increases while increasing the number of receivers. It can be noted from Fig. 6.6 that as the number of receivers is increased, the NMSE of the proposed opt-robust algorithm increases. This is reasonable since it is more likely

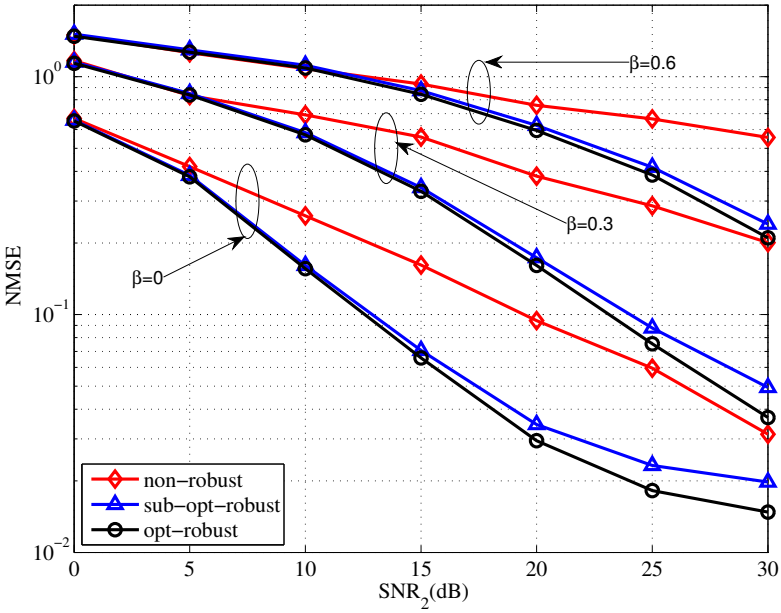

Figure 6.5: NMSE versus SNR_2 at different β. $L = 2$, $\sigma_e^2 = 0.005$, and $\alpha = 0$.

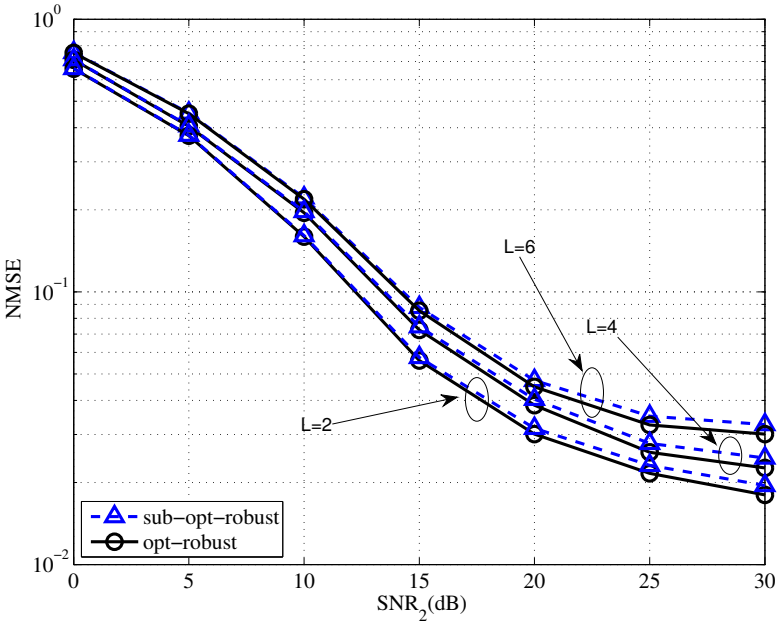

Figure 6.6: NMSE versus SNR_2 at different L. $\sigma_e^2 = 0.005$ and $\alpha = \beta = 0$.

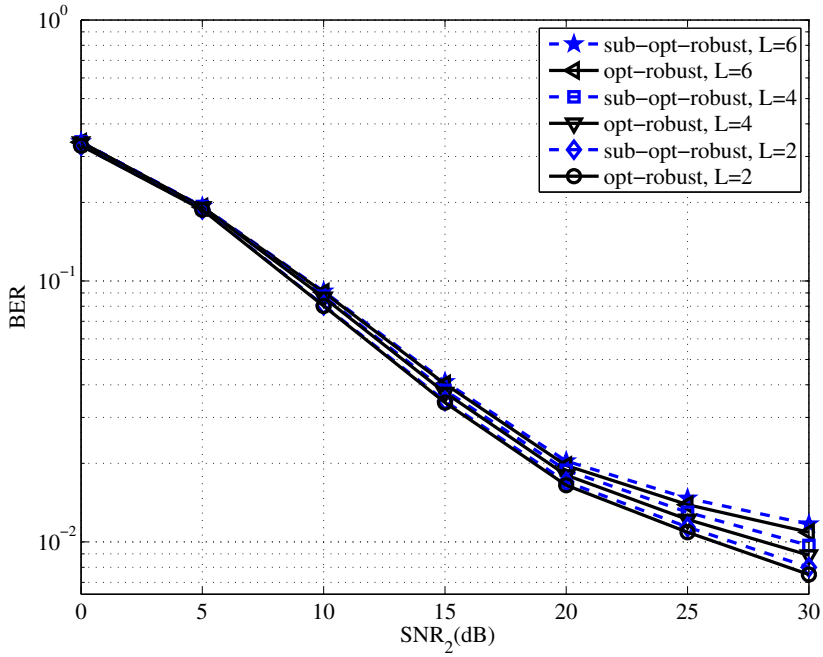

Figure 6.7: BER versus SNR_2 at different L. $\sigma_e^2 = 0.005$ and $\alpha = \beta = 0$.

to find a worse relay-receiver channel among the increased number of users and the worst-user MSE is chosen as the objective function.

For this example, the BER performance of the proposed algorithms is demonstrated in Fig. 6.7. It can be noted from Fig. 6.7 that similar to Fig. 6.6, the BER of the proposed algorithms increases with the number of receivers.

6.6 Chapter Summary

In this chapter, the challenging issues of robust transceiver optimization problems are addressed for multicasting MIMO relay systems when there is mismatch between the true and estimated channel matrices. The true channel matrices are assumed as Gaussian random matrices with the estimated channels as the mean value, and estimation error follows the well-known Kronecker model. In the proposed algorithms, the transmitter, relay, and receiver matrices are jointly optimized to minimize the maximal MSE of the signal waveform estimation at all destination nodes. Simulation results demonstrate that the proposed two robust transceiver design algorithms outperform the non-robust algorithm.

6.A Proof of Theorem 6.1

Let introduce

$$\mathbf{P}_i \triangleq tr\{\mathbf{G}\Xi\mathbf{G}^H\Psi_{2,i}\}\Sigma_{2,i} + \mathbf{I}_{N_D}, \qquad i = 1, \cdots, L. \tag{6.77}$$

The MSE function in (6.17) can be rewritten as

$$\begin{aligned} J_i(\mathbf{G},\mathbf{F}) = & tr\{\mathbf{I}_{N_B} - \mathbf{F}^H\hat{\mathbf{H}}_1^H\mathbf{G}^H\hat{\mathbf{H}}_{2,i}^H\big(\hat{\mathbf{H}}_{2,i}\mathbf{G}(\hat{\mathbf{H}}_1\mathbf{F}\mathbf{F}^H\hat{\mathbf{H}}_1^H + \boldsymbol{\Upsilon}) \\ & \times\mathbf{G}^H\hat{\mathbf{H}}_{2,i}^H + \mathbf{P}_i\big)^{-1}\hat{\mathbf{H}}_{2,i}\mathbf{G}\hat{\mathbf{H}}_1\mathbf{F}\}. \end{aligned} \tag{6.78}$$

By introducing

$$\tilde{\mathbf{G}} \triangleq \mathbf{G}\boldsymbol{\Upsilon}^{\frac{1}{2}}, \quad \tilde{\mathbf{H}}_1 \triangleq \boldsymbol{\Upsilon}^{-\frac{1}{2}}\hat{\mathbf{H}}_1, \quad \tilde{\mathbf{H}}_{2,i} \triangleq \mathbf{P}_i^{-\frac{1}{2}}\hat{\mathbf{H}}_{2,i} \tag{6.79}$$

The (6.78) can be rewritten as

$$\begin{aligned} J_i(\tilde{\mathbf{G}},\mathbf{F}) = & tr\{\mathbf{I}_{N_B} - \mathbf{F}^H\tilde{\mathbf{H}}_1^H\tilde{\mathbf{G}}^H\tilde{\mathbf{H}}_{2,i}^H\big(\tilde{\mathbf{H}}_{2,i}\tilde{\mathbf{G}}(\tilde{\mathbf{H}}_1\mathbf{F}\mathbf{F}^H\tilde{\mathbf{H}}_1^H + \mathbf{I}_{N_R}) \\ & \times\tilde{\mathbf{G}}^H\tilde{\mathbf{H}}_{2,i}^H + \mathbf{I}_{N_D}\big)^{-1}\tilde{\mathbf{H}}_{2,i}\tilde{\mathbf{G}}\tilde{\mathbf{H}}_1\mathbf{F}\} \\ = & tr\big\{\big[\mathbf{I}_{N_B} + \mathbf{F}^H\tilde{\mathbf{H}}_1^H\tilde{\mathbf{G}}^H\tilde{\mathbf{H}}_{2,i}^H\big(\tilde{\mathbf{H}}_{2,i}\tilde{\mathbf{G}}\tilde{\mathbf{G}}^H\tilde{\mathbf{H}}_{2,i}^H + \mathbf{I}_{N_D}\big)^{-1} \\ & \times\tilde{\mathbf{H}}_{2,i}\tilde{\mathbf{G}}\tilde{\mathbf{H}}_1\mathbf{F}\big]^{-1}\big\} \end{aligned} \tag{6.80}$$

where the matrix inversion lemma (6.29) has been applied to obtain (6.80). Using (6.79), the constraint (6.20) can be rewritten as

$$tr\big\{\tilde{\mathbf{G}}(\tilde{\mathbf{H}}_1\mathbf{F}\mathbf{F}\tilde{\mathbf{H}}_1^H + \mathbf{I}_{N_R})\tilde{\mathbf{G}}^H\big\} \leq P_r \tag{6.81}$$

Based on (6.21), (6.80), and (6.81), the MMSE-based transceiver optimization problem for the ith receiver can be written as

$$\min_{\mathbf{F},\tilde{\mathbf{G}}} \; J_i(\tilde{\mathbf{G}},\mathbf{F}) \tag{6.82}$$

$$s.t. \; tr\big\{\tilde{\mathbf{G}}(\tilde{\mathbf{H}}_1\mathbf{F}\mathbf{F}\tilde{\mathbf{H}}_1^H + \mathbf{I}_{N_R})\tilde{\mathbf{G}}^H\big\} \leq P_r \tag{6.83}$$

$$tr\{\mathbf{F}\mathbf{F}^H\} \leq P_s \tag{6.84}$$

It can be shown similar to [109] that the optimal $\tilde{\mathbf{G}}$ as the solution to the problem (6.82)-(6.84) can be written as

$$\tilde{\mathbf{G}} = \mathbf{T}\mathbf{F}^H\tilde{\mathbf{H}}_1^H(\tilde{\mathbf{H}}_1\mathbf{F}\mathbf{F}^H\tilde{\mathbf{H}}_1^H + \mathbf{I}_{N_R})^{-1} \tag{6.85}$$

And the objective function (6.82) can be decomposed into two MSE terms.

$$\begin{aligned} J_i(\mathbf{T},\mathbf{F}) = & tr\{(\mathbf{I}_{N_B} + \mathbf{F}^H\tilde{\mathbf{H}}_1^H\tilde{\mathbf{H}}_1\mathbf{F})^{-1}\} \\ & + tr\{(\tilde{\mathbf{R}}^{-1} + \mathbf{T}^H\tilde{\mathbf{H}}_{2,i}^H\tilde{\mathbf{H}}_{2,i}\mathbf{T})^{-1}\} \end{aligned} \tag{6.86}$$

where

$$\tilde{\mathbf{R}} = \mathbf{F}^H\tilde{\mathbf{H}}_1^H(\tilde{\mathbf{H}}_1\mathbf{F}\mathbf{F}^H\tilde{\mathbf{H}}_1^H + \mathbf{I}_{N_R})^{-1}\tilde{\mathbf{H}}_1\mathbf{F}. \tag{6.87}$$

Substituting $\tilde{\mathbf{G}}$ and $\tilde{\mathbf{H}}_1$ in (6.79) and $\boldsymbol{\Upsilon}$ in (6.24) into (6.85), $\mathbf{G}$ can be written as

$$\mathbf{G} = \mathbf{T}\mathbf{F}^H\widehat{\mathbf{H}}_1^H\boldsymbol{\Xi}^{-1},$$

which proves (6.22). By Substituting $\tilde{\mathbf{H}}_1$ in (6.79) into (6.87), $\tilde{\mathbf{R}}$ can be obtained as

$$\tilde{\mathbf{R}} = \mathbf{F}^H\widehat{\mathbf{H}}_1^H(\widehat{\mathbf{H}}_1\mathbf{F}\mathbf{F}^H\widehat{\mathbf{H}}_1^H + \boldsymbol{\Upsilon})^{-1}\widehat{\mathbf{H}}_1\mathbf{F} = \mathbf{R}$$

in (6.25). Moreover, by substituting (6.22) into (6.77), $\mathbf{P}_i$ can be written as

$$\begin{aligned} \mathbf{P}_i = & tr\left\{\mathbf{T}\mathbf{F}^H\widehat{\mathbf{H}}_1^H\boldsymbol{\Xi}^{-1}\widehat{\mathbf{H}}_1\mathbf{F}\mathbf{T}^H\boldsymbol{\Psi}_{2,i}\right\}\boldsymbol{\Sigma}_{2,i} + \mathbf{I}_{N_D} \\ = & tr\left\{\mathbf{T}\mathbf{R}\mathbf{T}^H\boldsymbol{\Psi}_{2,i}\right\}\boldsymbol{\Sigma}_{2,i} + \mathbf{I}_{N_D} \end{aligned} \tag{6.88}$$

Thus, from (6.79) and (6.86), $J_i(\mathbf{T},\mathbf{F})$ can be written as

$$\begin{aligned} J_i(\mathbf{T},\mathbf{F}) = & tr\{(\mathbf{I}_{N_B} + \mathbf{F}^H\widehat{\mathbf{H}}_1^H\boldsymbol{\Upsilon}^{-1}\widehat{\mathbf{H}}_1\mathbf{F})^{-1}\} \\ & + tr\{(\mathbf{R}^{-1} + \mathbf{T}^H\widehat{\mathbf{H}}_{2,i}^H\mathbf{P}_i^{-1}\widehat{\mathbf{H}}_{2,i}\mathbf{T})^{-1}\}. \end{aligned} \tag{6.89}$$

Finally, by substituting (6.88) into (6.89), (6.23) is proved.

Chapter 7

Conclusions and Future Work

In wireless communication systems, incorporating relay node between the transmitter and receiver is essential to provide reliable and cost effective, wide-area coverage for wireless networks in a variety of applications. Recent studies show that performing linear precoding at the relay in a non-regenerative MIMO relay system can provide higher rate data transmission than a single-antenna system in a scattered environment. In this dissertation, practical communication aspects of MIMO relay channel have been analyzed. The fundamental limits of MIMO relay channels with different degrees of CSI have been studied. Firstly, MIMO relay transceiver design has been analyzed with the assumption that the channel covariance information of the relay-destination link is available at the relay node. Next, joint design of the source and relay precoding matrices has been investigated in detail with the assumption that the mean and covariance information between the relay to destination nodes are available at the relay node. Then, the work has been extended to non-linear transceiver design with the assumption that the covariance information of the relay-destination link is available at the relay node. Finally, the transceiver design problem has been extended to multicasting MIMO relay systems.

7.1 Concluding Remarks

In this thesis, robust transceiver designs for non-regenerative MIMO relay systems have been investigated under channel uncertainty conditions. In Chapter 2, the optimal relay design problem has been considered for the non-regenerative MIMO relay communication system based on MMSE criterion. In the proposed design, it has been assumed that

the channel uncertainty condition has been considered between the relay-destination link. In the proposed design, nonconvex problem has been converted into convex problem and the problem is solved by conventional optimization tool. Simulation results demonstrate the effectiveness of the proposed design.

Then in Chapter 3, linear non-regenerative MIMO relay technique has been proposed to minimize the MSE of the signal waveform estimation at the destination node. In the proposed design, the existing results are generalized on the structure of the optimal relay amplifying matrix by considering the direct source-destination link. Further, it is assumed that channel uncertainty condition is considered between the relay-destination link and the source-destination link. Two design schemes are proposed to solve the transceiver design problem. In the proposed iterative design algorithm, the nonconvex optimization problem is converted into convex optimization problem and solved by projected gradient approach. Simulation results show that the proposed iterative algorithms outperform the existing covariance feedback based algorithms.

In Chapter 4, the general structures of the optimal source and relay precoding matrices have been derived for a linear non-regenerative MIMO relay communication system with channel uncertainty conditions between the relay-destination link. Two transceiver design schemes have been proposed to minimize the MSE of the symbol estimation at the destination with the assumption that the mean and covariance feedback of the relay-destination link is available at the relay node. In particular, it is shown that for both proposed design algorithms, the source and relay precoding matrices diagonalize the source-relay-destination channel.

Then in Chapter 5, the optimal TH, source, relay and receiver matrices design problem has been considered for a two-hop MIMO relay system based on MMSE criterion. In the proposed transceiver design scheme, it has been assumed that the full CSI of the source-relay link is known, while only the CCI of the relay-destination link is available at the relay node. Two transceiver design schemes are developed to solve the highly nonconvex joint TH, source, relay and receiver precoding matrix optimization problem. In the proposed iterative algorithm, the optimization problem is solved using the projected gradient approach. In particular, it is shown in the simplified algorithm that for given source precoding matrix, the optimal relay precoding matrix diagonalizes the source-relay-destination channel.

Finally in Chapter 6, robust multicasting optimization problem is considered in the downlink multiuser MIMO relay system where one transmitter multicasts common

message to multiple receivers through a relay node. In the proposed transceiver design, joint source and relay precoding design problem is investigated for multicasting non-regenerative MIMO relay system. In the proposed design scheme, the transmitter, relay, and receiver matrices are jointly optimized to minimize the maximal MSE of the signal waveform estimation among all receivers subject to power constraints at the transmitter and relay node. Due to the computation complexity of the proposed design scheme, a low complexity design scheme is proposed with mild approximation. In particular, it is shown that under (moderately) high source-relay link SNR assumption, both proposed transceiver design schemes are formulated as standard SDP problems and are efficiently solved using existing solvers.

7.2 Future Works

In this thesis, few advanced signal processing algorithms have been developed for non-regenerative MIMO relay systems with the assumption that the wireless channels undergo channel uncertainty conditions such as partial CSI and channel estimation errors. However, there are still many possibilities for extending this dissertation work. In Chapter 2, the optimal structure of the non-regenerative MIMO relay precoding matrix has been derived with the assumption that the relay knows the CCI of the relay-destination link and the full channel state information of the source-relay link. However, in the study, optimization of the source precoding matrix has been omitted and channel information of the source-relay link is considered as a full CSI. Hence, in the future work, the omitted parameters can be incorporated to obtain a closed form solution.

It will also be interesting to investigate the performance of the non-regenerative relaying algorithm in Chapter 3 with the assumption that the relay knows the covariance information of the source-destination link and relay-destination link. In the proposed non-regenerative MIMO relay systems, it has been assumed that there is a direct link between the source and destination nodes. In the future work, it can be assumed that the covariance information of the source-relay link is available at the relay node.

Extended work of the Chapter 2 has been investigated in Chapter 4. In the Chapter 4, an iterative joint source and relay precoder design scheme has been proposed to minimize the MSE of the symbol estimation at the destination with the assumption that the mean and covariance feedback of the relay-destination link is available at the relay. it has been assumed that the relay knows the full CSI of the source-relay link. In the

future work, the proposed transceiver designs in Chapter 4 can be extended with the assumption that mean and covariance information of the source-relay link are available at the relay node. For getting a closed form solution, direct link can be considered for obtaining the optimal transceiver design.

In Chapter 5, the performance of the TH precoder based non-linear transceiver design has been investigated for a non-regenerative MIMO relay system assuming that the full CSI of the source-relay link is known, while only the CCI of the relay-destination link is available at the relay node. In future work, it can be analyzed with the assumption that the mean and covariance information of all channels are available at the relay node.

Recently, there has been a growing interest on beamforming problems for multicasting in the non-regenerative MIMO relay systems. The existing dual-hop non-regenerative MIMO relay schemes have been extended to dual-hop non-regenerative multicasting MIMO relay systems in Chapter 6. The challenging issue of robust transceiver optimization has been investigated for multicasting MIMO relay systems when there is mismatch between the true and estimated channel matrices. The min-max MSE problem has been solved for multicasting multiple data streams. However, the min-max rate problem for multiple-stream multicasting still remains open as a challenging problem.

Bibliography

[1] E. Biglieri, R. Calderbank, A. Constantinides, A. Goldsmith, A. J. Paulraj, and H. V. Poor, *MIMO Wireless Communications*. Cambridge University Press, 2007.

[2] E. Telatar, "Capacity of multi-antenna gaussian channels," *AT&T Bell Labs, Tech. Memo.*, Murray Hill, NJ, Jun. 1995.

[3] S. M. Alamouti, "A simple transmit diversity technique for wireless communications," *IEEE J. Select. Areas Commun.*, vol. 16, pp. 1451–1458, Oct. 1998.

[4] D. Gesbert, M. Shafi, D.-S. Shiu, P. J. Smith, and A. Naguib, "From theory to practice: An overview of MIMO space-time coded wireless systems," *IEEE J. Sel. Areas Commun.*, vol. 21, pp. 281–302, Apr. 2003.

[5] A. J. Paulraj, D. A. Gore, R. U. Nabar, and H. Bölcskei, "An overview of MIMO communications–a key to gigabit wireless," *Proc. IEEE*, vol. 92, pp. 198–218, Feb. 2004.

[6] A. Goldsmith, S. A. Jafar, N. Jindal, and S. Vishwanath, "Capacity limits of MIMO channels," *IEEE J. Sel. Areas Commun.*, vol. 21, pp. 684–702, Jun. 2003.

[7] D. Tse and P. Viswanath, *Fundamentals of Wireless Communication*. Cambridge University Press, 2005.

[8] A. Goldsmith, *Wireless Communications*. Cambridge University Press, 2005.

[9] G. J. Foschini, "Layered space-time architecture for wireless communication in a fading environment when using multi-element antennas," *Bell Labs Tech. J.*, vol. 1, pp. 41–59, Autumn 1996.

[10] G. J. Foschini and M. J. Gans, "On limits of wireless communications in a fading environment when using multiple antennas," *Wireless Pers. Commun.*, vol. 6, pp. 311–335, Mar. 1998.

[11] D.-S. Shiu, G. Foschini, M. Gans, and J. Kahn, "Fading correlation and its effect on the capacity of multielement antenna systems," *IEEE Trans. Commun.*, vol. 48, pp. 503–513, Mar. 2000.

[12] M. Shafi, H. Huang, A. Hottinen, P. J. Smith, and R. A. Valenzuela, "MIMO systems and applications: Field experience, practical aspects, limitations and challenges," *IEEE J. Sel. Areas Commun.*, vol. 26, pp. 841–844, Guest Editorial, Aug. 2008.

[13] T. M. Cover and A. A. El Gamal, "Capacity theorems for the relay channel," *IEEE Trans. Inf. Theory*, vol. 25, pp. 572–584, Sep. 1979.

[14] R. Pabst, B. H. Walke, D. C. Schultz, D. C. Herhold, H. Yanikomeroglu, S. Mukherjee, H. Viswanathan, M. Lott, W. Zirwas, M. Dohler, H. Aghvami, D. D. Falconer, and G. P. Fettweis, "Relay-based deployment concepts for wireless and mobile broadband radio," *IEEE Commun. Mag.*, vol. 42, pp. 80–89, Sep. 2004.

[15] I. Kang, W. Sheen, R. Chen, and S. L. C. Hsiao, "Throughput improvement with relay-augmented cellular architecture," *IEEE 802.16mmr-05 008*, http://www.wirelessman.org, Sep. 2005.

[16] V. Genc, S. Murphy, Y. Yu, and J. Murphy, "IEEE 802.16j relay-based wireless access networks: An overview," *IEEE Wireless Commun.*, vol. 15, pp. 56–63, Oct. 2008.

[17] J. N. Laneman, D. N. C. Tse, and G. W. Wornell, "Cooperative diversity in wireless networks: Efficient protocols and outage behavior," *IEEE Trans. Inf. Theory*, vol. 50, pp. 3062–3080, Dec. 2004.

[18] A. Wittneben and B. Rankov, "Impact of cooperative relays on the capacity of rank-deficient MIMO channels," in *Proc. 12th IST Summit on Mobile and Wireless Communications*, Aveiro, Portugal, Jun. 2003, pp. 421-425.

[19] J. N. Laneman and G. W. Wornell, "Distributed space-time-coded protocols for exploiting cooperative diversity in wireless networks," *IEEE Trans. Inf. Theory*, vol. 49, pp. 2415–2425, Oct. 2003.

[20] D. P. Palomar, J. M. Cioffi, and M. A. Lagunas, "Joint Tx-Rx beamforming design for multicarrier MIMO channels: A unified framework for convex optimization," *IEEE Trans. Signal Process.*, vol. 51, pp. 2381–2401, Sep. 2003.

[21] O. Muñoz-Medina, J. Vidal, and A. Agustín, "Linear transceiver design in nonregenerative relays with channel state information," *IEEE Trans. Signal Processing*, vol. 55, pp. 2593–2604, Jun. 2007.

[22] X. Tang and Y. Hua, "Optimal design of non-regenerative MIMO wireless relays," *IEEE Trans. Wireless Commun.*, vol. 6, pp. 1398–1407, Apr. 2007.

[23] W. Guan and H. Luo, "Joint MMSE transceiver design in non-regenerative MIMO relay systems," *IEEE Commun. Lett.*, vol. 12, pp. 517–519, Jul. 2008.

[24] A. S. Behbahani, R. Merched, and A. M. Eltawil, "Optimizations of a MIMO relay network," *IEEE Trans. Signal Process.*, vol. 56, pp. 5062–5073, Oct. 2008.

[25] Y. Rong, X. Tang, and Y. Hua, "A unified framework for optimizing linear non-regenerative multicarrier MIMO relay communication systems," *IEEE Trans. Signal Process.*, vol. 57, pp. 4837–4851, Dec. 2009.

[26] Y. Rong and F. Gao, "Optimal beamforming for non-regenerative MIMO relays with direct link," *IEEE Commun. Lett.*, vol. 13, pp. 926–928, Dec. 2009.

[27] Y. Rong, "Optimal joint source and relay beamforming for MIMO relays with direct link," *IEEE Commun. Lett.*, vol. 14, pp. 390–392, May 2010.

[28] F. S. Tseng and W. R. Wu, "Linear MMSE transceiver design in amplifyand-and-forward MIMO relay systems," *IEEE Tran. Veh. Technol*, vol. 59, pp. 754–765, Feb. 2010.

[29] H. W. Je, B. Lee, S. Kim, and K. B. Lee, "Design of non-regenerative MIMO-relay systems with partial channel state information," in *Proc. IEEE Int. Conf. Commun*, Beijing, China, May. 19-23, 2008, pp. 4441-4445.

[30] C. Jeong and H.-M. Kim, "Precoder design of non-regenerative relays with covariance feedback," *IEEE Commun. Lett.*, vol. 13, pp. 920 – 922, Dec. 2009.

[31] C. Jeong, B. Seo, S. R. Lee, H.-M. Kim, and I.-M. Kim, "Relay precoding for non-regenerative MIMO relay systems with partial CSI feedback," *IEEE Trans. Wireless Commun.*, vol. 11, pp. 1698–1711, May 2012.

[32] L. Gopal, Y. Rong, and Z. Zang, "Joint MMSE transceiver design in non-regenerative MIMO relay systems with covariance feedback," in *Proc. IEEE 17th Asia-Pacific Conf. Commun*, Sabah, Malaysia, Oct. 2-5, 2011, pp. 290-294.

[33] K. Dae-Hyun and H.-M. Kim, "MMSE precoder design for a non-regenerative MIMO relay with covariance feedback," in *Proc. IEEE 21st Int. Sym. Per. Ind. Mobile Radio Commun.*, Istanbul, Turkey, Sep. 26-30, 2010, pp. 461-464.

[34] L. Gopal, Y. Rong, and Z. Zang, "Channel covariance information based transceiver design for AF MIMO relay systems with direct link," in *Proc. IEEE 18th Asia-Pacific Conf. Commun.*, Jeju Island, Korea, Oct. 15-17, 2012, pp. 1-6.

[35] ——, "MMSE based transceiver design for MIMO relay systems with mean and covariance feedback," in *Proc. 77th IEEE Veh. Technol. Conf.*, Dresden, Germany, Jun. 2-5, 2013, pp. 1-5.

[36] Y. Rong and M. R. A. Khandaker, "On uplink-downlink duality of multi-hop MIMO relay channel," *IEEE Trans. Wireless Commun.*, vol. 10, pp. 1923–1931, Jun. 2011.

[37] L. Sanguinetti, A. A. D'Amoco, and Y. Rong, "A tutorial on the optimization of amplify-and-forward MIMO systems," *IEEE J. Sel. Areas Commun.*, vol. 30, pp. 1331–1346, Sep. 2012.

[38] R. F. H. Fischer, C. Windpassinger, A. Lampe, and J. H. Huber, "Space time transmission using Tomlinson-Harashima precoding," in *Proc. 4th ITC Conf. Source Channel Coding*, 2002.

[39] A. A. D'Amico and M. Morelli, "Joint Tx-Rx MMSE design for MIMO multicarrier systems with Tomlinson-Harashima precoding," *IEEE Trans. Wireless Commun.*, vol. 7, pp. 3118–3127, Aug. 2008.

[40] F.-S. Tseng, M.-Y. Chang, and W.-R. Wu, "Joint Tomlinson-Harashima source and linear relay precoder design in amplify-and-forward MIMO relay systems via MMSE criterion," *IEEE Trans. Veh. Technol.*, vol. 60, pp. 1687–1698, May 2011.

[41] C. Xing, M. Xia, F. Gao, and Y.-C. Wu, "Robust transceiver with Tomlinson-Harashima precoding for amplify-and-forward MIMO relaying systems," *IEEE J. Sel. Areas Commun.*, vol. 30, pp. 1370–1382, Sep. 2012.

[42] A. P. Millar, S. Weiss, and R. W. Stewart, "THP transceiver design for MIMO relaying with direct link and partial CSI," *IEEE Commun. Lett.*, vol. 17, pp. 1204–1207, Jun. 2013.

[43] F.-S. Tseng, M.-Y. Chang, and W.-R. Wu, "Robust Tomlinson-Harashima source and linear relay precoders design in amplify-and-forward MIMO relay systems," *IEEE Trans. Commun.*, vol. 60, pp. 1124–1137, Apr. 2012.

[44] F. A. Dietrich, P. Breun, and W. Utschik, "Robust Tomlinson-Harashima precoding for the wireless broadcast channel," *IEEE Trans. Signal Process.*, vol. 55, pp. 631–644, Feb. 2007.

[45] M. R. A. Khandaker and Y. Rong, "Precoding design for MIMO relay multicasting," *IIEEE Tran. Wireless Commun.*, vol. 12, pp. 3544–3555, Jul. 2013.

[46] ——, "Multicasting MIMO relay optimization based on min-max MSE criterion," in *Proc. 13th IEEE Int. Conf. Commun. Syst.*, Singapore, Nov. 21-23, 2012, pp. 16-20.

[47] S. Serbetli and A. Yener, "Transceiver optimization for multiuser MIMO systems," *IEEE Trans. Signal Process.*, vol. 52, pp. 214–226, 2004.

[48] F. Kaltenberger, M. Kountouris, L. Cardoso, R. Knopp, and D. Gesbert, "Capacity of linear multi-user MIMO precoding schemes with measured channel data," in *Proc. IEEE 9th Workshop on Signal Process. Adv. Wireless Commun.*, Recife, Brazil, Jul. 6-9, 2008, pp. 580-584.

[49] L. Gopal, Y. Rong, and Z. Zang, "Tomlinson-Harashima precoding based transceiver design for MIMO relay systems with channel covariance information," *IIEEE Tran. Signal Process.*, submitted, Aug. 2014.

[50] S. Berger, M. Kuhn, A. Wittneben, T. Unger, and A. Klein, "Recent advances in amplify-and-forward two-hop relaying," *IEEE Commun. Mag.*, vol. 47, pp. 50 – 56, Jul. 2009.

[51] H. Bölcskei, R. U. Nabar, O. Oyman, and A. J. Paulraj, "Capacity scaling laws in MIMO relay networks," *IEEE Trans. Wireless Commun.*, vol. 5, pp. 1433–1443, Jun. 2006.

[52] B. Wang, J. Zhang, and A. Host-Madsen, "On the capacity of MIMO relay channels," *IEEE Trans. Inf. Theory*, vol. 51, pp. 29–43, Jan. 2005.

[53] O. Muñoz, J. Vidal, and A. Agustin, "Non-regenerative MIMO relaying with channel state information [cellular example]," in *Proc. IEEE Int. Conf. Acoustics, Speech, and Signal Process.*, Mar.18-23, 2005, vol. 3, pp. iii/361 - iii/364.

[54] R. Mo and Y. H. Chew, "Precoder design for non-regenerative MIMO relay systems," *IEEE Trans. Wireless Commun.*, vol. 8, pp. 5041 – 5049, Oct. 2009.

[55] A. S. Behbahani, R. Merched, and A. Eltawil, "On signal processing methods for MIMO relay architectures," in *Proc. IEEE Global Telecommun. Conf.*, Washington, DC, USA, Nov. 26-30, 2007, pp. 2967-2971.

[56] B. Zhang, Z. He, K. Niu, L. Zhang, and X. Wang, "Joint linear transceiver design in amplify-and-forward MIMO relay system using an MMSE criterion," in *Proc. IEEE Int. Conf. Network Infrastructure and Digital Content*, Beijing, China, Nov. 6-8, 2009, pp. 936-940.

[57] N. Khajehnouri and A. H. Sayed, "Distributed MMSE relay strategies for wireless sensor networks," *IEEE Tran. Signal Process.*, vol. 55, pp. 3336–3348, Jul. 2007.

[58] B. Aygün and A. Soysal, "Achieving the lower bound of fading MIMO relay channels with covariance feedback at the transmitters," in *Proc. 7th Int. Wireless Commun. Mobile Computing Conf.*, Istanbul,Turkey, Jul. 4-8, 2011, pp. 900-905.

[59] S. M. Kay, *Fundamentals of Statistical Signal Processing: Estimation Theory.* Englewood Cilffs, NJ: Prentice Hall, 1993.

[60] D. Bernstein, *Matrix Mathematics: Theory, Facts, and Formulas.* Princeton University Press, 2011.

[61] E. K. P. Chong and S. H. Zak, *Introduction to optimization*. New York, NY:Wiley-Interscience, 2001.

[62] F.-S. Tseng, W.-R. Wu, and J.-Y. Wu, "Joint source/relay precoder design in nonregenerative cooperative systems using an MMSE criterion," *IEEE Trans. Wireless Commun.*, vol. 8, pp. 4928 – 4933, Oct. 2009.

[63] C.-H. Wu, W.-H. Chung, and C.-E. Chen, "MMSE-based precoder design in non-regenerative relay systems with direct link," in *Proc. IEEE 77th Veh. Tech. Conf.*, Dresden, Germany, Jun. 2-5, 2013, pp. 1-5.

[64] F.-S. Tseng, W.-R. Wu, and J.-Y. Wu, "Joint source/relay precoder design in amplify-and-forward relay systems using an MMSE criterion," in *Proc. IEEE Wireless Commun. Network Conf.*, Budapest, Hungary, Apr. 5-8, 2009, pp. 1-5.

[65] A. W. Marshall, I. Olkin, and B. C. Arnold, *Inequalities: Theory of Majorization and Its Applications*. Springer, 2011.

[66] T. Ando, "Concavity of certain maps on positive definite matrices and applications to hadamard products," *Linear Algebra and Its Applications*, vol. 26, pp. 203–241, Aug. 1979.

[67] B. Zhang, X. Wang, K. Niu, and Z. He, "Joint linear transceiver design for non-regenerative MIMO relay systems," *Electronics Letters*, vol. 45, pp. 1254–1256, Nov. 2009.

[68] Z. Chen, H. Liu, and W. Wang, "Optimal transmit strategy of a two-hop decode-and-forward MIMO relay system with mean and covariance feedback," *IEEE Commun. Lett.*, vol. 14, pp. 530 – 532, Jun. 2010.

[69] P. A. Angel and M. Kaveh, "On the performance of distributed space-time coding system with one and two non-regenerative relays," *IEEE Trans. Wireless Commun.*, vol. 5, pp. 682–692, Mar. 2006.

[70] M. B. Shenouda and T. N. Davidson, "Nonlinear and linear broadcasting with QoS requirements: Tractable approaches for bounded channel uncertainties," *IEEE Tran. Signal Process.*, vol. 57, pp. 1936–1947, May 2009.

[71] A. A. D'Amico, "Tomlinson-Harashima precoding in MIMO systems: A unified approach to transceiver optimization based on multiplicative schur-convexity," *IEEE Tran. Signal Process.*, vol. 56, no. 8, pp. 3662–3677, Aug 2008.

[72] R. F. H. Fischer, "Tomlinson-Harashima precoding in space-time transmission for low-rate backward channel," in *Proc. Int. Zurich Seminar Broadband Commun. Access, Transmission, Networking*, Zurich, Switzerland, Feb.19-21, 2002, pp. 7-1 - 7-6.

[73] L. Sanguinetti and M. Morelli, "Non-linear pre-coding for multipleantenna multi-user downlink transmissions with different QoS requirements," *IEEE Trans. Wireless Commun.*, vol. 6, pp. 852–856, Mar. 2007.

[74] A. A. D'Amico, "Tomlinson-Harashima precoding in MIMO systems: A unified approach to transceiver optimization based on multiplicative Schur-convexity," *IEEE Trans. Signal Process.*, vol. 56, pp. 3662–3677, Aug. 2008.

[75] L. Sun and M. Lei, "Quantized CSI-based Tomlinson-Harashima precoding in multiuser MIMO systems," *IEEE Trans. Wireless Commun.*, vol. 12, pp. 1118–1126, Mar. 2013.

[76] S. S. Christensen, R. Agarwal, E. de Carvalho, and J. M. Cioffi, "Weighted sum-rate maximization using weighted MMSE for MIMO-BC beamforming design," *IEEE Trans. Wireless Commun.*, vol. 7, pp. 4791–4790, Dec. 2008.

[77] ——, "Weighted sum-rate maximization using weighted MMSE for MIMO-BC beamforming design," in *Proc. IEEE Int. Conf. Commun.*, Dresden, Germany, Jun. 14-18, 2009, pp. 1-6.

[78] M. B. Shenouda and T. N. Davidson, "A framework for designing MIMO systems with decision feedback equalization or Tomlinson-Harashima precoding," *IEEE J. Sel. Areas Commun.*, vol. 26, pp. 401–411, Feb. 2008.

[79] F.-S. Tseng and W.-R. Wu, "Joint source/relay precoders design in amplify-and-forward relay systems: A geometric mean decomposition approach," in *Proc. IEEE Int. Conf. Acoustics, Speech and Signal Process*, Taipei, Taiwan, Apr.19-24, 2009, pp. 2641-2644.

[80] W. Liu, C. Li, J.-D. Li, and L. Hanzo, "Geometric-mean-decomposition-based optimal transceiver for a class of two-hop MIMO-aided amplify-and-forward relay channels," *IEEE Trans. Wireless Commun.*, vol. 63, pp. 948 – 952, Feb. 2014.

[81] Y. Jiang, W. Hager, and J. Li, "The geomatric mean decomposition," *Linear Algebra Appl*, vol. 396, pp. 373–384, Feb. 2005.

[82] Y. Jiang, J. Li, and W. W. Hager, "Joint transceiver design for MIMO communications using geometric mean decomposition," *IEEE Tran. Signal Process.*, vol. 53, no. 10, pp. 3791–3803, Oct 2005.

[83] D. P. Bertsekas, *Nonlinear Programming*, 2nd. Edition, Ed. Athena Scientific, Belmont, 1995.

[84] T. M. Cover and J. A. Thomas, *Elements of Information Theory.* New York: Wiley, 1991.

[85] A. P. Millar, S. Weiss, and R. W. Stewart, "Robust transceiver design for MIMO relay systems with Tomlinson Harashima precoding," in *Proc. 20th European Signal Process. Conf.*, Bucharest, Romania, Aug. 27-31, 2012, pp. 1374-1378.

[86] I. Olkin and J. Pratt, "A multivariate Tchebycheff inequality," *Ann. Math. Statist*, vol. 29, pp. 226–234, Mar. 1958.

[87] S. Boyd and L. Vandenberghe, *Convex Optimization.* Cambridge, U. K.: Cambridge University Press, 2004.

[88] M. A. Khojastepour, A. Salehi-Golsefidi, and S. Rangarajan, "Towards an optimal beamforming algorithm for physical layer multicasting," in *Proc. IEEE Inf. Theory Workshop*, Paraty, Brazil, Oct. 16-20, 2011, pp. 395-399.

[89] N. Jindal and Z.-Q. Luo, "Capacity limits of multiple antenna multicast," in *Proc. IEEE ISIT*, Seattle, USA, Jul. 9-14, 2006, pp.1841-1845.

[90] S. Y. Park, D. Love, and D. H. Kim, "Capacity limits of multi-antenna multicasting under correlated fading channels," *IEEE Tran. Commun.*, vol. 58, pp. 2002–2013, Jul. 2010.

[91] N. D. Sidiropoulos, T. N. Davidson, and Z.-Q. T. Luo, "Transmit beamforming for physical-layer multicasting," *IEEE Trans. Signal Process.*, vol. 54, pp. 2239–2251, Jun. 2006.

[92] E. Chiu and V. K. N. Lau, "Precoding design for multi-antenna multicast broadcast services with limited feedback," *IEEE Systems Journal*, vol. 4, pp. 550–560, Dec. 2010.

[93] E. Matskani, N. D. Sidiropoulos, Z.-Q. Luo, and L. Tassiulas, "Efficient batch and adaptive approximation algorithms for joint multicast beamforming and admission control," *IEEE Trans. Signal Process.*, vol. 57, pp. 4882–4894, Dec. 2009.

[94] M. A. Khojastepour, A. Khajehnejad, K. Sundaresan, and S. Rangarajan, "Adaptive beamforming algorithms for wireless link layer multicasting," in *Proc. IEEE PIMRC*, Toronto, Canada, Sep. 11-14, 2011, pp. 1994-1998.

[95] M. Kaliszan, E. Pollakis, and S. Stańczak, "Efficient beamforming algorithms for MIMO multicast with application-layer coding," in *Proc. IEEE ISIT*, St. Petersburg, Russia, Jul. 31-Aug. 5, 2011, pp. 928-932.

[96] S. Shi, M. Schubert, and H. Boche, "Physical layer multicasting with linear MIMO transceivers," in *Proc. 42nd Annual Conf. Information Sciences and Systems*, Princeton, NJ, USA, Mar. 19-21, 2008, pp. 884-889.

[97] H. Zhu, N. Prasad, and S. Rangarajan, "Precoder design for physical layer multicasting," *IEEE Tran. Signal Process.*, vol. 60, no. 11, Nov 2012.

[98] B. Du, X. Xu, Z. Zhang, and X. Dai, "Precoder design for dual-stream MIMO multicasting," in *Proc. Int. Conf. Wireless Commun. Signal Process*, Hangzhou, China, Oct . 24-26, 2013, pp. 1 - 6.

[99] H. Zhang, X. You, G. Wu, and H. Wang, "Cooperative multi-antenna multicasting for wireless networks," in *Proc. IEEE GLOBECOM*, Miami, FL, USA, Dec. 6-10, 2010.

[100] L. Musavian, M. R. Nakhai, M. Dohler, and A. H. Aghvami, "Effect of channel uncertainty on the mutual information of MIMO fading channels," *IEEE Trans. Veh. Technol.*, vol. 56, pp. 2798–2806, Sep. 2007.

[101] Y. Rong, "Robust design for linear non-regenerative MIMO relays with imperfect channel state information," *IEEE Trans. Signal Process.*, vol. 59, pp. 2455–2460, May 2011.

[102] C. Xing, S. Ma, and Y.-C. Wu, "Robust joint design of linear relay precoder and destination equalizer for dual-hop amplify-and-forward MIMO relay systems," *IEEE Tran. Signal Process.*, vol. 58, pp. 2273 – 2283, Apr. 2010.

[103] C. Xing, S. Ma, Y.-C. Wu, T.-S. Ng, and H. V. Poor, "Linear transceiver design for amplify-and-forward MIMO relay systems under channel uncertainties," in *Proc. IEEE Wireless Commun. Networking Conf.*, Sydney, Australia, Apr. 18-21, 2010, pp. 1-6.

[104] H. Shen, J. Wang, W. Xu, Y. Rong, and C. Zhao, "A worst-case robust MMSE transceiver design for nonregenerative MIMO relaying," *IEEE Trans. Wireless Commun.*, vol. 13, pp. 695–709, Feb. 2014.

[105] L. Zhang, Y. Cai, R. C. de Lamare, and M. Zhao, "Robust multibranch Tomlinson-Harashima precoding design in amplify-and-forward MIMO relay systems," *IEEE Trans. Commn.*, vol. 62, pp. 3476 – 3490, Oct. 2014.

[106] B. K. Chalise and L. Vandendorpe, "Joint linear processing for an amplify-and-forward MIMO relay channel with imperfect channel state information," *EURASIP J. Adv. Signal Process.*, vol. Article ID 640186, 13 pages, Aug. 2010.

[107] Z. He, W. Jiang, and Y. Rong, "Robust design for amplify-and-forward MIMO relay systems with direct link and imperfect channel information," *IEEE Trans. Wireless Commun.*, to be appear 2014.

[108] J. Liu, F. Gao, and Z. Qiu, "Robust transceiver design for multi-user multiple-input multiple-output amplify-and-forward relay systems," *IET Commun.*, vol. 8, pp. 2162–2170, Mar. 2014.

[109] Y. Rong, "Simplified algorithms for optimizing multiuser multi-hop MIMO relay systems," *IEEE Trans. Commun.*, vol. 59, pp. 2896–2904, Oct. 2011.

[110] M. Ding and S. D. Blostein, "MIMO minimum total MSE transceiver design with imperfect CSI at both ends," *IEEE Trans. Signal Process.*, vol. 57, no. 3, pp. 1141–1150, Mar 2009.

[111] X. Zhang, D. P. Palomar, and B. Ottersten, "Statistically robust design of linear MIMO transceivers," *IEEE Tran. Signal Process.*, vol. 56, no. 8, pp. 3678–3689, Aug 2008.

[112] L. Zhang, Y. Cai, R. C. de Lamare, and M. Zhao, "Robust multi-branch Tomlinson-Harashima source and relay precoding scheme in nonregenerative MIMO relay systems," in *Proc. 77th IEEE Veh. Tech. Conf.*, Dresden, Germany, Jun. 2-5, 2013, pp. 1-5.

[113] C. Xing, S. Ma, Y.-C. Wu, and T.-S. Ng, "Robust beamforming for amplify-and-forward MIMO relay systems based on quadratic matrix programming," in *Proc. IEEE Int. Conf. Acoustics Speech Signal Process.*, Dallas, TX, USA, Mar. 14-19, 2010, pp. 3250-3253.

[114] C. Xing, S. Ma, and Y.-C. Wu, "Bayesian robust linear transceiver design for dual-hop amplify-and-forward MIMO relay systems," in *Proc. IEEE Global Telecommun. Conf.*, Honolulu, HI, USA, Nov. 30-Dec. 4, 2009, pp. 1 - 5.

[115] C. Xing, S. Ma, Z. Fei, Y.-C. Wu, and J. Kuang, "Joint robust weighted LMMSE transceiver design for dual-hop AF multiple-antenna relay systems," in *Proc. IEEE Global Telecommun. Conf.*, Houston, TX, USA, Dec. 5-9, 2011, pp. 1 - 5.

[116] A. Gupta and D. Nagar, *Matrix Variate Distributions*. London, U.K.: Chapman & Hall/CRC,, 2000.

[117] M. Grant and S. Boyd, "Cvx: Matlab software for disciplined convex programming (web page and software)." *http://cvxr.com/cvx*, April, 2010.

[118] C. Xing, S. Ma, Y. C. Wu, and T. S. Ng, "Transceiver design for dual-hop non-regenerative MIMO-OFDM relay systems under channel uncertainties," *IEEE Trans. Signal Process.*, vol. 58, pp. 6325–6339, Dec. 2010.